University of Alberta

Modulation of Ercc1 protein expression in human cells through the use of antisense-*ERCC1* cDNA

by

Loretta Vallee-Lucic

A thesis submitted to the Faculty of Graduate Studies and Research in partial fulfillment of the requirements for the degree of Master of Science

Medical Sciences – Oncology

Edmonton, Alberta
Spring, 2004

Your file Votre référence
ISBN: 0-612-96560-0
Our file Notre référence
ISBN: 0-612-96560-0

ABSTRACT

An attempt to make a null of the mutant *ERCC1* DNA repair gene in a human background was undertaken using antisense-*ERCC1* cDNA transfected into SV40-transformed GM00637A human fibroblast cells. Transfected cells harboring the antisense-*ERCC1* cDNA and expressing antisense-*ERCC1* mRNA did not demonstrate a significant decrease in Ercc1 protein expression with a corresponding increase in either ultraviolet light/phosphoramide mustard sensitivity. The half-life of the Ercc1 protein in GM00637A cells (6-24 h) indicated an increase in protein stability when compared to the non-transformed cell line GM38 (<2 h) suggesting that SV40-transformation could influence Ercc1 protein stability, which in turn may directly impact nucleotide excision repair and interstrand crosslink repair and its modulation. A parallel preliminary study for *ERCC1* mRNA stability also showed an increase in *ERCC1* mRNA half-life in SV40-transformed vs. non-transformed human fibroblast cells. Although down-regulation of the Ercc1 protein was not achieved in this study, results suggest that examination of *ERCC1* mRNA and protein expression in malignant cells might lead to more effective chemotherapeutic strategies.

DEDICATION

I would like to dedicate this thesis to those that I love so dearly. To my parents Wayne and Judy Vallee who were so happy just to see me graduate from high school and were ecstatic to see me continue to expand my horizons. To my sisters Sonyau Stavely and Melonie Vallee who make me laugh at myself when I get too involved with work. To my two wonderful children, McKayla and Daniel, and my husband John Lucic who have helped me in find the strength and courage to complete my thesis and get my degree.

ACKNOWLEDGEMENTS

First and foremost, I would like to thank my supervisor Dr. David Murray for his guidance and support, particularly in writing this thesis. I would also like to thank my supervisory committee, Charlotte Spencer and John Bell. I am very grateful to Dr. Micheal Weinfeld, who was so generous in loaning me his ChemDraw program. I am also grateful to all the staff and students that work (or have worked) in the research department of the Cross Cancer Institute who were very helpful and supportive. In particular: Sharon Barker, Taunja Palmer-Stone, Beth Rosenberg, Sherry Perdue, Sandy Dieb, Roseline Godbout, Allan Franko, Stacey Bleoo, Ray Roland, Louise Enns, April Scott and the many other people who assisted me in my work and who were so very understanding.

Financial support from the Department of Oncology, University of Alberta, is gratefully acknowledged. These studies were variously funded by the NIH/NCI (USA) and the NCI (Canada) as well as the CIHR (Canadian Institutions for Health Research).

TABLE OF CONTENTS

LIST OF TABLES

LIST OF FIGURES

LIST OF ABBREVIATIONS

αE1	antisense ERCC1
AGT	O^6-alkylguanine-DNA alkyltransferase
ALDH	aldehyde dehydrogenase
AO-ORF	antisense overlapping-open reading frame
BSA	bovine serum albumin
CHO	Chinese hamster ovary
CMV	cytomegalovirus
CP	cyclophosphamide
CPD	cyclopbutane pyrimidine dimer
CPM	counts per minute
CRS	cross-link induced repair synthesis
CS	Cockayne's syndrome
C-terminus	protein carboxy terminus
cDNA	complementary deoxyribonucleic acid
dH_2O	distilled water
DMEM	Dulbecco's modified Eagles medium
DTT	dithiothreitol
EDTA	disodium ethylenediaminetetraacetate
EGTA	ethylene glycol-bis (β-aminoethyl ether) – *N,N,N',N'*-tetraacetic acid
ERCC	excision repair cross complementing
FBS	fetal bovine serum
GGR	global genome repair
4HC	4-hydroperoxycyclophosphamide
HCl	hydrochloric acid
HEPES	*N*-2-hydroxyethylpiperazine-*N'*-2-

	ethanesulfonic acid
4HOCP	4-hydroxycyclophosphamide
hRAD	human homolog of rad
HR	homologous recombination
HRP	horseradish peroxidase
IgG	immunoglobin G
ISC	interstrand cross-link
kb	kilobase
kDa	kilodaltons
mAb	monoclonal antibody
$MgCl_2$	magnesium chloride
MMC	Mitomycin C
MMR	mismatch repair
MOPS	morpholinopropanesulfonic acid
mQH_2O	distilled deionized water
mRNA	messenger ribonucleic acid
NER	nucleotide excision repair
N-terminus	protein amino terminus
PBS	phosphate-buffered saline
PBST	phosphate-buffered saline with Tween 20
PCNA	proliferating-cell nuclear antigen
pD3	pcDNA3 mammalian expression vector
PM	phosphoramide mustard
PMSF	phenylmethylsulfonyl fluoride
RFC	replication factor C
RPA	replication protein A
rpm	revolutions per minute

SDS	sodium *n*-dodecyl sulfate
SDS-PAGE	sodium *n*-dodecyl sulfate polyacrylamide gel electrophoresis
SV40	simian virus 40
TBE	Tris-borate-EDTA buffer
TBS	Tris-buffered saline
TCR	transcription coupled repair
TFIIH	transcription factor IIH
UV-C	ultraviolet light wavelength C (254 nm)
XP	xeroderma pigmentosum
XRCC	x-ray cross complementary

CHAPTER 1: INTRODUCTION

In the course of treating various types of cancer, chemotherapeutic agents that appear to be the most broadly effective include the bifunctional alkylating and platinating agents such as mitomycin C (MMC), cyclophosphamide (CP), melphalan and cisplatin. The effectiveness of these agents is dependent upon a number of factors that also appear to influence the development of drug resistance in tumor cells. Although these agents can react with many biological target molecules, cytotoxicity has generally been attributed to the formation of DNA adducts such as monoadducts, intrastrand crosslinks (within the same DNA strand), and interstrand cross-links (between two strands of DNA) (see Figure 1-1; Chabner et al. 1996, Colvin 2000).

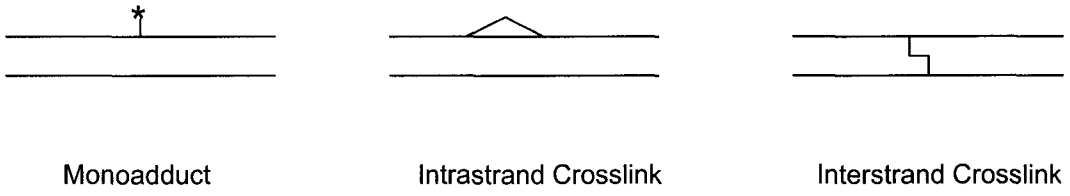

Figure 1-1. DNA adducts that can be formed by bifunctional alkylating and platinating agents.

The presence of DNA adducts interferes with the fundamental mechanisms of cellular activity, in particular DNA replication and cell division, and if left unrepaired can result in cell death and mutagenesis (Chabner et al. 1996, Colvin 2000, Dronkert and Kanaar 2001). DNA adducts can also actively trigger responses such as apoptosis, possibly involving detector proteins such as mismatch repair (MMR) factors (Fink et al. 1998). In order for a cell to continue to function effectively, these DNA adducts must be repaired. To effect the repair of DNA damage produced by bifunctional alkylating/platinating agents, particular pathways of repair are required depending on the type of lesion induced and its location in the genomic

DNA. Monoadducts and intrastrand cross-linked DNA adducts can be effectively repaired by the nucleotide excision repair (NER) pathway. Interstrand cross-links (ISCs), however, require an alternative method of repair because both strands of the DNA helix are locally covalently linked. The repair of ISCs is thought to require proteins from both the NER and homologous recombination (HR) repair pathways (Dronkert and Kanaar 2001). The protein heterodimer Ercc1 (excision repair cross complementing 1)-Xpf (xeroderma pigmentosum f) is thought to provide a critical activity in both NER and ISC repair. To this end, the Ercc1 protein in particular has become a target for modulation in tumor cells in an attempt to help make the bifunctional alkylating and platinating agents more effective in cancer treatment.

1.1 Bifunctional alkylating/platinating agents (ISC-forming agents)

Bifunctional alkylating agents such as MMC and CP and the platinating agents such as cisplatin and carboplatin are effective in the treatment of many tumors. These agents are capable of affecting cells at any stage of the cell cycle, although cytotoxicity is markedly enhanced in rapidly proliferating tissues where there is disruption of DNA synthesis and cell division (Chabner et al. 1996). The cytotoxic effects of these agents have been directly related to the alkylation of DNA, which results in chemically stable DNA lesions such as monoadducts, intrastrand cross-links and ISCs that require an efficient, but not necessarily an error-free, mechanism of repair (Chabner et al. 1996). The proposed critical lesions that dictate the effectiveness of a particular agent are the DNA ISCs (Dronkert and Kanaar 2001). Experiments have demonstrated a correlation between cytotoxicity and the formation of ISCs by bifunctional alkylating agents (Colvin 2000). However, DNA damage is influenced by a number of cellular factors that can limit the lesions produced, and DNA adducts are not always produced randomly throughout the genome, because chromatin structure can influence adduct formation (Dronkert and Kanaar 2001). ISCs represent a small percentage of the total adducts formed by cisplatin, CP and MMC (see Table 1-1), and ISCs produced by these agents have been examined in some detail in order to determine how they affect a cell.

The 3-D structure of an ISC differs with the ISC-inducing agent and could influence the efficiency of ISC recognition and repair (Dronkert and Kanaar 2001).

Table 1-1. Properties of some ISC-inducing agents (adapted from Dronkert and Kanaar 2001).

ISC-inducing Agent	DNA sequence of major ISCs	Percentage ISCs[a]	DNA distortion[b]
Mitomycin C	5' - CG - 3' / 3' - GC - 5'	5-13	Minor
Cisplatin	5' - GC - 3' \ 3' - CG - 5'	5-8	Major
Cyclophosphamide	5' - GNC - 3' \ 3' - CNG - 5'	1-5	Major

[a]Percentage of total DNA adducts formed by the ISC-inducing agent *in vitro*.
[b]Distortion of the DNA double helix by the ISC. Potential DNA distortions include kinks, bends, and unwinding of DNA strands.

The acquisition of resistance to an alkylating or platinating agent by tumor cells is a common event, and often resistance acquired to such agents can result in cross-resistance to other chemotherapeutic agents (Chabner et al. 1996). Cellular resistance mechanisms are critical determinants of the effectiveness of anticancer therapy, and include decreased uptake or increased efflux of the drug, increased intracellular inactivation of the drug, enhanced repair of DNA damage, and absence of cellular factors that would otherwise generate a cytotoxic response to DNA damage (Chabner et al. 1996, Colvin 2000). However, when assessing the role of DNA repair in drug resistance it is important to consider that (1) increased phenotypic repair of DNA adducts does not necessarily indicate which repair pathway is involved; (2) *in vitro* studies can demonstrate that a particular repair pathway(s) is

important for the removal of a particular type of adduct, but this does not necessarily indicate that the repair pathway(s) is actually increased in a particular drug-resistant cell line; and (3) increased levels of an individual repair enzyme in resistant cell lines does not automatically prove that the activity of a multi-enzyme repair pathway is enhanced (Chaney and Sancar 1996).

1.1.1 Cisplatin

Cisplatin is a platinum coordination complex (see Figure 1-2) that appears to enter cells by diffusion and can produce DNA lesions by reacting predominantly with N-7 of guanines (Chabner et al. 1996, Colvin 2000, Siddik 2002). The DNA adducts formed cause a major distortion of the DNA helix, with the majority of these lesions being intrastrand cross-links and a small percentage of the total adducts being ISCs (Dronkert and Kanaar 2001). The level of cisplatin-DNA adducts correlates well with cytotoxicity, and although there is considerable evidence that these DNA adducts are cytotoxic, the mechanism by which the cytotoxic effect is mediated has not been conclusively associated with a single type of adduct (Chabner et al. 1996, Colvin 2000, de Silva 2002). As with cytotoxicity, the mechanisms of drug resistance are unknown even though a number of factors have been shown to influence cellular sensitivity to cisplatin. Factors determined to affect cisplatin sensitivity are decreased uptake/increased efflux, increased inactivation by glutathione (GSH) or metallothionein, increased DNA repair activity, and loss of proteins that can recognize cisplatin-DNA adducts, such as the MMR protein hMSH2 and the high mobility group (HMG) proteins (Chabner et al. 1996, Fink et al 1998, Gamcsik et al. 1999, Colvin 2000, Niedner et al. 2001).

1.1.2 Mitomycin C (MMC)

MMC is a natural antitumor antibiotic (see Figure 1-2) that requires either intracellular or spontaneous chemical reduction for activation (Chabner et al. 1996, Dronkert and Kanaar 2001). Activated MMC reacts preferentially with N-2 of guanines specifically in d(CpG)

sequences (Rink et al. 1996, Dronkert and Kanaar 2001). Li et al. (2000b) found that methylation of cytosine in CpG sites greatly enhances MMC adduct formation, and these authors propose that methylation of genomic DNA may determine MMC sensitivity, which in turn may play a crucial role in the antitumor activities of the drug. Of the total adducts formed by MMC, 5-13% are ISCs which cause little distortion of the DNA helix (Dronkert and Kanaar 2001). Palom et al. (2002) were able to show that ISCs are probably the critical lesions resulting in cytotoxicity with MMC.

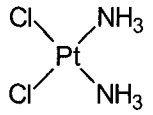

Cisplatin

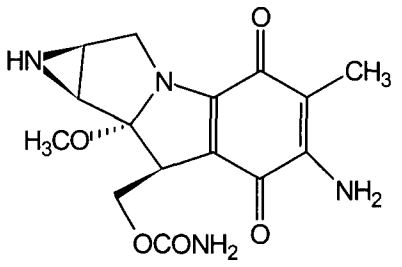

Mitomycin C
(MMC)

Figure 1-2. Chemical structures for the bifunctional alkylating agent MMC and the platinating agent cisplatin.

1.1.3 Cyclophosphamide (CP)

CP is a nitrogen mustard derivative (see Figure 1-3) that is activated by cytochrome P450-mediated microsomal oxidation in the liver to form predominantly the 4-hydroxycyclophosphamide (4HOCP) metabolite. 4HOCP is relatively non-polar at physiologic pH, allowing it to diffuse into the blood and be transported to sites of action (Colvin 2000). Upon entry into a cell, 4HOCP can produce the primary cytotoxic agent phosphoramide mustard (PM) through spontaneous decomposition of the aldophosphamide intermediate (see Figure 1-3) (Chabner et al. 1996, Gamcsik et al. 1999, Ludeman 1999, Colvin 2000). PM is highly

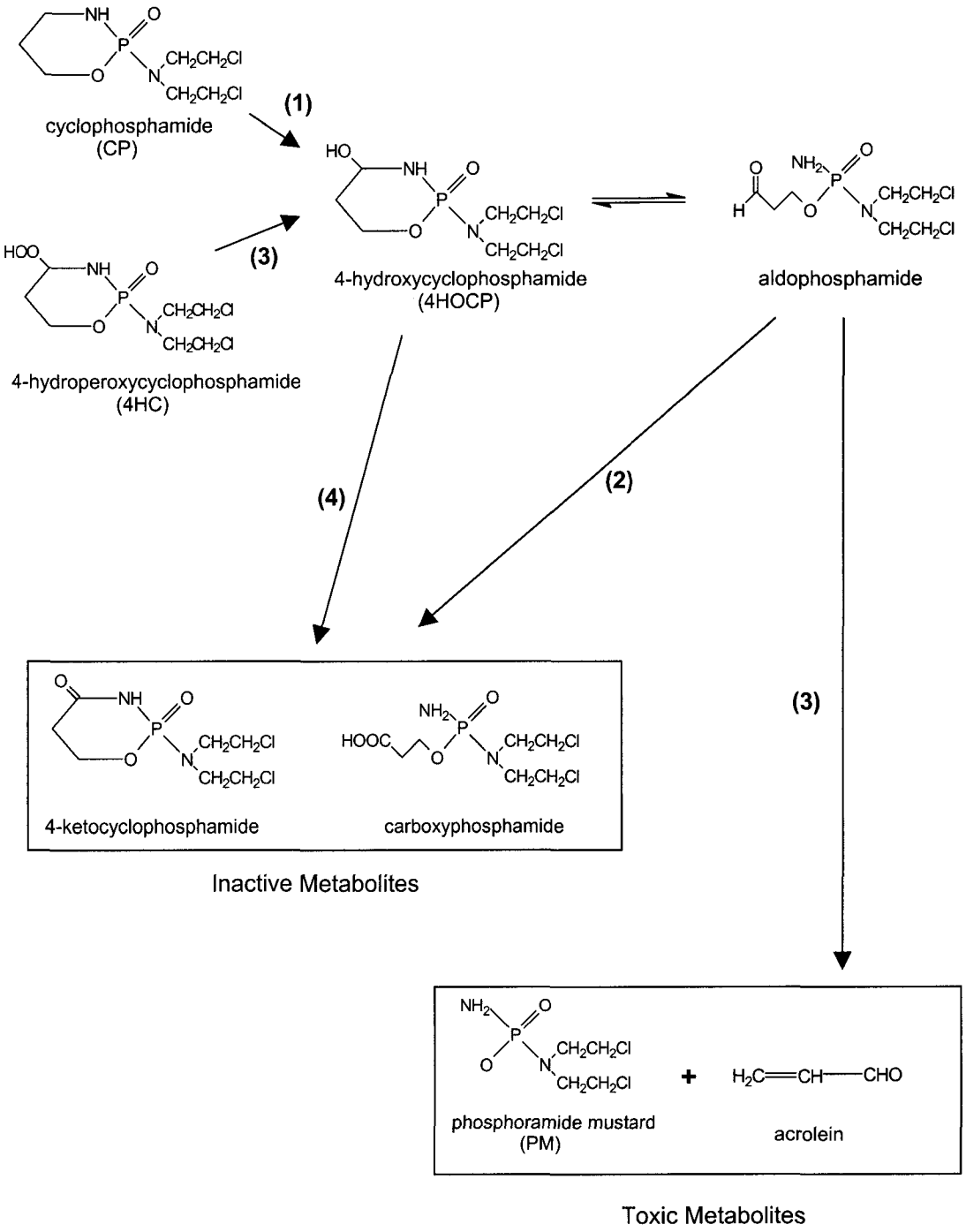

Figure 1-3. Cyclophosphamide metabolism. (1) hepatic cytochrome P450 system, (2) aldehyde dehydrogenase, (3) nonenzymatic, (4) enzymatic (Reproduced from Chabner et al. 1996).

reactive, being able to form DNA adducts with the N-7 atom of guanine, thereby generating lesions such as guanine monoadducts, intrastrand cross-links, as well as ISCs in the sequence d(GpNpC) that cause major distortion of the DNA helix (Chabner et al. 1996, Dronkert and Kanaar 2001). Cellular resistance to CP is likely the result of a combination of interrelated factors (Gamcsik et al. 1999). The more common mechanisms of CP resistance are the interaction of CP metabolites with either the aldehyde dehydrogenases (ALDHs) or GSH, the latter reaction either occurring spontaneously or catalyzed by the glutathione-S-transferases (Gamcsik et al. 1999). In addition, increased efflux of the GSH-CP conjugates via the multiple drug resistance (MDR) system may enhance the rate of detoxification and lead to drug resistance (Gamcsik et al. 1999).

For the purpose of experimental studies, the production of DNA adducts by CP *in vitro,* without the use of P450-mediated activation, can be achieved by using 4-hydroperoxycyclophosphamide (4HC). 4HC spontaneously converts to 4HOCP in solution, which then generates the other active metabolites of CP through non-enzymatic conversions (see Figure 1-3, Flowers et al. 2000). Although 4HC is useful in experimental studies as a model for clinical CP, generation of the PM metabolite is accompanied by the generation of the additional metabolites aldophosphamide and acrolein, with the relative proportions being dependent on pH (see Figure 1-3, Ludeman 1999). Aldophosphamide not only generates PM and acrolein, but ALDH can also convert aldophosphamide to the inactive metabolite carboxyphosphamide; thus, an increase in this enzyme will decrease the amount of PM being produced (see Figure 1-3). The acrolein metabolite can also produce DNA adducts that may contribute to CP cytotoxicity and mutagenesis, and these adducts can be repaired by O^6-alkylguanine-DNA alkyltransferase (AGT) (Ludeman 1999). The use of PM to treat cells *in vitro* avoids the production of unwanted metabolites that may interfere with drug sensitivity or even action. However, PM also has inherent problems as an experimental reagent. PM is very polar at pH 7.4, so it has poor membrane permeability and it is very unstable, having a half-life of ~18 min at 37°C (Ludeman 1999, Colvin 2000). When PM is used in experimental

studies it is a considerably less potent inducer of ISCs and cytotoxicity than is 4HC at equimolar concentrations (Ludeman 1999). PM has also been found to be 50-100 times less effective at producing ISCs on a per mole basis than mechlorethamine (nitrogen mustard) or melphalan (Bauer and Povirk 1997). Reactions of PM with either GSH or metallothionein have been observed, and they represent an important mechanism of detoxification that may contribute to acquired drug resistance (Ludeman 1999, Wei et al. 1999).

1.2 The nucleotide excision repair pathway

The ability of human cells to defend themselves against various forms of DNA damage requires an efficient mechanism to deal with these lesions. DNA damage can derive from a variety of sources, including intracellular/endogenous sources (such as free radicals, incorrect nucleotide incorporation, spontaneous hydrolysis or chemical alterations) and extracellular/exogenous sources (such as ionizing radiation, ultraviolet (UV) light and electrophilic chemicals) (Dronkert and Kanaar 2001, Friedberg 2001). Damage to a DNA base may result in a signal cascade that ultimately leads to various cellular responses in eukaryotic cells, such as activation of cell-cycle checkpoint pathways, transcriptional activation of specific genes, apoptosis, damage tolerance, or DNA repair (Friedberg 2001). Several DNA repair pathways exist in human cells that specifically repair a wide variety of DNA lesions (Friedberg 2001). Of particular interest is the NER pathway, which is the most versatile of the repair pathways and is capable of repairing large, bulky DNA lesions induced by a wide variety of agents. It is capable of recognizing and repairing many types of base damage that often have little, if any, structural or chemical similarity; however, the pathway is restricted to substrate DNA adducts that significantly distort the DNA helix (Wood 1999, Friedberg 2001). In mammalian cells, the process of NER apparently proceeds in two distinct steps requiring the sequential operation of multiprotein complexes (Friedberg 2001). The first step involves damage recognition and excision of the lesion, and the second step involves

repair synthesis followed by DNA ligation in order to restore DNA integrity (see Figure 1-4, Friedberg 2001).

Damage recognition in NER is an intricate process that utilizes one of two sub-pathways, depending on the transcriptional activity of the damaged sequence. Transcription coupled repair (TCR) operates preferentially on transcriptionally active DNA and involves the detection of arrested RNA polymerase II transcription machinery, whereas global genome repair (GGR) operates on the transcriptionally inactive regions of the genome and involves the recognition of DNA damage by Xpc (xeroderma pigmentosum c)-hRad23B (human homolog of rad23B) (Friedberg 2001, Hanawalt 2001a). Although there appears to be two subpathways involved in NER, they do converge at the point where Xpa (xeroderma pigmentosum a) and Rpa (replication protein a) are believed to facilitate specific recognition of base damage (Friedberg 2001). Upon binding of these proteins, sequential assembly of the excision complex commences. The TFIIH (transcription factor IIH) complex contains two helicases, Xpb (xeroderma pigmentosum b) and Xpd (xeroderma pigmentosum d), that promote unwinding of the DNA duplex around the site of base damage, generating a bubble structure (Friedberg 2001). The heterodimer complex Ercc1-Xpf is a 5′ endonuclease and Xpg (xeroderma pigmentosum g) is a 3′ endonuclease that bind to the assembled complex and together perform bimodal excision of the DNA strand containing the lesion, generating an oligonucleotide fragment ~27-30 nucleotides long (Friedberg 2001). Once the lesion has been excised, repair synthesis-DNA ligation via DNA polymerase δ/ε, Pcna (proliferating-cell nuclear antigen), Rpa, Rfc (replication factor c), and ligase I restores the covalent integrity of the DNA strand using the opposite, undamaged DNA strand as a template (Friedberg 2001).

The NER pathway has been well defined in mammalian cells using a series of NER-deficient rodent and human cell lines which have defects in various proteins involved in NER. Numerous Chinese hamster ovary (CHO) mutant cell lines were obtained by extensive mutagenesis followed by selection for sensitivity to UV light, and these cells have provided

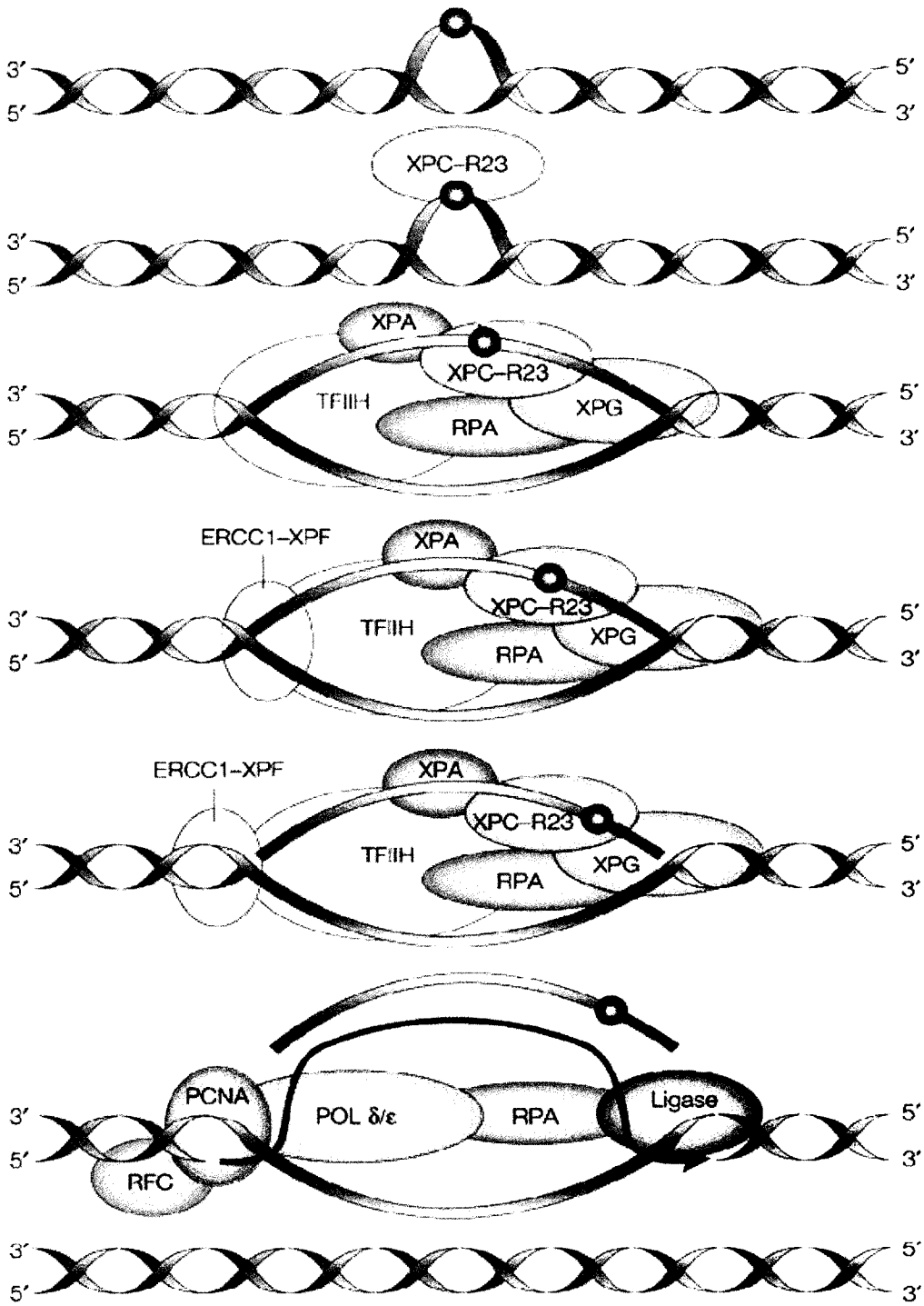

Figure 1-4. The essential features of nucleotide excision repair. (Reproduced from Friedberg 2001).

valuable insight into the process of NER. However, differences between rodent and human cells often make it difficult to extend the knowledge gained from observing rodent cells to human cells. Of particular interest is the "rodent paradox", reported by Hanawalt (2001b). Hanawalt noted that cultured normal rodent and human cells typically display similar sensitivities in the clonogenic survival assay following exposure to UV light, even though cultured rodent cells are generally deficient in excision repair of UV-induced cyclobutane pyrimidine dimers (CPDs) whereas cultured human cells are proficient in repairing these lesions. This relative inability of cultured rodent cells to repair CPD damage appears to be the result of a deficient p53-dependent mechanism that activates GGR (Hanawalt 2001b). The lack of GGR does not dramatically affect clonogenic survival because rodent cells have proficient TCR, such that they are not hypersensitive; however, it does pose a problem to investigators when comparing the repair of specific DNA lesions between rodent and human cell free extracts (Hanawalt 2001b). Thus, it becomes important to study the NER pathway in a human background, especially in studies where the information will be applied to clinical questions.

The process of NER in human cells is understood mostly from work with NER-deficient human cell lines derived from patients with the hereditary disease xeroderma pigmentosum (XP). XP is characterized by defective DNA repair and a markedly increased risk of skin cancer that is associated with exposure to UV light (Friedberg 2001). There are seven known complementation groups of XP, which are denoted XPA through XPG, as well as the XP variant (XPV). Further understanding of the TCR sub-pathway of NER has come from studies of the human hereditary disease Cockayne's Syndrome (CS). Humans with mutations in either the *CSA* or *CSB* genes exhibit this syndrome, which manifests with neuroskeletal abnormalities but no predisposition to sunlight-induced skin cancer (Chaney and Sancar 1996). The molecular mechanism of TCR is not known, although it appears that only genes transcribed by RNA polymerase II and only lesions that block the progression of this enzyme are subject to this process (Chaney and Sancar 1996, Friedberg 2001).

1.3 Interstrand cross-link (ISC) repair

Although NER can effectively repair a broad spectrum of bulky DNA lesions such as monoadducts and intrastrand cross-links, repair of ISCs is more complex. ISCs represent a small fraction of the total adducts formed by a given alkylating/platinating agent, and the main determinant of cytotoxicity is thought to be through their inhibition of DNA strand separation, thus directly influencing DNA replication, transcription and segregation (Dronkert and Kanaar 2001). It is also possible that ISCs could be recognized by a detector system that in turn activates signaling pathways resulting in apoptosis (Fink et al. 1998). Much of the knowledge about ISC repair in mammalian cells has been derived from either mammalian (mostly hamster) or yeast mutant cell lines (Dronkert and Kanaar 2001). Although there is a high degree of conservation between the two species, there are also important differences between yeast and mammalian ISC repair, possibly reflecting the importance of specific pathways required to repair ISCs, as well as the number of proteins involved (Dronkert and Kanaar 2001). From studies with mutant cell lines, the repair of ISCs appears to involve two types of mechanisms – error-free and error-prone – that involve proteins from pathways such as NER, HR, and replicative/translesion bypass (Chaney and Sancar 1996, Dronkert and Kanaar 2001). In mammalian cells, the recombination-dependent mechanism appears to be the predominant pathway for ISC repair and involves proteins from both NER and HR (Wang et al. 2001).

In order for a cell to elicit an effective response to an ISC, it needs to be able to recognize these lesions. However, the 3-D structures of ISCs can differ, and this may influence the efficiency of recognition and subsequent repair (Dronkert and Kanaar 2001). Nuclear protein complexes in human and rodent cell lines were found that could recognize and bind with high affinity to site-specific MMC-DNA ISCs that were generated by reaction of the drug with an oligonucleotide (Warren et al. 1998). The Ercc1 protein was identified as being part of the nuclear protein complexes isolated, implicating Ercc1 and its partner Xpf as having a role in ISC repair (Warren et al. 1998). Further evidence that the Ercc1-Xpf

heterodimer is involved in ISC repair is the extreme sensitivity of CHO cell lines such as UV20 (*ERCC1*$^{-}$) and UV41 (*XPF*$^{-}$) to ISC-inducing agents such as MMC and CP analogs (Busch et al. 1980, Thompson et al. 1980, 1982, Hoy et al. 1985, Sorenson and Eastman 1988, Andersson et al. 1996, Damia et al. 1996). The *ERCC1*$^{-}$ and *XPF*$^{-}$ rodent mutants were also found to be defective in the incision and "unhooking" step of ISC repair *in vitro* (de Silva et al. 2000). Other important ISC repair genes identified to date are *XRCC2* and *XRCC3* (homologs of *RAD51*), where a mutation in either gene results in hypersensitivity to ISC-inducing agents; these proteins are presumed to catalyze recombination (Gamcsik et al. 1999, Thompson and Schild 2001). Aside from the requirement for Ercc1-Xpf, Xrcc2 and Xrcc3, there is little information on which other components of the mammalian homology-driven recombination apparatus act to repair ISCs (McHugh et al. 2001, Legerski and Richie 2002).

A proposed model for ISC repair in dividing mammalian cells, based on observations with site-specific ISCs, is shown in Figure 1-5 (Kuraoka et al. 2000, de Silva et al. 2000, McHugh et al. 2001). In dividing cells, the ISC inhibits the progression of the replication fork and somehow generates a DSB (Kuraoka et al. 2000, de Silva et al. 2000). The result is DNA unpaired on the 3′ side providing a substrate for Xpf-Ercc1 (in conjunction with Rpa) to make incisions flanking the ISC, or digestion of the DNA past the crosslink via the Ercc1-Xpf 3′-to-5′ exonucleolytic activity (Mu et al. 2000, Kuraoka et al. 2000, de Silva et al. 2000, McHugh et al. 2001). After gap resection, Xrcc2 and Xrcc3 mediate recombination events where the invading strand is used as the template to fill the gap by repair synthesis (Kuraoka et al. 2000, de Silva et al. 2000, McHugh et al. 2001). The DNA that was replaced by repair synthesis can then be used in a second excision-resynthesis event in which the ISC-adduct is eliminated (Kuraoka et al. 2000, de Silva et al. 2000, McHugh et al. 2001).

Aside from the requirement of the HR pathway for repairing ISC-adducts, other pathways that play a minor role in the repair of ISCs have also been identified in mammalian cells. The process of post-replication repair represents an error-prone method of bypassing

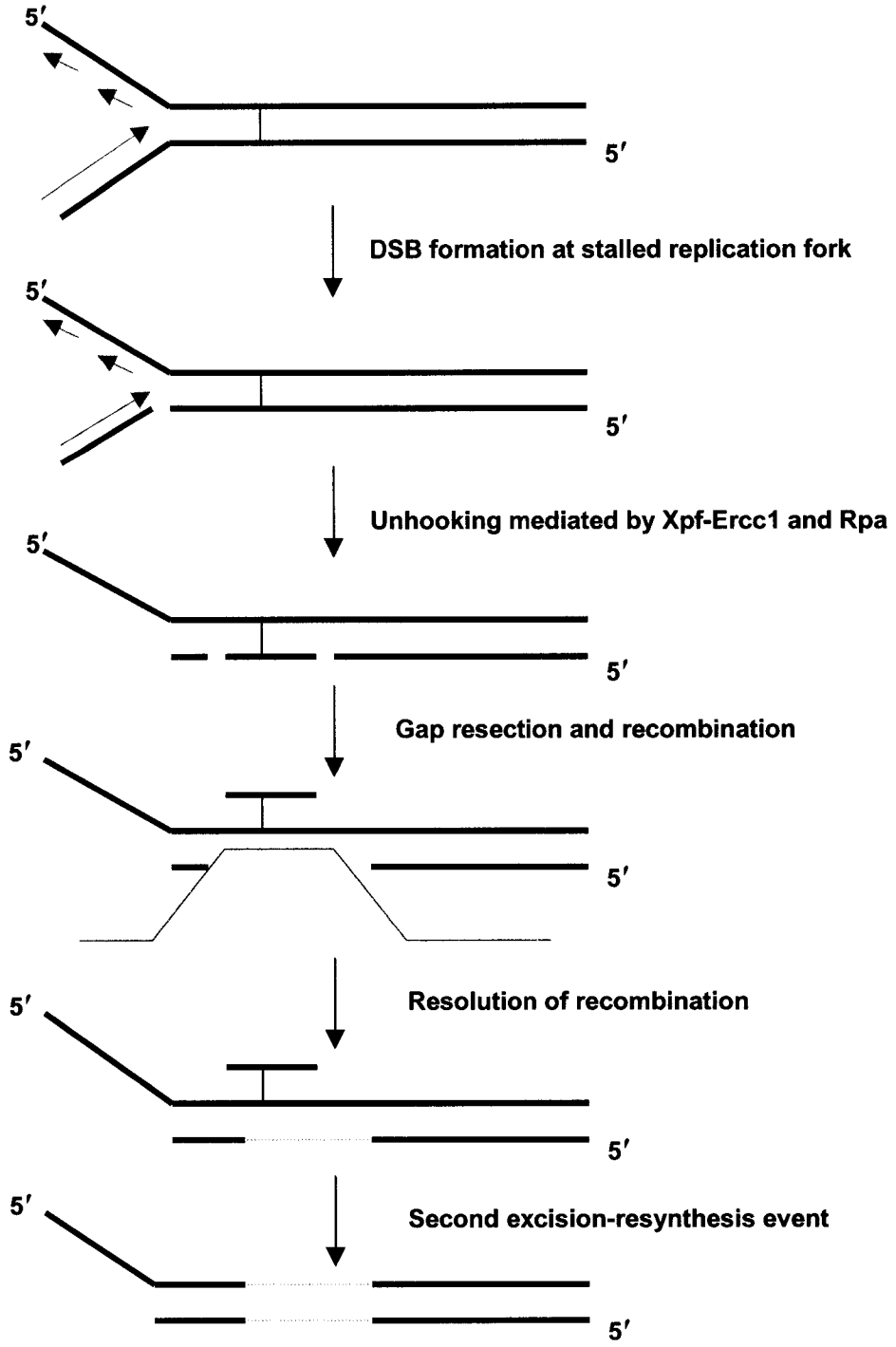

Figure 1-5. Proposed model for the repair of an ISC in dividing mammalian cells (Reproduced from McHugh et al. 2001). Green represents replication, red represents recombination, and blue represents repair synthesis.

the damaged DNA. Mechanisms of post-replication repair suggested by Chaney and Sancar (1996) are replicative/translesion bypass, activation of alternate origins of replication near a site of damage, and template switching, where the DNA polymerase could use the complementary daughter strand as a template instead of the damaged parental strand. Evidence that a DNA polymerase can replicate past a psoralen ISC has been demonstrated (Masutani et al. 2000). Many of the studies involving translesion bypass involve the use of psoralen + UV; however, Zheng et al. (2003) demonstrated translesion bypass by DNA pol η (POLH) using a site-specific MMC ISC. Repair of the MMC ISC also involved TCR, requiring all five NER factors involved in the incision step (Xpc-hRad23B, Xpa, TFIIH (Xpb and Xpd), Ercc1-Xpf, and Xpg). The result is a recombination-independent and pro-mutagenic mechanism for ISC repair (Zheng et al. 2003).

1.4 *ERCC1* (Excision Repair Cross Complementing 1)

The designation of ERCC (excision repair cross complementing) refers to the correction of an NER mutant phenotype in CHO cells with human DNA. The cross complementation of NER proteins between human and CHO cells enabled the cloning of the genes involved in NER such as *ERCC1* (Friedberg et al. 1995). The human *ERCC1* gene was cloned and sequenced by van Duin et al. (1986, 1987) and mapped to chromosome 19q13.2-13.3 (Brook et al. 1985). It consists of 10 exons spanning ~15 kb (see Figure 1-6A). A strong conservation of the *ERCC1* gene has been noted in various eukaryotes such as *Drosophila*, mammals, reptiles, birds and fish, with human *ERCC1* having significant homology with yeast *RAD10*, mouse *ERCC1* and *E. coli UvrA* and *UvrC* (van Duin et al. 1986, 1987, 1988). The promoter region of the human *ERCC1* gene was examined by van Duin and colleagues (van Duin et al. 1987) and shown not to contain "classical" promoter elements, although several other sequence motifs of unknown significance were identified. However, the sequence examined for promoter elements by these authors only encompassed ~0.5 kb upstream of exon 1. Examination of the region 5 kb upstream of

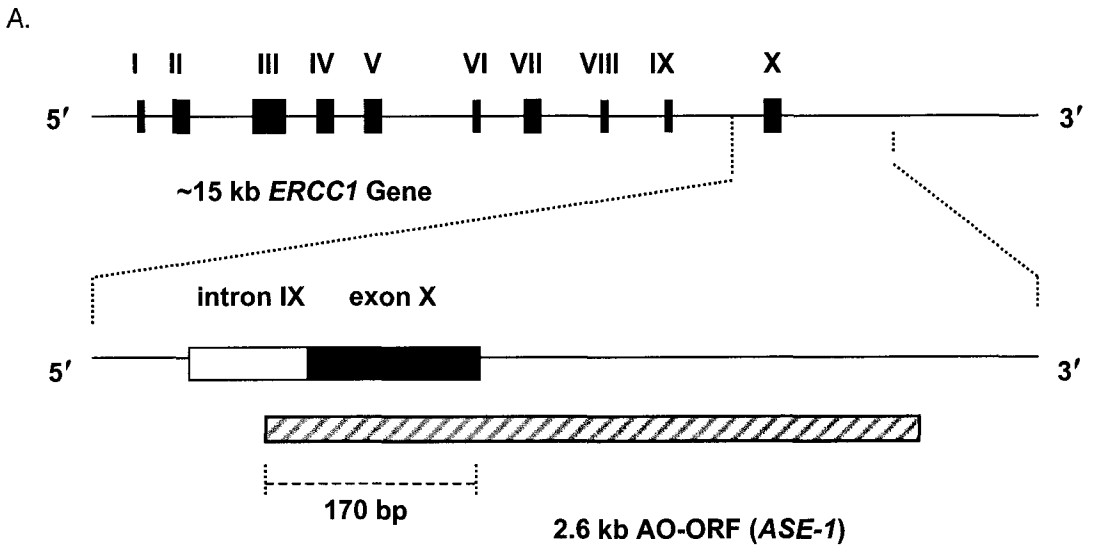

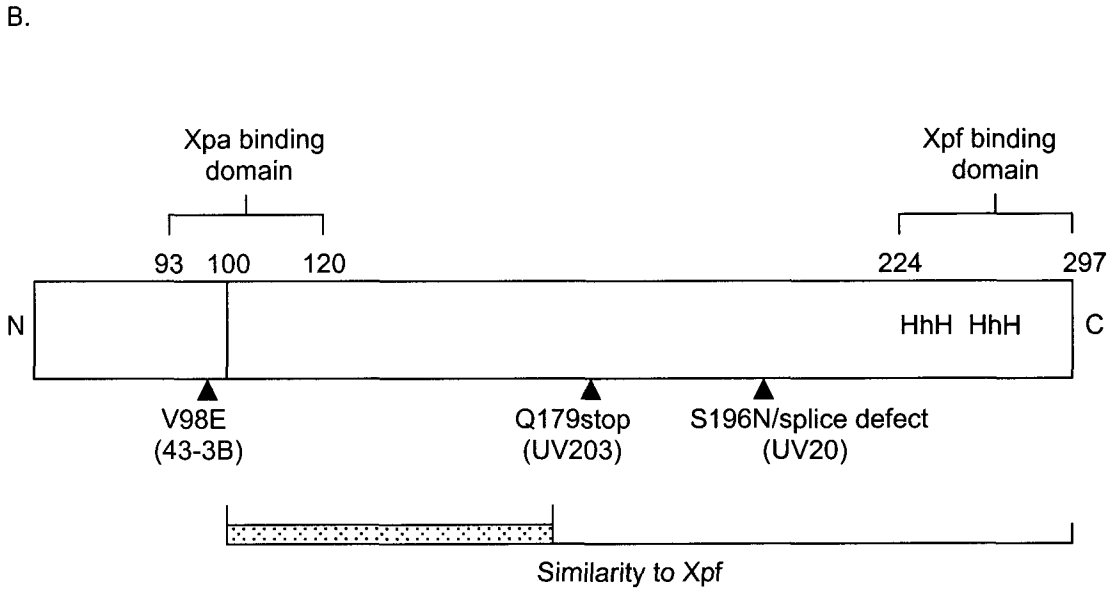

Figure 1-6. Schematic representations of the *ERCC1* gene and Ercc1 protein. (A) *ERCC1* gene organization of 10 exons (black boxes) and antisense overlapping-open reading frame (AO-ORF) identified as *ASE-1* that overlaps ~170 bp of *ERCC1* gene at the 3′ end (striped bar) (van Duin et al. 1986, Belt et al. 1991, Whitehead et al. 1997). (B) Ercc1 protein binding domains (stippled bar represents the highly conserved region between Ercc1 and Xpf) and identified mutations in rodent cell lines (▲). (Reproduced in part from van Duin et al. 1988, Li et al. 1994, Sijbers et al. 1996a, de Laat et al. 1998, and Gaillard and Wood 2001). HhH – Helix-hairpin-Helix motif.

exon 1 revealed a CpG island that contained "classical" promoter elements such as a TATA box, as well as classical regulatory elements (Zhong et al. 2000, Wilson et al. 2001). The co-localization of the CpG island and promoter region would suggest a possible role in gene regulation (Wilson et al. 2001).

The *ERCC1* gene directs the synthesis of low levels of transcripts that can be differentially polyadenylated, resulting in several transcripts being detected by Northern blotting with sizes of 3.8 kb, 3.4 kb and 1.1 kb (van Duin et al. 1986, 1987, 1989b). An additional *ERCC1* transcript was isolated that lacked exon VIII (–72 bp) and was determined to be a splice variant of the full length *ERCC1* mRNA (van Duin et al. 1986, 1987). Transfection studies indicated the 1.1 kb *ERCC1* mRNA to be biologically significant and to be translated into a 297-amino acid protein with a calculated molecular weight of 32,562 Da (van Duin et al. 1986). Although the alternatively spliced *ERCC1* transcript, lacking exon VIII, was unable to correct the *ERCC1*-deficency in CHO 43-3B cells, it is still capable of encoding a protein of 29,992 Da (van Duin et al. 1986, Yu et al. 1998).

Mutational analysis of the human Ercc1 protein has determined the Xpa binding domain to be located at amino acids 93-120 and the Xpf binding domain to be at amino acids 224-297 (see Figure 1-6B; Li et al. 1994, de Laat et al. 1998, Gaillard and Wood 2001). Ercc1 was found to contain a region of similarity to Xpf that includes two areas of the C-teminal domain located between amino acids 100-297 (see Figure 1-6B; Gaillard and Wood 2001). The first region of similarity is located between amino acids 100-174 and is the most conserved, and the second region of similarity is near the C-terminal end which is predicted to have 2 helix-hairpin-helix motifs (see Figure 1-6B; Gaillard and Wood 2001). The use of mutational analysis has also established the minimum size of the Ercc1 protein required to correct the MMC- and UV-sensitive phenotype in an *ERCC1*-deficient rodent cell line (43-3B) (Sijbers et al. 1996a). An N-terminal deletion of 91 amino acids can still provide NER function; however, an N-terminal deletion of 102 amino acids results in a loss of NER function (Sijbers et al. 1996a). A C-terminal deletion of more than 4 amino acids also

resulted in a loss of NER function even though a stable Ercc1 protein was produced (Sijbers et al. 1996a). A deletion of 7 amino acids from the C-terminal end resulted in both loss of NER function and a loss of protein expression (Sijbers et al. 1996a). The C-terminus of Ercc1 contains the Xpf binding domain (see Figure 1-6B) and the subsequent loss of both Ercc1 protein expression and NER function directly links Ercc1-Xpf complex formation ability with repair capability (van Duin et al. 1988, Sijbers et al 1996a, de Laat et al. 1998).

Most missense mutations introduced in the central area of the Ercc1 protein, which has homology to Rad10 (amino acids 93-120), reduces the amounts of detectable Ercc1 protein and results in incomplete complementation of the 43-4B (*ERCC1*$^{-}$) repair defect (Sijbers et al. 1996a).

The Ercc1 protein binds tightly to the Xpf protein to form a heterodimeric complex that is primarily found in the nucleus (van Vuuren et al. 1993, de Laat et al. 1998, Houtsmuller et al. 1999). The Ercc1-Xpf complex has structure-specific endonuclease activity, making an incision on the 5′-side of a DNA lesion in the NER pathway (Sijbers et al. 1996b). The activity of the Ercc1-Xpf heterodimer has been demonstrated to cleave model stem loops and bubble structures on the 5′ side near the borders between the double-stranded and single-stranded DNA regions, and is Rpa-dependent (Matsunaga at al. 1996 , Sijbers et al. 1996b, Bessho et al. 1997). The stability of both the Ercc1 and the Xpf proteins appears to depend on their tight association with each other. This is supported by the finding that exogenous excess Ercc1 protein is quickly degraded within 1 h, and that only a moderate increase in Ercc1 protein levels (~3-4 fold) can be achieved by the continuous over-expression of the *ERCC1* gene (100-1000 fold) in mammalian cells (van Vuuren et al. 1993, Sijbers et al. 1996a). Over-expression of the Ercc1 protein also did not result in elevated MMC resistance, suggesting that Ercc1 protein levels should be carefully determined before conclusions can be drawn with respect to its involvement in drug resistance (van Vuuren et al. 1993). Interestingly, simultaneously over-expressing the *ERCC1* and *XPF* genes from separate

vectors within a cell did significantly increase resistance to MMC (Dr. L. H. Thompson, personal communication to David Murray).

1.4.1 *ERCC1* antisense overlapping-open reading frame (AO-ORF)

The use of a genomic *ERCC1* probe led to the detection of a 2.6 kb mRNA that did not encode an Ercc1 protein (van Duin et al. 1989a). The transcript was found to overlap ~170 bp in the 3′ region of the *ERCC1* gene in the antisense direction (*ASE-1*), encompassing exon X and terminating in intron IX (see Figure 1-6A; van Duin et al. 1989a). Similar overlapping antisense transcription units have also been found in the 3′ regions of the yeast *RAD10* gene (*ASR10*) and the mouse *ERCC1* gene (van Duin et al. 1989a). This phenomenon of overlapping antisense gene organization is not unusual and has also been observed in other higher eukaryotes such as *Drosophila* (Henikoff et al. 1986, Nepveu and Marcu 1986, Spencer et al. 1986, Williams and Fried 1986, Adelman et al. 1987, Chen et al. 1987, Merino et al. 1994). The *ASE-1* gene encodes a protein that has been shown to have a biologically important role as a novel nucleolar factor, and does not appear to have a connection in function to the Ercc1 protein (Whitehead et al. 1997). It is not known, however, whether the *ERCC1* and *ASE-1* mRNAs can bind to each other to inhibit either *ERCC1* or *ASE-1* translation or if association of the two mRNAs could possibly mediate their transport to a common location in the cytoplasm and perhaps protect against degradation (van Duin et al. 1989a, Whitehead et al. 1997).

1.4.2 Clinical relevance of *ERCC1*

Clinical studies have correlated high tumor cell levels of *ERCC1* mRNA expression with an increase in drug resistance (Dabholkar et al. 1992, Metzger et al. 1998, Li et al. 1998, Li et al. 2000a, Shirota et al. 2001, Lord et al. 2002, Murray 2002). The increased levels of *ERCC1* mRNA expression could be mediated through such mechanisms as polymorphisms, changes in gene copy number, transcriptional regulation and altered mRNA stability.

Polymorphisms, or genetic variation, can result in an amino acid substitution that could impact mRNA stability or protein synthesis through the generation of rare and/or under-utilized codons or by altering protein function (Shen et al. 1998, Chen et al. 2000, Goode et al. 2002). Polymorphisms within the *ERCC1* gene represent a possible mechanism that can effect an increase or decrease in DNA repair capacity by altering the rate of *ERCC1* mRNA transcription, Ercc1 protein translation, or Ercc1 protein function (Dabholkar et al. 1993, Yu et al. 1997, 2000b, Shen et al. 1998, Goode et al. 2002). Shen et al. (1998) identified 7 single-nucleotide polymorphisms in the *ERCC1* gene, but none of these resulted in an amino acid substitution, and no amino acid substitutions in known regulatory elements were identified. Other reports, however, have shown a significant association of an *ERCC1* polymorphism with either an increased risk of brain tumors or cisplatin resistance in a human ovarian carcinoma cell line (Yu et al. 1997, 2000b, Chen et al. 2000). In the studies by Yu and colleagues (Yu et al. 1997, 2000b), the *ERCC1* polymorphism was associated with an ~50% reduction in codon usage that could affect transcription rate and/or translation rate.

An increase in gene copy number is another means of increasing *ERCC1* mRNA expression. Clinical analysis of the *ERCC1* gene in human gliomas and normal cells by Liang et al. (1995) revealed that abnormalities in the copy number of the *ERCC1* gene is common in glial tumors, although a direct relationship between copy number and clinical outcome with chemotherapy was not observed. Alteration in *ERCC1* gene copy number, however, is not a common event in human ovarian cancer or in normal cells (from cancer patients) with either a high or low *ERCC1* mRNA expression, which suggests that other mechanisms must be invoked to explain these differences in *ERCC1* mRNA levels (Dabholkar et al. 1993, Yu et al. 2000a).

Transcriptional regulation of the *ERCC1* gene, mediated by a signal transduction pathway, is another likely candidate for an increase in *ERCC1* mRNA transcripts. Identification of an AP-1-like site in the promoter region of the *ERCC1* gene and the identification of AP-1 sites in other NER genes would suggest that signal transduction

pathways that modulate AP-1 may be important in the regulation of DNA repair (Li et al. 1999a, Li et al. 1999b, Zhong et al. 2000). This likelihood is supported by an increase seen in both *c-FOS* and *c-JUN* mRNA levels upon exposure to cisplatin in human ovarian cancer cells preceding the *ERCC1* mRNA increase, suggesting AP-1 is involved in transcriptional modulation of *ERCC1* gene expression (Li et al. 1998). The involvement of either the Junk/Sapk or Erk signal transduction pathways have been implicated in influencing AP-1 activity, and thus *ERCC1* mRNA expression (Yu et al. 2000b, Yacoub et al. 2003). An increase in *ERCC1* mRNA expression by activating the Ras-Erk-dependent pathway has been demonstrated following the activation of the human insulin receptor by insulin or over-expression of the human insulin receptor in CHO cells (Lee-Kwon et al. 1998, Perfetti et al. 1997). However, no significant correlation was observed between the insulin-mediated expression of *ERCC1* mRNA and UV resistance (Perfetti et al. 1997). A possible explanation is that controls operating at the transcriptional and post-transcriptional levels (such as mRNA stability) might participate in both the basal and insulin-induced increase of *ERCC1* mRNA (Perfetti et al. 1997). An increase in *ERCC1* mRNA stability has been identified in human ovarian cancer cells upon exposure to cisplatin, reflecting a possible role in drug resistance (Li et al. 1998).

A noteworthy finding was the identification of AP-1 as a common activator for all of the NER genes assessed, indicating that AP-1 is an important transcriptional activator for the NER pathway (Zhong et al. 2000). This may best be demonstrated by experimental studies that examined the order of activation of the expression of NER genes following exposure to a drug such as cisplatin (Dabholkar et al. 1993, Cheng et al. 1999, Reed et al. 2000). In human ovarian cancer cells there appears to be a defined order to NER gene activation, with *ERCC1* possibly leading the cascade (Reed et al. 2000). However, these researchers caution that the order of mRNA expression of NER genes may not mimic the order of protein activities within the cell. Coordinate expression of NER genes is thought to be optimal in the normal situation, and coordinate expression may be disrupted as a tumor moves from low

grade to high malignancy (Zhong et al. 2000). Normal individuals with low levels of expression of DNA repair genes may have low DNA repair capacity, which may result in the accumulation of genetic alterations involved in carcinogenesis (Cheng et al. 1999).

Studies that have shown a correlation between *ERCC1* mRNA levels and resistance to alkylating agents have usually measured total *ERCC1* mRNA levels and did not measure Ercc1 protein levels or take into account the possible effects of the alternatively spliced variant of *ERCC1* mRNA (lacking exon VIII). In a paper by Britten et al. (2000), the authors were unable to demonstrate an obvious relationship between Ercc1 protein levels and cisplatin resistance among a panel of human cervical carcinoma cell lines. In fact, there was no correlation between *ERCC1* mRNA and Ercc1 protein levels in that study. They suggest that the observed association of *ERCC1* mRNA levels with drug resistance may be an epiphenomenon, that is, the level of *ERCC1* mRNA may be a surrogate marker for some other determinant of chemotherapeutic response (Britten et al. 2000). This suggestion appears to be supported by the finding that mRNA levels of *ERCC1* and *XPF* do not correlate with each other and the 'apparent order of appearance' of mRNA expression of NER genes may not mimic the order of proposed protein activities within the cell (Vogel et al. 2000). In a paper by Codegoni et al. (1997) high levels of *ERCC1* gene expression in ovarian cancers did not correlate with poor response to chemotherapy. Rather, these authors were able to show a weak correlation between high *ERCC1* mRNA expression and a high probability of response resulting in longer survival (Codegoni et al. 1997). Other researchers have measured not only total *ERCC1* mRNA levels but have also measured independently the full-length *ERCC1* mRNA and the alternatively spliced variant of *ERCC1* mRNA (Dabholkar et al. 1994, 1995a, 1995b, Lin et al. 1998, Yu et al. 1998). In three of the studies the data showed, with respect to cisplatin resistance, that alternatively spliced variant *ERCC1* mRNA levels have a strong inverse relation to DNA repair activity, suggesting a possible inhibitory influence (Dabholkar et al. 1995a, 1995b, Yu et al. 1998). This was most evident in the experimental study done by Yu et al. (1998), who determined the ratio of full-length to

alternatively spliced *ERCC1* mRNA or Ercc1 protein and demonstrated an association between the alternatively spliced mRNA/protein and a reduction in cellular capacity to repair cisplatin-DNA damage. The data they presented suggest that measuring the total *ERCC1* mRNA or Ercc1 protein may be insufficient to obtain a true assessment of biologically effective Ercc1 activity (Yu et al. 1998). In the study by Lin et al. (1998) the authors detected an abnormally migrating product of the *ERCC1* gene in a patient with acute MLL (mixed lineage leukemia) that correlated well with clinical onset and relapse of the disease. The possibility that *ERCC1* mRNA splice variants might contribute to the regulation of *ERCC1* mRNA and/or Ercc1 protein expression was also determined through the identification of splice variants in published sequences (Wilson et al. 2001). Therefore, in light of the above findings, examining the resulting Ercc1 protein expression would likely give a more accurate indication of NER capability than mRNA levels alone.

1.5 Experimental objectives

There are many clinical studies where tumor cells have been analyzed to determine a correlation between DNA repair capacity and drug resistance. Some cancer cells so analyzed show an increase in NER gene expression, such as *ERCC1* mRNA, and this appears to be a major determinant of drug resistance (Dabholkar et al. 1992, 1994, Li et al. 1998, Metzger et al. 1998, Yu et al. 1998, Britten et al. 2000, Cheng et al. 2002, Lord et al. 2002). The importance of DNA repair pathways such as NER and ISC repair in the resistance to chemotherapeutic drugs makes them a possible target for modulation for the purpose of improving treatment outcome for a particular cancer. Since many of the more successful chemotherapeutic drugs are bifunctional alkylating and platinating agents that exert their cytotoxic effects at least in part through the induction of ISCs, targeting a protein that is involved in repairing ISCs would be a likely candidate for chemosensitization. An attractive target for such modulation is the Ercc1 protein, which has been shown to be involved in both NER and ISC repair. Studies based on the phenotypes of the mutant CHO

lines UV20 (*ERCC1*$^-$) and UV41 (*XPF*$^-$) demonstrating their dramatic sensitivity to cross-linking agents support this concept, and indicate that an Ercc1-Xpf dependent recombinational repair process mediates ISC repair (Thompson et al. 1996). Unfortunately, information on the role of the Ercc1 and Xpf proteins in human cells is limited to XPF cell lines because no known disease has been associated with a deficiency in the Ercc1 protein.

In the present study we have examined the sensitivity of NER-deficient human cell lines, in particular XPF$^-$ (XP2YOSV) and XPA$^-$ (XP12T703) cell lines, to the CP analog, PM. Of the XP lines, XPF is obviously the most interesting given the extraordinary sensitivity of the corresponding CHO mutants (e.g., UV41) to such agents. The sensitivity of the XPA cell line was also examined in order to determine if the human Xpa protein has a significant role in ISC repair.

In order to assess the role of the Ercc1 protein in the repair of ISCs induced by DNA-damaging agents in human cells, an attempt to make a null *ERCC1* mutant in a human background was undertaken because no human *ERCC1* mutant has been isolated to date. Modulation of the Ercc1 protein has been attempted using a vector carrying an antisense-*ERCC1* cDNA that can integrate into the genome of a target cell for continuous, stable expression of the antisense-*ERCC1* mRNA.

CHAPTER 2: MATERIALS AND METHODS

2.1 Human cell lines and culture conditions

Dr. Michael Weinfeld generously provided GM00637A, a normal SV40-transformed human fibroblast cell line. Dr. Malcolm Paterson provided the NER-deficient, SV40-transformed, fibroblast cell lines XP12T703 and XP2YO(SV) which were originally isolated from human patients with the hereditary disorder XP, and have been previously assigned to the complementation groups XPA and XPF, respectively. The cell line termed XP12T703 was originally cited by Miyakoshi et al. (1991) but is more frequently referred to as either XP12RO(SV) or XP12RO. The primary human fibroblast cell line GM38 was provided by Dr. Razmik Mirzayans. All cell lines were grown as monolayer cultures in Dulbecco's modified Eagles medium/Ham's F12 (DMEM/F12, Gibco-BRL, Burlington, ON) supplemented with 10% fetal bovine serum, 1% L-glutamine, and 1% penicillin-streptomycin (all from Gibco-BRL). Cell cultures were incubated at 37°C in a fully humidified 5% CO_2/95% air atmosphere and stock cultures were passaged by trypsinization every 4-5 days for GM00637A, GM38 and XP12T703 cultures or every 7-10 days for XP2YO(SV) cultures to maintain exponential growth. Cells were detached from the tissue culture flasks/dishes by incubating with 0.05% Trypsin-EDTA at 37°C for 3 min, and the trypsin activity was quenched by adding supplemented growth medium. Cell numbers were determined using a Coulter® Multisizer II (Coulter, Hialeah, FL, USA).

2.2 Survival Assay

2.2.1 Phosphoramide Mustard

PM was provided by Dr. R. F. Struck of the Southern Research Institute in Birmingham, Alabama. Stock solutions were prepared by dissolving the PM in phosphate-buffered saline (PBS, Gibco-BRL) immediately prior to use.

2.2.2 **Clonogenic (colony-forming) assay**: PM sensitivity

Human SV40-transformed fibroblast cell lines GM00637A, XP12T703 and XP2YO(SV) were examined for their sensitivity to the drug PM. Cell cultures were exposed to trypsin and plated at 3 x 10^5 cells per 60-mm tissue culture dish 24 h prior to treatment with the drug. Drug treatment involved washing the cells with warm PBS, adding an appropriate dilution of PM in PBS, and incubating for 15 min at 37°C. After incubation, the dishes were examined under a microscope to ensure that there was no significant cell detachment, and then the PM was removed. Cells were washed twice with warm PBS, detached by exposure to trypsin, and cell numbers were determined using the Coulter® Multisizer II. Serial dilutions were made in supplemented growth medium. The cells were plated in 100-mm dishes in triplicate and incubated for 2-3 weeks at 37°C. The growth medium was replaced once each week. Cells were stained with 5% crystal violet in ethanol, and colonies with greater than 50 cells were counted. The surviving fraction of drug-treated cells was defined as the ratio of the plating efficiencies of drug-treated cells and untreated control cells (Murray et al. 2002). The survival data were analyzed through the computer program Prizm™ 3.0 (Graphpad, San Diego, CA, USA) using the linear-quadratic model: $-\ln SF(C) = \alpha C + \beta C^2$; where SF is the surviving fraction at a drug concentration C, and α and β are constants (Murray et al. 2002).

2.2.3 Growth inhibition assay: Ultraviolet light - C (UV-C) and PM sensitivity

Transformed cell lines (GM00637A $\pm$ α*ERCC1*) and the parental GM00637A cell line were analyzed for UV-C and PM sensitivity using the growth inhibition assay, which is a modification of a protocol supplied by Dr. Razmik Mirzayans. Briefly, cell lines were exposed to trypsin and plated at 10^5 cells per 60-mm dish 24 h prior to treatment with UV-C (254 nm) or plated at 4 x 10^5 cells per 100-mm dish 24 h prior to treatment with PM. UV-C treatment involved removing the medium and exposing the cells to a pre-determined UV-C dose in an UV-C box where exposure of 1 s = 1 J/m^2. PM treatment involved washing the cells with warm PBS and incubating in a dilution of PM in PBS for 15 min at 37°C. After incubation, the

PM was removed and the cells were washed with warm PBS. Fresh supplemented growth medium was added upon completion of the treatment with either UV-C or PM, and the dishes were incubated undisturbed for 5 days at 37°C. Adherent cells were recovered by exposure to trypsin, and cell numbers were determined using the Coulter® Multisizer II. The surviving fraction was calculated as the ratio of the total number of cells in the treated dish and the untreated control dish.

2.3 Electroporation

2.3.1 Plasmids and primers

The full length *ERCC1* cDNA of 1098 bp was provided by Dr. Jan Hoeijmakers (Erasmus University, The Netherlands); pcDNA3 (pD3) was provided by Dr. Richard Britten. The *ERCC1* cDNA was restricted with *Bam* HI and *Kpn* I, resulting in a 629 bp fragment. The 629 bp fragment of *ERCC1* was ligated into the pcDNA3 (pD3αE1) multiple cloning site (MCS) using the *Bam* HI and *Kpn* I restriction sites, in the antisense orientation (see Figure 2-1).

2.3.2 Transfection of GM00637A cells with the pD3αE1 construct

The pD3αE1 construct was linearized with *Pvu* I (pD3αE1/*Pvu* I) and used to transfect GM00637A cells. Controls were pcDNA3 vector linearized with *Pvu* I (pD3/*Pvu* I) and no vector. Briefly, 0.9 x 10^7 GM00637A cells in ice-cold serum-free medium, either with or without 500 μg/ml sheared salmon sperm DNA (carrier DNA), was placed in a pre-chilled 0.4 cm gap electroporation cuvette (Gene Pulser® Cuvette, Bio-Rad, Mississauga, ON). The pD3αE1/*Pvu* I construct was added to each sample and electroporated (Gene Pulser® Transfection Apparatus, Bio-Rad) at one of three voltages - 0.22 kV, 0.25 kV, or 0.32 kV - with the electroporation settings for each electroporation being - capacitance: 960 μF, time constant: 31-44 ms. The controls used were pD3/*Pvu* I ± carrier and mock ± carrier (no added vector). Samples were plated in 100-mm dishes containing supplemented growth

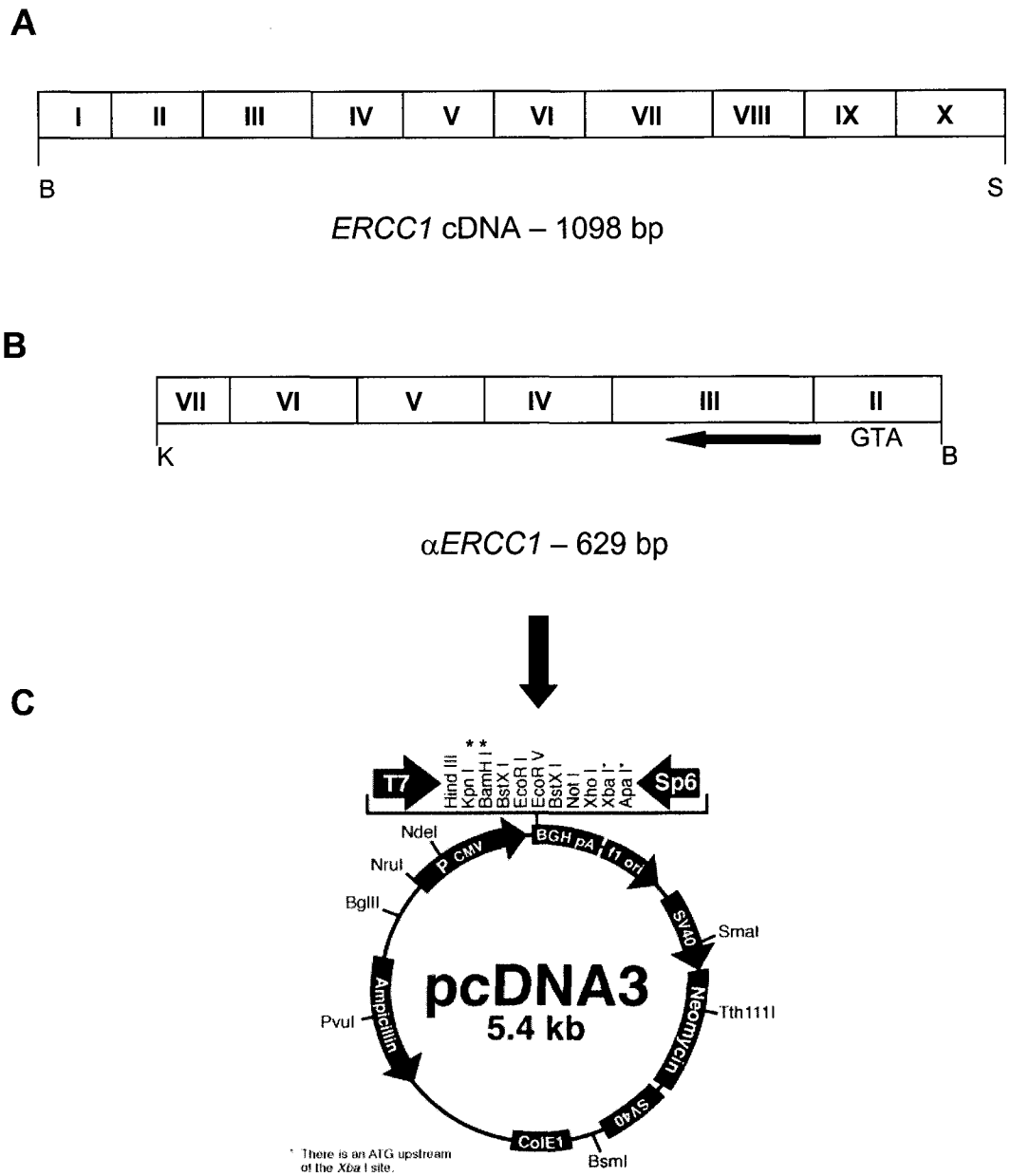

Figure 2-1. Schematic representation of the construction of a plasmid harboring the antisense-*ERCC1* cDNA insert. **A.** Organization of the *ERCC1* cDNA. **B.** The antisense-*ERCC1* (αERCC1) cDNA used in this study. The αERCC1 cDNA was ligated into the pcDNA3 MCS using the *Bam* HI site in exon II, and includes 70% of the coding region up to and including the *Kpn* I site in exon VII. **C.** The mammalian expression vector pcDNA3 with a transcription cassette consisting of the CMV (cytomegalovirus) promoter, MCS flanked by T7/Sp6 promoters, and bovine GH polyadenylation signal.
Abbreviations: B – *Bam* HI; K – *Kpn* I; *denotes restriction sites used in pcDNA3.

medium and incubated at 37°C for 3 days, after which selection was begun using G418 (Gibco-BRL) at 400 μg/ml in supplemented growth medium. The G418-containing growth medium was replaced every 3-4 days. Surviving colonies were sub-cloned by trypsinization using cloning rings and re-seeding to 24-well plates for several passages in selective medium.

2.4 Protein analysis

2.4.1 Nuclear protein extraction

The method of Chen and Sun (1998) was modified and used to isolate the nuclear protein from each cell line. Briefly, exponentially growing cells were exposed to trypsin and washed with PBS. Pelleted cells were placed on ice. Buffer 1 (10 mM HEPES [pH 7.9], 10 mM KCl, 0.1 mM EGTA [pH 8.0], 0.1 mM EDTA [pH 8.0], 1 mM dithiothreitol (DTT), 0.5 mM phenylmethylsulfonyl fluoride (PMSF), 1% aprotinin) was added to each of the pellets. Each sample was mixed and incubated on ice for 15 min. Buffer 1 containing Nonidet P-40 at a final concentration of 0.6% was added to each sample. Each sample was then mixed by inversion and pelleted by centrifugation at 1,000*g* for 15 min at 4°C. Supernatants (containing cytoplasmic proteins) were removed and the pellets (unlysed nuclei) were washed with Buffer 1. The integrity of the nuclei was checked by Trypan blue staining. The isolated nuclei were lysed in Buffer 2 (20 mM HEPES [pH 7.9], 400 mM NaCl, 1 mM EGTA [pH 8.0], 1 mM EDTA [pH 8.0], 10% glycerol, 1 mM DTT, 1 mM PMSF, 1% aprotinin). Each sample was gently mixed and incubated for 30 min at 4°C with rocking. The lysed nuclei were pelleted by centrifugation at 12,000*g* for 10 min at 4°C. Supernatants were removed to new tubes and the pellets discarded. Aliquots were frozen at –80°C after adding 0.5 μl of leupeptin (10 mg/ml) to every 100 μl of sample. Protein concentrations were determined using 5 μl of sample in duplicate in the BioRad Protein Assay with bovine serum albumin (BSA) (New England Biolabs, Beverly, MA, USA) at 1 mg/ml used for the standard curve.

2.4.2 Whole cell lysate protein extraction

Whole cell extracts were prepared from a monolayer culture as outlined by Santa Cruz Biotech (Santa Cruz, CA, USA) (www.scbt.com, protocols) using the RIPA buffer (1X PBS, 1% Nonidet P-40, 0.5% sodium deoxycholate, 0.1% SDS, 0.1 mg/ml PMSF, 0.1 mg/ml aprotinin, 1 mM sodium orthovanadate). Briefly, exponentially growing cells were exposed to trypsin and washed twice with PBS. Cells were pelleted by centrifugation at 1,000*g* for 10 min at 4°C and placed on ice. For every 2 x 10^7 cells, 1.0 ml of RIPA buffer was added, and each tube was gently mixed and incubated on ice for 30 min. Each sample was passed through a 21-gauge needle 4-5 times to further disrupt the cells. To each sample, 10 μl of PMSF (10 mg/ml) was added, followed by incubation for 30 min on ice. The samples were centrifuged at 12,000*g* for 10 min at 4°C. Supernatants were removed to new tubes and the pellets discarded. Aliquots of the supernatants were frozen at –80°C. The protein concentration of the supernatants was determined by using 5 μl of sample in duplicate in the BioRad Protein Assay with BSA at 1 mg/ml used for the standard curve.

2.4.3 *Immunologic reagents*

Primary antibodies used include:

(i) Ercc1 (clone 8F1) affinity-purified mouse monoclonal antibody raised against the full length, His-tagged recombinant human Ercc1 protein (PharMingen, San Diego, CA, USA, 1:100).

(ii) p53 (Pab 1801) affinity-purified mouse monoclonal antibody raised against the amino-terminal epitope mapping between amino acids 32-79 of human origin (Santa Cruz, 1:1,000).

(iii) Xpf rabbit polyclonal antibody, which was generously provided by Maureen Biggerstaff (Imperial Cancer Research Fund, Hertfordshire, England) for detection of human Xpf (1:15,000).

(iv) Actin (1-19) goat polyclonal antibody (IgG) raised to the carboxy terminus of human actin, which recognizes a broad range of actin isoforms (Santa Cruz, 1:800).

Secondary antibodies used include peroxidase-conjugated, affinity-purified, goat anti-rabbit IgG (H+L) (Jackson ImmunoResearch, West Grove, PA, USA, 1:10,000); peroxidase-conjugated goat anti-mouse IgG (H+L) (Jackson , 1:10,000); and peroxidase-conjugated donkey anti-goat IgG antibody (sc 2020; Santa Cruz, 1:1,000).

2.4.4 Western blot analysis

Protein samples of 50 μg were denatured by adding sample buffer (0.125 M Tris-HCl [pH 6.8], 20% glycerol, 4% SDS, 10% β-mercaptoethanol, 0.0025% bromophenol blue) and boiling for 10 min. Samples were loaded onto a 4-12% Tris-Glycine (pH 6.8-8.8) gradient gel in a MiniProtean II electrophoresis apparatus (BioRad). The gel was run in running buffer (25 mM Tris, 192 mM Glycine, 0.1% SDS) at 150 V until the dye front had run close to the bottom. The run was then stopped and the gels removed to transfer buffer for 10 min at room temperature. Gels were transferred to nitrocellulose membranes (Trans-Blot™, BioRad) in transfer buffer (25 mM Tris, 192 mM Glycine, 20% Methanol) at either 100 V for 1 h or 30 V overnight. Nitrocellulose membranes were blocked in PBST (PBS + 0.05% Tween 20) + 5% skim milk at room temperature for 1 h with rocking. The membranes were then placed in a solution containing primary antibody diluted in PBST + 5% skim milk and incubated at room temperature for 1-2 h or overnight at 4°C with rocking. The membranes were washed 3 times for 10 min in PBST at room temperature with rocking and then placed in a solution containing secondary antibody conjugated to horseradish peroxidase in PBST + 5% skim milk and incubated for 1 h at room temperature or overnight at 4°C with rocking. The membranes were washed 3 times for 10 min in PBST at room temperature with rocking. Detection of protein bands was performed using ECL or ECL plus (Amersham Pharmacia Biotech, Piscataway, NJ, USA) added at 2 ml/membrane followed by incubation for 1-5 min at room temperature. The membranes were wrapped in Saran wrap and exposed to Kodak XR-5

x-ray film. Protein bands detected on Western blots were quantitated by densitometry as outlined in section 2.4.6.

2.4.5 Cyclohexamide time course assay

Protein half-lives were determined by exposing exponentially growing cultures to cyclohexamide (Sigma-Aldrich, Oakville, ON) and harvesting the cells at varying time points. Briefly, cells were plated at 1.5 x 10^6 in 150-mm dishes containing supplemented growth medium 24 h prior to treatment with cyclohexamide. The next day the medium was removed, 20 μg/ml of cyclohexamide in supplemented growth medium was added, and the dishes were incubated at 37°C. Cells were harvested at various times later by trypsinization and pelleted in a 50 ml conical centrifuge tube by centrifugation at 1,000*g* for 10 min at 4°C. The supernatant was decanted and the pellet resuspended in 1 ml of ice-cold PBS. The pellet was transferred to a 1.5 ml Eppendorf tube and centrifuged as above. The supernatant was removed and the pellet washed 2 more times with PBS. After the final wash, as much of the supernatant was removed as possible and the pellet was frozen at –80°C. Protein extracts were obtained as outlined in sections 2.4.1 and 2.4.2.

2.4.6 Densitometry

The bands detected by Western or Northern blotting were quantitated by densitometry from developed film. Each image was captured using a video camera linked to the Interactive Image Acquisition and Processing Program Version 3.4 Cancer Imaging (IPRO program with grain count, from the BC Cancer Research Agency). Quantitation of band intensities was done by outlining a band six different times and, using the computer program mentioned above, the integrated optical density (OD) was determined. The average band intensity for each protein or mRNA band was calculated and normalized to the average actin band intensity, within an experiment, according to:

$$\text{Normalized band intensity} = \frac{\text{average OD of protein or mRNA band}}{\text{average OD of actin protein or mRNA band}}$$

The band intensities obtained for protein and mRNA above are, therefore, relative.

2.5 DNA Analysis

2.5.1 DNA extraction

Exponentially growing cells were detached by exposure to trypsin and 3 x 10^6 cells were transferred to a 15 ml conical centrifuge tube and pelleted by centrifugation at 1,000*g* for 15 min at 4°C. Pellets were washed twice by resuspension in PBS and centrifugation as above. After the last wash, cells were resuspended in 0.5 ml of PBS and transferred to a microcentrifuge tube to be pelleted again, as above. As much of the supernatant as possible was removed, and to each pellet was added 100 μl of digestion buffer (100 mM NaCl, 10 mM Tris-HCl [pH 8.0], 25 mM EDTA [pH 8.0], 0.1% SDS, 1 mg/ml proteinase K) for every 10^6 cells. Samples were mixed and incubated at 50°C overnight. Genomic DNA was phenol-chloroform extracted by the method outlined by the Current Protocols in Molecular Biology Vol. 1 (1993). The resulting pellet was dissolved in 500 μl of T buffer (10 mM Tris-HCl [pH 8.0]) containing DNAse-free pancreatic RNAse at 20 μg/ml, incubated at room temperature for 1 h, and isopropanol precipitated. The resulting pellet was dissolved in 500 μl of T buffer. DNA concentrations were determined on an UV spectrophotometer at wavelengths 260 nm and 280 nm.

2.5.2 PCR analysis of genomic DNA

PCR analysis was used to determine if the antisense-*ERCC1* cDNA of the pD3αE1 construct had integrated into the genomic DNA of the GM00637A transfected cell lines. Genomic DNA was extracted from each of the GM00637A and transfected cell lines as outlined in section 2.5.1. The promoter primers T7 (5'-TAA TAC GAC TCA CTA TAG G-3')

and Sp6 (5'-ATT TAG GTG ACA CTA TAG-3') were used for the PCR amplification reaction; these primers correspond to the promoter regions in the pcDNA3 vector on either side of the MCS (see Figure 2-1). The amplification reaction involved an initial denaturation at 94°C for 3 min; 30 cycles of denaturation at 94°C for 1 min, annealing at 55°C for 1 min, elongation at 72°C for 1 min; and a final extension at 72°C for 7 min. The resulting PCR product corresponds to 775 bp (antisense-*ERCC1*) or 146 bp (no antisense-*ERCC1*, i.e. empty vector) when run out on a 0.8% agarose gel and stained with 0.5 μg/ml ethidium bromide.

2.5.3 Southern blot analysis

Samples of genomic DNA were aliquoted to give 10 μg in a 1.5 ml microcentrifuge tube, incubated in restriction enzyme buffer at 4°C for ~2 h, and then restricted with *Bam* HI. The samples were concentrated by ethanol precipitation to 15 μl in sterile mQH_2O. To each sample was added sample buffer (0.25% xylene cyanol, 0.25% bromophenol blue, 40% sucrose) and the samples were loaded onto a 0.8% agarose gel made with 0.5X TBE (Tris-borate-EDTA buffer). The samples were allowed to sit for 2-3 min to allow DNA diffusion in the well. Gels were run in 0.5X TBE at 12 V for 18-20 h. The genomic DNA was visualized on the gel by staining with 0.5 μg/ml ethidium bromide in dH_2O. Transfer of the genomic DNA was accomplished by the standard protocol of Sambrook et al. (1989). Briefly, the DNA was denatured by soaking the gel in a denaturing solution (0.5 M NaOH, 1.5 M NaCl) for 45 min with gentle shaking. The gel was rinsed briefly in dH_2O then soaked in a neutralizing solution (0.5 M Tris, 1.5 M NaCl [pH 7.5]) two times, once for 30 min and a second time for 15 min. The DNA was blotted onto a nylon membrane (Hybond-N+, Amersham Pharmacia Biotech) overnight using the standard procedure outlined in Sambrook et al. (1989). The next day, the membrane was dried for 1 h at 80°C and then stored at –20°C. Membranes were probed using ^{32}P-radiolabelled *ERCC1* cDNA produced from the single strand DNA synthesis reaction outlined by Feinberg and Vogelstein (1983, 1984). The reaction used the T7 primer, [α-^{32}P]dCTP (3000 Ci/mmol, DNA Core Services, University of Alberta) and *E. coli* Klenow

(Amersham Pharmacia Biotech). Unused nucleotides were removed using Bio-Spin 30 columns (BioRad). Membranes were prehybridized at 68°C for 20 min in RapidHyb™ (Amersham Pharmacia Biotech) and then hybridized for 2 h with ^{32}P-labeled probe. Membranes were washed once with 2X SSC/0.1% SDS for 20 min at room temperature, twice with 1.0X SSC/0.1% SDS for 15 min at 65°C, and twice with 0.1X SSC/0.1% SDS for 15 min at 65°C. Membranes were wrapped in Saran wrap and exposed to Kodak XR-5 x-ray film with an intensifying screen for 3 days at –80°C.

2.6 RNA Analysis

2.6.1 RNA Extraction

Total RNA was isolated from cells using TRIzol™ reagent (Invitrogen, Carlsbad, CA, USA) according to the manufacturers instructions with slight modifications. Briefly, cells were grown to ~80% confluence, detached by exposure to trypsin, and pelleted in 15 ml conical tubes by centrifugation at 1,000*g* for 10 min at 4°C. Pellets were resuspended in 1 ml of ice-cold PBS and transferred to 1.5 ml Eppendorf tubes and centrifuged as above. Pellets were washed 2 more times in 1 ml of ice-cold PBS and the final pellet was resuspended in 1 ml TRIzol™. Samples were incubated at room temperature for 3 min, after which 200 µl of chloroform was added. The samples were mixed, incubated at room temperature for 2-3 min and centrifuged at 12,000*g* for 15 min at 4°C. The top (aqueous) layer was removed to a new tube. The TRIzol™ (lower) layer was back-extracted with 100 µl of 10 mM Tris-HCl (pH 8.0), and the aqueous (upper) layer was removed and added to the tube containing the previously extracted aqueous layer. The samples were extracted with phenol-chloroform, isopropanol precipitated, and the RNA pellet was rinsed twice with 1 ml of ice-cold 75% ethanol. Pellets were dried at room temperature and resuspended in sterile mQH_2O. Samples were stored at –80°C. RNA concentrations were determined by spectrophotometric analysis at a wavelength of 260 nm.

2.6.2 Actinomycin D time course assay

Actinomycin D (Amersham Pharmacia Biotech) was used to determine the half-life of *ERCC1* mRNA. Cells from either GM38 or GM00637A cultures were aliquoted at 1.0–1.5 x 10^6 cells per 150-mm dish containing supplemented growth medium and incubated for 24 h prior to treatment with actinomycin D. The next day, the medium was removed and replaced with 15 ml of supplemented growth medium containing 5 μg/ml actinomycin D. The dishes were then incubated at 37°C for various times until they were harvested. Harvesting the treated cells involved removing the drug and washing the cells with warm PBS. The cells were detached by exposure to trypsin, after which they were transferred to a 50-ml conical centrifuge tube and centrifuged at 1,000*g* for 10 min at 4°C. Cell numbers were determined using the Coulter® Multisizer II. The cell pellets were washed 3 times with 1 ml of ice-cold PBS, with the first PBS wash being used to transfer the suspension to a 1.5 ml Eppendorf tube. All washes were as above. As much of the supernatant was removed as possible and 1 ml of TRIzol™ was added. Each of the samples was mixed by inversion and placed at –80°C. RNA extraction with TRIzol™ was done as outlined in section 2.6.1.

2.6.3 Northern blot analysis

Samples of total RNA were aliquoted to give 17 μg in a 1.5 ml microcentrifuge tube and were concentrated by ethanol precipitation to a volume of 7 μl in sterile mQH_2O. To each sample, 23 μl of sample buffer (6% deionized formaldehyde, 50% deionized formamide, 20 mM morpholinopropanesulfonic acid (MOPS)) was added and the samples were incubated at 65°C for 15 min then cooled on ice. After incubation, 3 μl of loading dye (50% glycerol, 1 mM EDTA, 0.4% bromophenol blue plus 0.4% xylene cyanol) and 0.5 μl of ethidium bromide (10 mg/ml) were added to each sample. RNA samples were loaded onto a 1.4% denaturing agarose-formaldehyde gel in MOPS running buffer (400 mM MOPS, 100 mM sodium acetate, 10 mM EDTA) containing 6% formaldehyde. The RNA gel was run in MOPS buffer and electrophoresed for 3-5 h at 90 V. After electrophoresis, the gel was

rinsed in dH_2O for 30 min and the RNA was transferred onto a nylon membrane (Hybond-N+, Amersham Pharmacia Biotech) overnight using the standard procedure outlined in Sambrook et al. (1989). The following day, the membrane was dried between two pieces of Whatmann 3-MM paper for 1 h at 80°C and stored at –20°C. Equal RNA loading was determined by visualization of the 18S and 28S ribosomal RNA bands on ethidium bromide stained gels using a UV light.

The *ERCC1* probe was prepared and used as outlined in section 2.5.3. The β-*actin* probe was produced using the Rediprime II DNA labeling system (Amersham Pharmacia Biotech) and used as outlined in section 2.5.3. RNA bands detected on Northern blots were quantitated by densitometry as outlined in section 2.4.6.

2.6.4 RT-PCR

RT-PCR analysis of transfectant (GM00637A + pD3αE1/PvuI) and GM00637A mRNA was accomplished using 1 μg total RNA in a reaction with oligo(dT) and Superscript II reverse transcriptase (Invitrogen) to produce the single strand cDNA, as outlined by the manufacturer. The single strand cDNA was amplified by using 1 μl in a PCR reaction containing the appropriate primers. For the detection of the antisense-*ERCC1* mRNA, the T7 and Sp6 promoter primers (sequences can be found in section 2.5.2) were used. The amplification reaction involved an initial denaturation at 94°C for 3 min; 30 cycles of denaturation at 94°C for 1min, annealing at 55°C for 1 min, elongation at 72°C for 1 min; and a final extension at 72°C for 7 min. The resulting band size for the amplified antisense-*ERCC1* mRNA was 775 bp (a band of 146 bp would be produced if the empty control vector transcribes mRNA).

The β-*actin* primer pairs identified by Raff et al. (1997), which avoid the co-amplification of contaminating genomic DNA, were used for the detection of the human β-*actin* mRNA: β-*actin* 1-1 (5'-CCT CGC CTT TGC CGA TCC-3') and β-*actin* 1-2 (5'-GGA TCT TCA TGA GGT AGT CAG TC-3'). The amplification reaction for β-*actin* involved an

initial denaturation at 94°C for 5 min; 30 cycles of denaturation at 94°C for 1 min, annealing at 60°C for 1 min, elongation at 72°C for 1 min; and a final extension at 72°C for 7 min. The resulting band size for the β-*actin* was 626 bp.

CHAPTER 3: RESULTS

3.1 Sensitivity of GM00637A, XPF, and XPA cells to phosphoramide mustard

The sensitivity of the GM00637A (normal), XP2YO(SV) (XPF) and XP12T703 (XPA) human cell lines to PM can be seen in Figure 3-1. The IC_{90} (inhibiting concentration of drug resulting in 90% growth arrest) values derived from these survival curves were: GM00637A, 530 μg/ml; XP2YO(SV) (XPF), 301 μg/ml; and XP12T703 (XPA), 646 μg/ml (Murray et al. 2002). The unexpectedly modest sensitivity of the XP2YO(SV) cells to PM of ~1.75 fold is far less than the 22-fold sensitivity of the corresponding CHO mutant UV41 (*XPF*$^{-}$) to PM (Andersson et al. 1996). The human XP12T703 (XPA) cell line was assessed for its sensitivity to PM because it is not known if the Xpa protein is required for ISC repair. No CHO mutants for *XPA* have been isolated, and the XPA$^{-/-}$ knockout mice generated by Nakane et al. (1995) and de Vries et al. (1995) have not been tested for their sensitivity to crosslinking agents to our knowledge. As seen in Figure 3-1, XP12T703 (XPA) cells have normal PM sensitivity compared to GM00637A cells. This may imply that the Xpa protein does not have a significant role in ISC repair.

3.1.1 Ercc1 protein expression in XP2YO(SV) cells

The level of Ercc1 protein in XP2YO(SV) cells, as well as the non-transformed parental line XP2YO, has been reported by Yagi and colleges (Yagi et al. 1997, 1998a, 1998b) to be very low even though the level of *ERCC1* mRNA transcripts had been reported to be normal (Yagi et al. 1998a, van Duin et al. 1989b). As shown in Figure 3-2, GM00637A cells expressed high levels of Ercc1 protein, whereas XP2YO(SV) cells did not express Ercc1 protein at levels detectable by Western blotting. The undetectable Ercc1 protein level in the nuclear fraction of XP2YO(SV) cells correlates well with previously published results of Ercc1 protein expression in these cells (Biggerstaff et al. 1993, van Vuuren et al. 1995, Yagi et al. 1997, 1998a, 1998b).

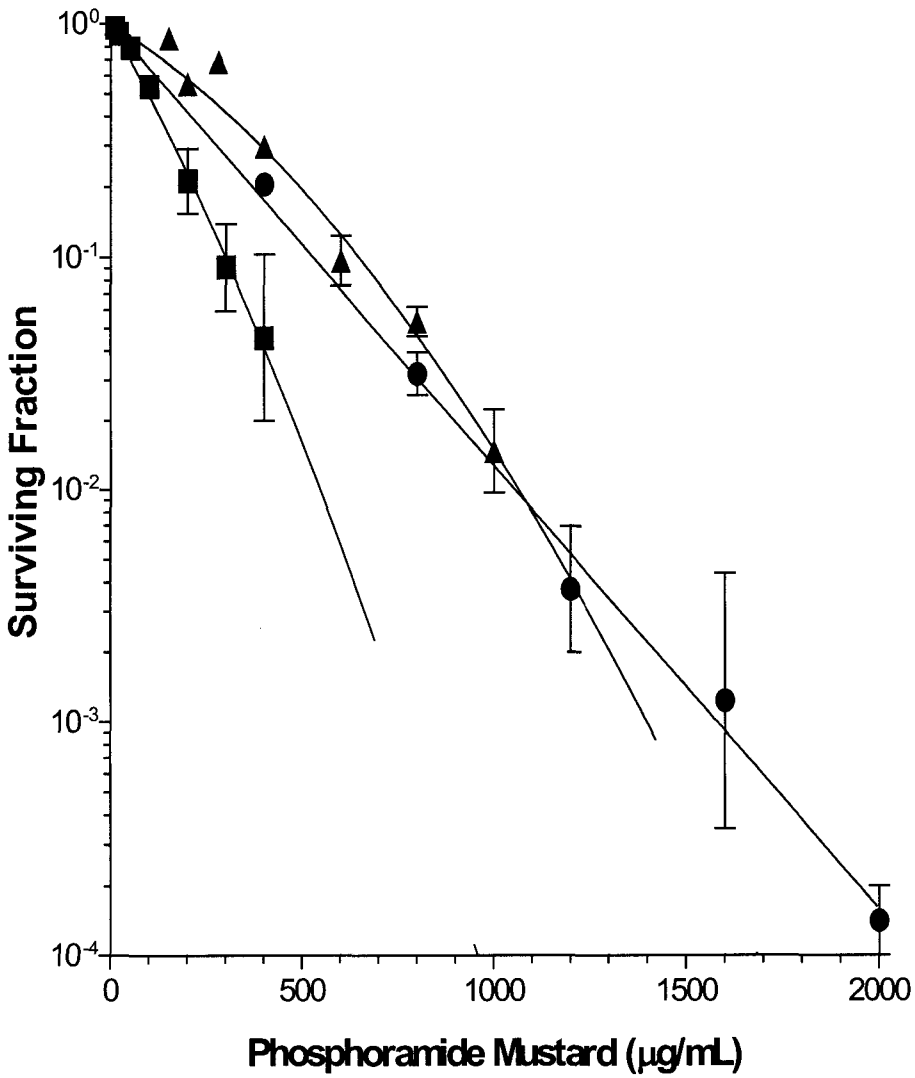

Figure 3-1. Sensitivity of GM00637A (normal ●), XP12T703 (XPA ▲), and XP2YO(SV) (XPF ■) human SV40-transformed fibroblasts exposed to PM for 15 minutes at 37°C, assessed using the clonogenic survival assay. The graph is the result of 3 separate experiments for each cell line.

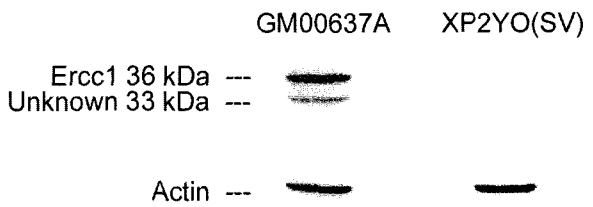

Figure 3-2. Western blot analysis of Ercc1 protein expression in nuclear extracts of GM00637A and XP2YO(SV) cell lines. Expression of the actin protein was also measured as a control.

3.2 Antisense-*ERCC1* cDNA expression in normal human cells.

Eliminating the expression of a specific NER protein in the human fibroblast cell background could help to determine its role in a particular repair pathway. With Xpf and Ercc1, creating a human cell line deficient in either protein would help delineate their functions not only in NER but also in ISC repair. At the time this project was begun, the human *XPF* gene had not been cloned and no human cell line deficient in the Ercc1 protein was available. However, van Duin et al. (1987) had determined the DNA sequence of the *ERCC1* gene. An antisense-*ERCC1* cDNA was used in an attempt to make a "null" *ERCC1* mutant in a human background. The full-length *ERCC1* cDNA (1098 bp) was modified and used to produce a 629 bp fragment that contained 70% of the coding region starting in exon II, where the translation (ATG) start site is located, up to and including part of exon VII (see Figures 2-1A, and 2-1B). This modified *ERCC1* fragment was inserted into the MCS of the mammalian expression vector pcDNA3 in the reverse orientation (Figure 2-1C). The pcDNA3 vector allows for stable, but random, integration into the human genome, and contains a CMV (cytomegalovirus) promoter for high expression of the antisense-*ERCC1* cDNA insert. The resulting pD3αE1 construct was linearized with *Pvu* I and used to transfect the normal SV40-transformed human fibroblast cell line GM00637A. Protic-Sabljic et al. (1985) had previously

reported that GM00637A cells were suitable for gene transfer, resulting in a high frequency of transfection and plasmid DNA gene expression, whereas primary non-transformed human cell lines generally gave a low transfection efficiency and did not allow prolonged culture of transformants. Stable transfectants were selected by growing the cells in G418 (geneticin)-containing medium. Transfectants were screened for UV-C sensitivity, PM sensitivity, Ercc1 protein expression, presence of the antisense-*ERCC1* cDNA within the transfectant genome, and antisense-*ERCC1* mRNA expression. Nomenclature pertaining to the antisense transfectants (A) and the transfectant controls (B) are shown in the following examples:

A. 637pD3αE1-**22C.1**	where:	637	transfected cell line GM00637A
		pD3	plasmid pcDNA3 used for transfection
		αE1	antisense-*ERCC1* cDNA insert in pD3
		22	220 volts used in electroporation
		C	carrier DNA added to electroporation
		.1	subclone number
B. 637pD3-**22B.3B**	where:	22	220 volts used in electroporation
		B	blank, i.e., no antisense-*ERCC1* cDNA
		.3B	subclone number

The transfectant nomenclature throughout will be referred to in an abbreviated form (in bold above) containing only the reference to the voltage used for electroporation, presence/absence of carrier DNA, and the subclone number.

3.3 UV-C and PM growth inhibition assays

3.3.1 UV-C growth inhibition assay of GM00637A transfectant cell lines

If the transfectant cell lines have an impaired NER pathway in relation to the presence of the antisense-*ERCC1* cDNA then an increase in UV-C sensitivity would be expected. The growth inhibition assays showing the sensitivity of the various GM00637A transfectants to UV-C can be found in Appendix A (see Figures A-1 to A-4).

The control transfectant cells 22B.1A, 22B.3A and 22B.3B had modest UV-C resistance and 22B.2A had a high UV-C resistance (~1.8 fold), when compared to GM00637A cells (see Figure A-1). These results suggest that the vector alone can exert a significant influence on UV-C sensitivity. This may be the result of the random integration of the vector into the genome or the transfection and/or selection of the resulting clones.

Transfectant cell lines obtained using the vector plus the antisense-*ERCC1* insert have varying UV-C sensitivities; however, only a few of these exhibited the high UV-C resistance that was characteristic of the control transfectants (see Appendix A, Figures A-1 to A-4). The most UV-C resistant transfectant cell line was 25.4 (~1.4 fold; see Appendix A, Figure A-3). Most of the transfectant cell lines had either modest UV-C resistance or UV-C sensitivity approaching normal when compared to GM00637A cells. Transfectant cell lines 22.3, and 22.11 (see Figures A-1 and A-2) had modest UV-C sensitivity when compared to GM00637A cells, with 22.3 cells being the most UV-C sensitive (~1.2 fold; see Appendix A, Figure A-1).

3.3.2 PM growth inhibition assay of GM00637A transfectant cell lines

Transfectant cell lines that were sensitive to UV-C, with respect to the presence of the antisense-*ERCC1* cDNA, would also be expected to be sensitive to PM. An initial screen of all of the transfectant cell lines using a single concentration of 600 μg/ml PM (Figures 3-3 and 3-4) showed that the various GM00637A transfectants exhibited a range of responses from modest sensitivity to high resistance.

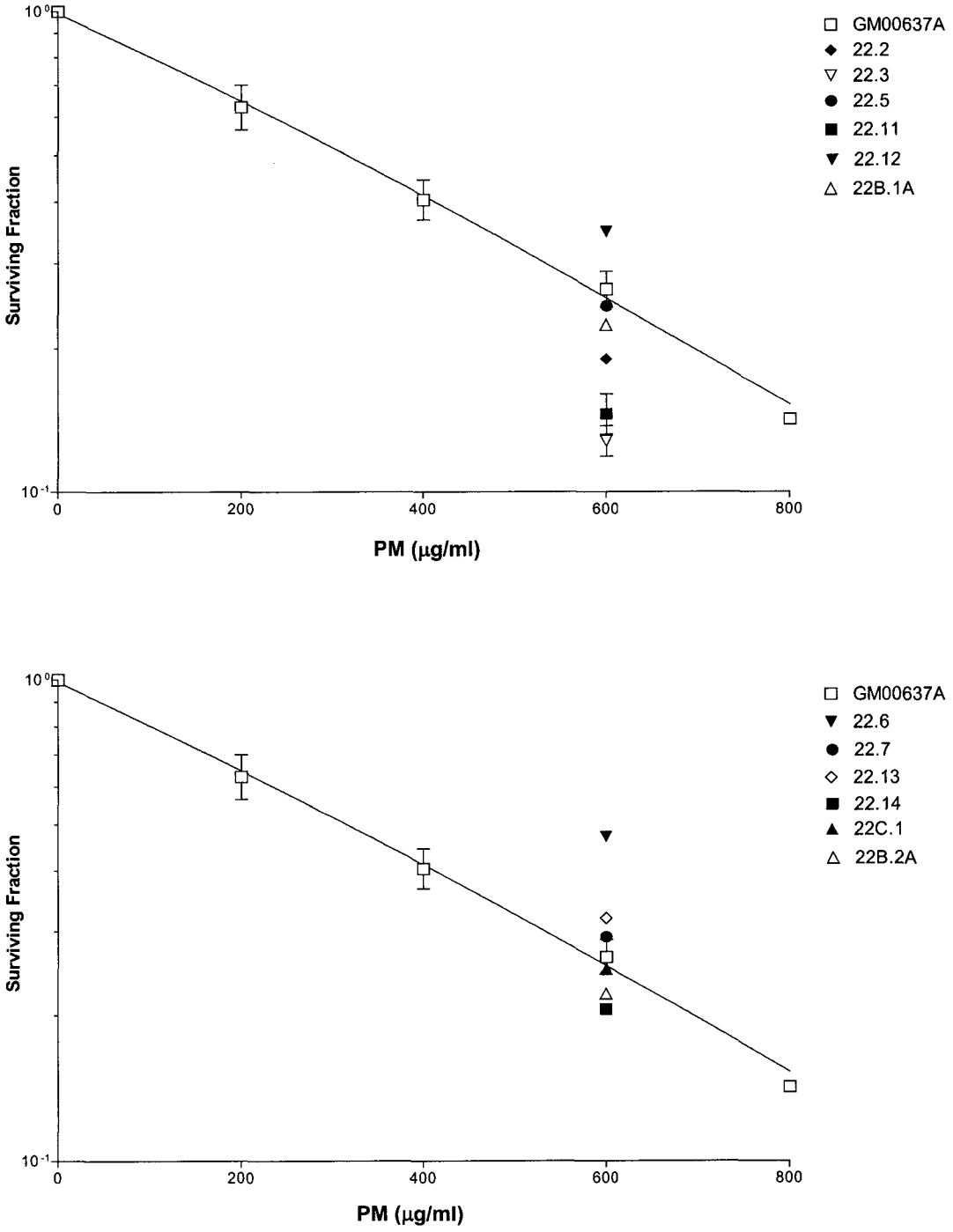

Figure 3-3. Sensitivity of GM00637A transfectant cell lines exposed to PM for 15 minutes at 37°C as measured using the growth inhibition assay. Transfectants were obtained using 220 volts to electroporate GM00637A cells without carrier DNA and with carrier DNA (22C.1). Analysis of each assay was done with the Prism™ 3.0 computer program.

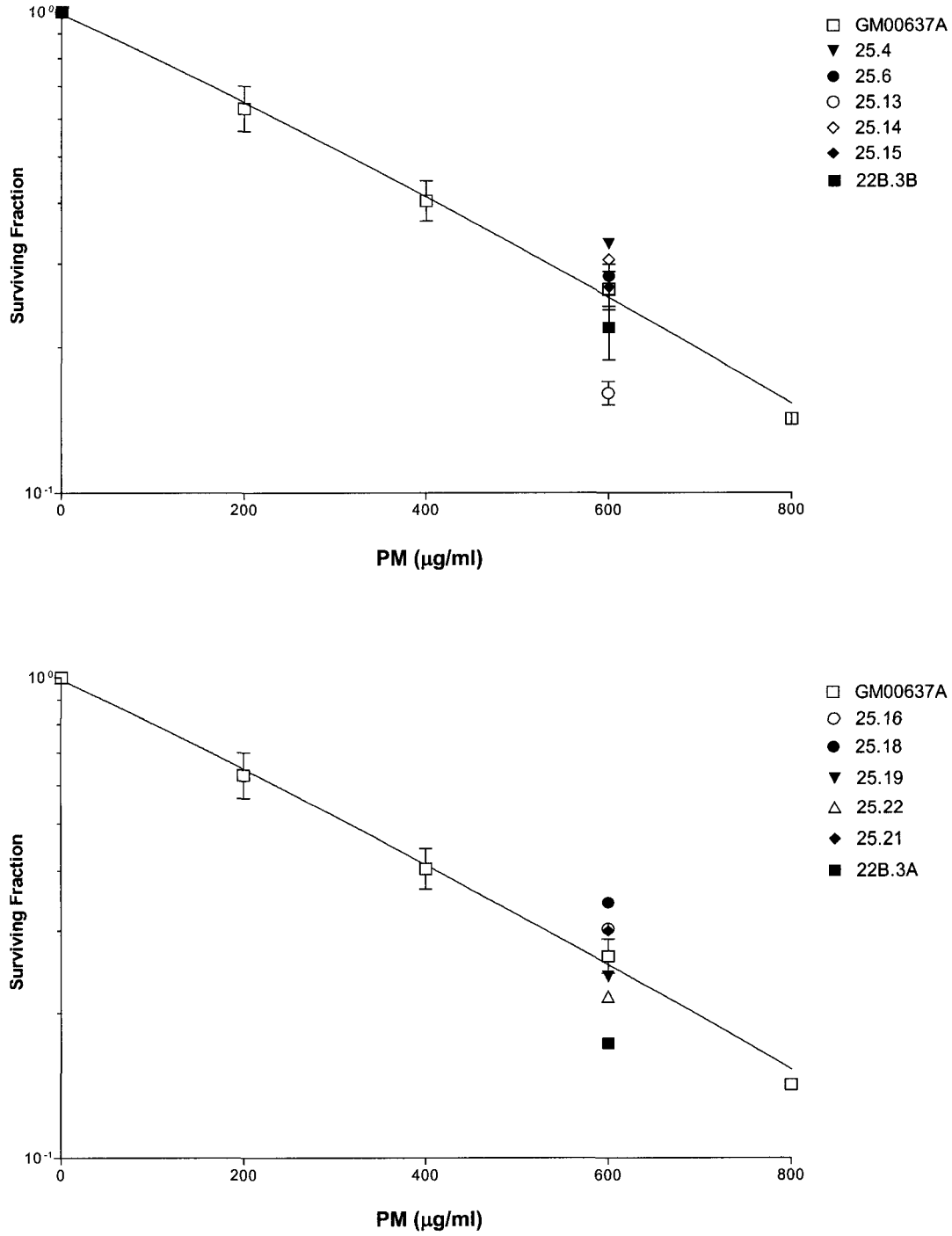

Figure 3-4. Sensitivity of GM00637A transfectant cell lines exposed to PM for 15 minutes at 37°C as measured using the growth inhibition assay. Transfectants were obtained using 250 volts to electroporate GM00637A cells without carrier DNA. Analysis of each assay was done with the Prism™ 3.0 computer program.

The control transfectant cells appear to vary in sensitivity, with 22B.3A being the most PM sensitive and the other three (22B.1A, 22B.2A, and 22B.3B) showing no significant difference when compared to GM00637A cells. This result was somewhat unexpected since all control transfectant cells were UV-C resistant and might, therefore, have been expected to be PM resistant.

Transfectant cell lines obtained using the vector plus the antisense-*ERCC1* insert also displayed varying sensitivities to PM. Transfectant cells that exhibit a response to PM comparable to GM00637A in this assay were 22.5, 22.7, 22C.1, 25.6, 25.15, and 25.19. Transfectant cells that ranged from high to moderate PM resistance were 22.6 > 22.12 ≈ 25.18 > 25.4 > 22.13 > 25.14 ≈ 25.16 ≈ 25.21. Transfectant cells that ranged from high to moderate PM sensitivity were 22.3 > 22.11 > 25.13 > 22.2 > 22.14 > 25.22. Transfectant cells that showed the highest PM resistance (22.12, 25.18, and 25.4), with the exception of 22.6, were also UV-C resistant.

Those transfectant cell lines determined to be the most sensitive to PM (22.3 and 22.11) were further analyzed in a more extensive PM growth inhibition assay, along with transfectant cell lines 25.15 and 22B.3B for comparison (Figure 3-5). The sensitivity of 22.3 and 22.11 cells was ~1.50 fold and ~1.36 fold respectively, compared to the GM00637A cell line (see Figure 3-5). When the PM sensitivities of 22.3 and 22.11 cells were compared to their UV-C sensitivities, only 22.3 cells showed both the NER ($UV\text{-}C^s$) and ISC (PM^s) repair pathways being inhibited. This may indicate that in this particular cell line, the antisense-*ERCC1* mRNA is indeed affecting the sense-*ERCC1* mRNA expression and ultimately Ercc1 protein expression. However, for the 22.11 cell line there appears to be a differential phenotypic effect with high sensitivity to PM but not to UV-C, suggesting that the ISC repair pathway is inhibited but the NER pathway remains unaffected.

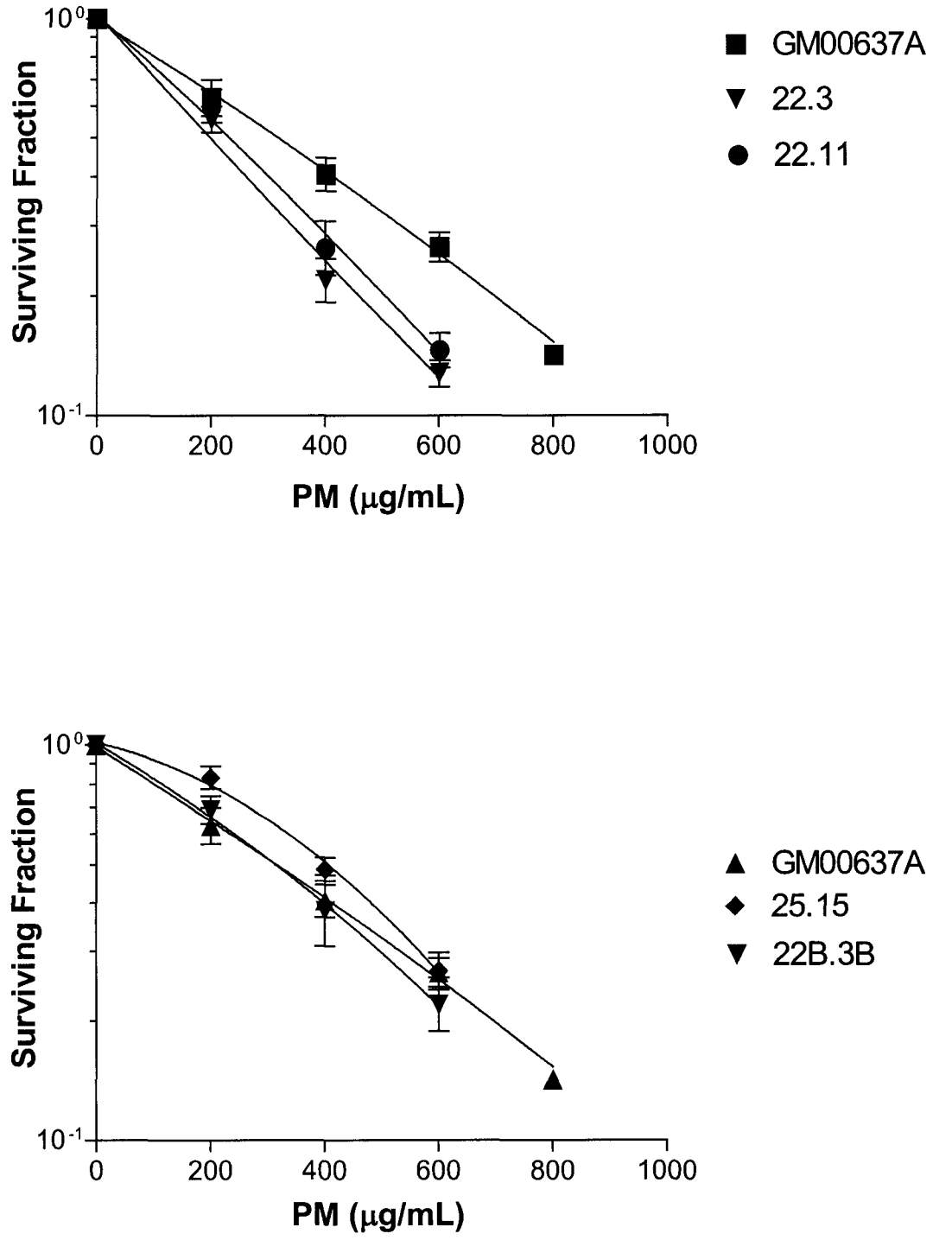

Figure 3-5. Sensitivity of GM00637A transfectant cell lines (22.3, 22.11, 25.15 and 22B.3B) exposed to PM for 15 minutes at 37°C as measured using the growth inhibition assay. Analysis of each assay was done with the Prism™ 3.0 computer program. The graph is the result of 3 separate experiments for each cell line.

3.3.3 Scatter plot analysis of UV-C D_{90} and PM IC_{90} values

Using the PM data points of Figures 3-3 and 3-4, a linear relationship between –log(SF) and drug concentration was assumed based on the linear nature of the survival curve for the GM00637A cell line. This enabled the calculation of a PM IC_{90} value (and thus of a dose modifying factor) for each of the GM00637A transfectants. The dose modifying factor for the PM growth inhibition assay was used in conjunction with the determined UV-C D_{90} (dose resulting in 90% growth inhibition) value for each of the transfectant cell lines in order to generate a scatter plot relating the relative responses of the cell lines to the growth-inhibitory effects of PM and UV-C (Figure 3-6). When the derived UV-C D_{90} and PM IC_{90} values were plotted using GM00637A cells as the normal control, the majority of the transfectant cells were seen to be UV-C resistant but to have a wide range of PM sensitivities (Figure 3-6A). When the UV-C D_{90} and PM IC_{90} values were plotted after normalizing to an average of all the control transfectant cells, the majority of the antisense transfectant cell lines appear to be UV-C sensitive and more of the transfectant cell lines display apparent PM resistance (Figure 3-6B). All of the antisense transfectant cell lines except for 25.4 showed some degree of UV-C sensitization, but only three of the antisense transfectant cell lines (22.3, 22.11, and 25.13) displayed obvious UV-C and PM sensitivity (Figure 3-6B).

3.4 Western blotting of whole cell extracts and nuclear extracts

Ercc1 protein levels in each of the GM00637A transfectant cells were measured to examine whether the antisense-*ERCC1* mRNA was affecting the expression of the Ercc1 protein. Whole cell extracts, as well as nuclear extracts, were prepared and Western blotting was performed using the anti-Ercc1 monoclonal antibody obtained from PharMingen. If the antisense-*ERCC1* mRNA was inhibiting the sense-*ERCC1* mRNA, a decrease in the Ercc1 protein levels would be expected.

A.

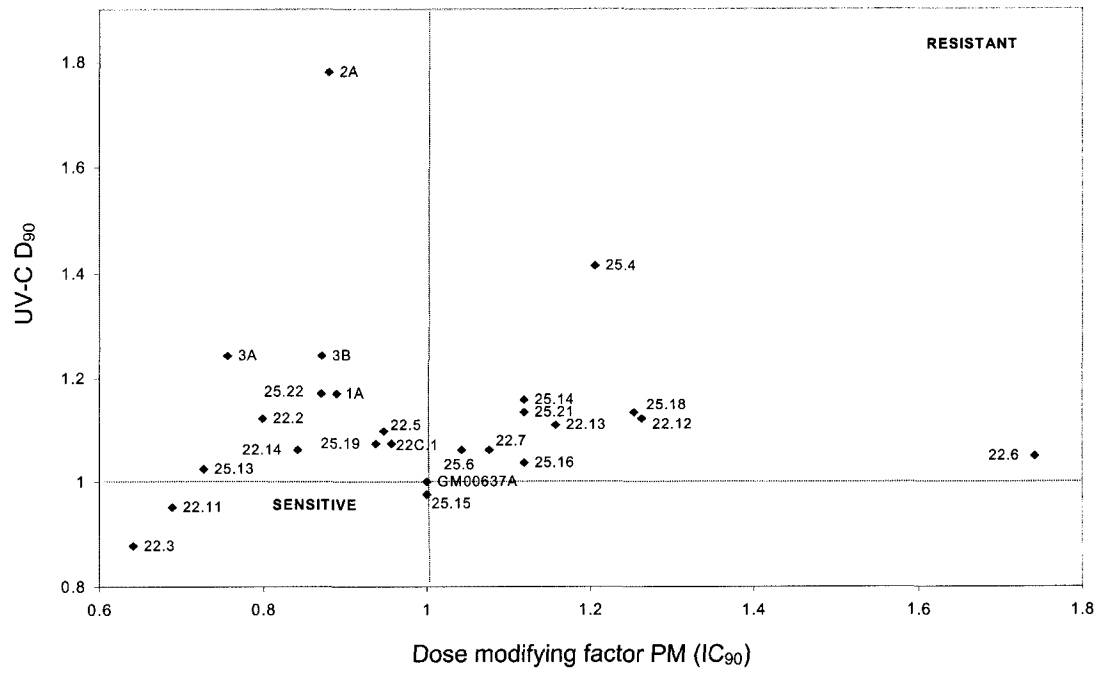

B.

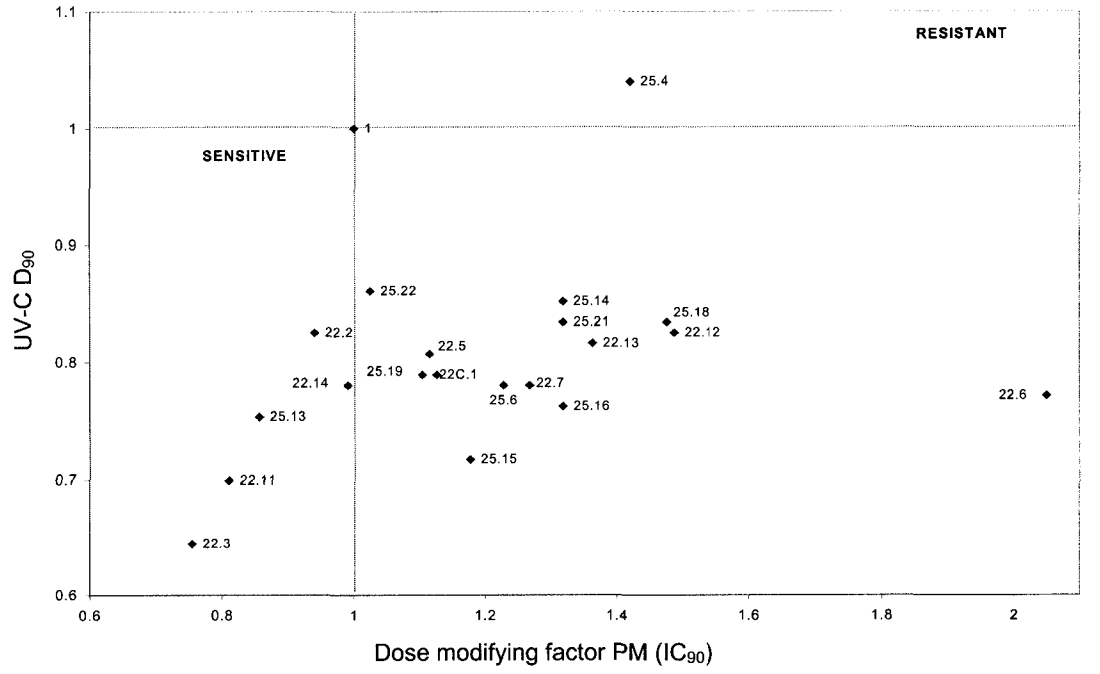

Figure 3-6. Scatter plot of UV-C D_{90} vs. PM IC_{90} (dose modifying factor) for each transfectant cell line (A) relative to the transformed parental cell line GM00637A (GM37) and (B) relative to the average of the GM00637A transfectant control cells (22B.1A, 22B.2A, 22B.3A, and 22B.3B) – represented by the intersecting lines.

3.4.1 Ercc1 protein levels in whole cell extracts

The expression of the Ercc1 protein in whole cell extracts was determined in all GM00637A transfectant cell lines, as shown in Figure 3-7. Protein bands detected in Western blots were quantitated by densitometry in order to detect changes in protein levels. Protein band intensities were normalized to actin within the same experiment and plotted in Excel (Figures 3-8). The control transfectant cell lines 22B.1A and 22B.3B have an Ercc1 protein expression comparable to GM00637A cells, whereas the Ercc1 protein expression in 22B.2A and in 22B.3A cells is higher and lower, respectively, when compared to GM00637A cells. The variation in Ercc1 protein levels apparent in the empty-vector controls was also evident in the antisense transfectant cell lines.

Transfectant cell lines determined to have a lower Ercc1 protein expression than GM00637A cells were 22.2, 22.6, 22.11, 22.12, 22.13, 22.14, 22C.1, 25.14, and 25.21 (Figures 3-8). Transfectant cell lines determined to have a higher expression of the Ercc1 protein than GM00637A cells were 22.3, 22.5, 22.7, 25.4, 25.6, 25.13, 25.16, 25.18, 25.19, and 25.22 (Figures 3-8). Only the 25.15 cell line had an Ercc1 protein level similar to GM00637A cells.

It should be noted that Western blotting of whole cell extracts only measures the total amount of Ercc1 protein within a cell. Yu et al. (1998) suggested that measurement of the total amount of Ercc1 protein might be insufficient to obtain a true assessment of the biologically effective Ercc1 protein. Indeed, Houtsmuller et al. (1999) demonstrated a predominantly homogenous nuclear distribution of the Ercc1-GFP/Xpf complex in CHO cells that was equivalent to that seen in the human HeLa cell line using an anti-Ercc1 antiserum. Therefore, detection of Ercc1 protein expression in the nuclear extract may give a more relevant estimate of the biologically effective Ercc1 protein.

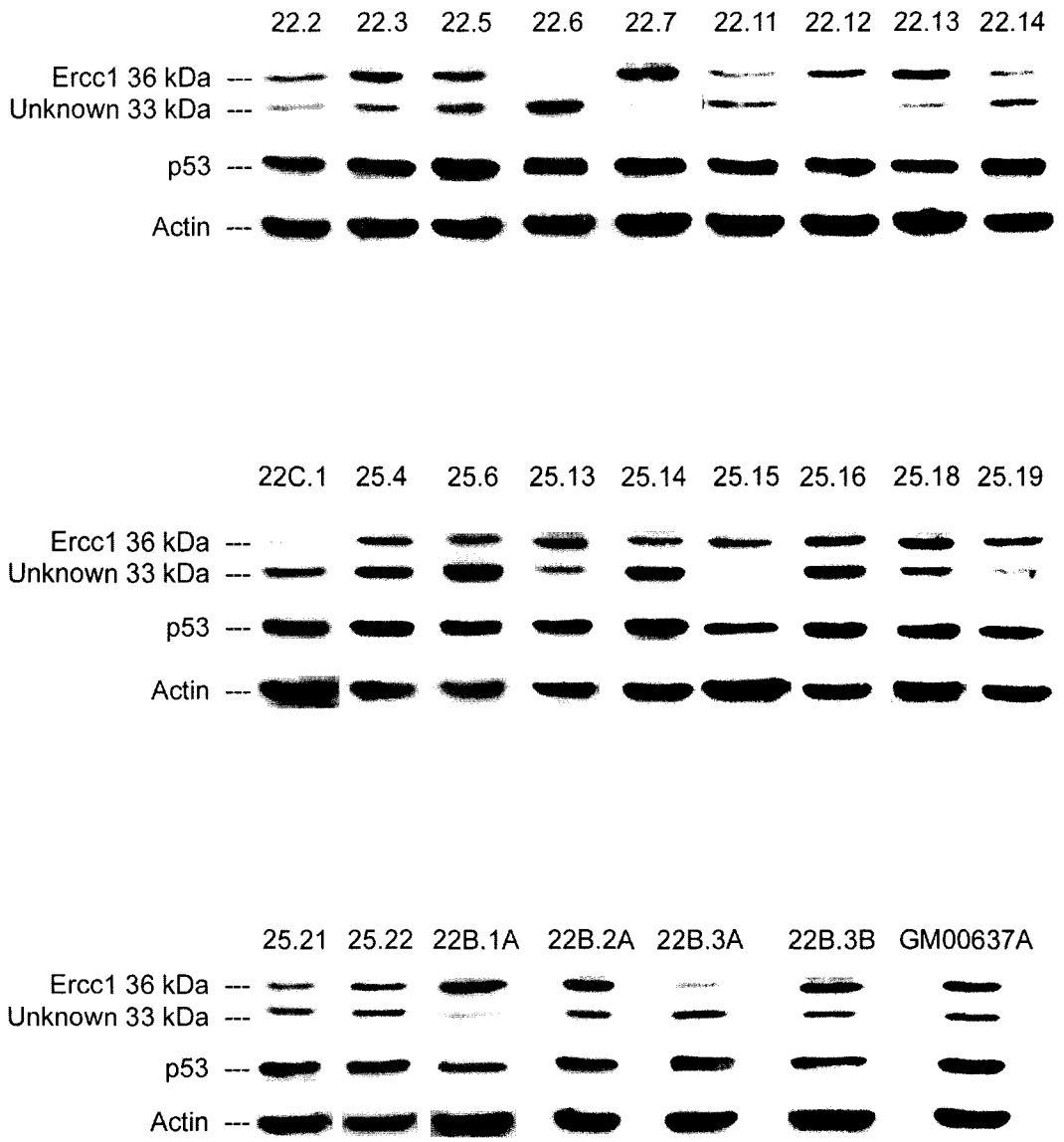

Figure 3-7. Western blot analysis of Ercc1 protein expression in whole cell extracts from GM00637A transfectant cell lines. Expression of p53 and actin proteins were also measured as controls.

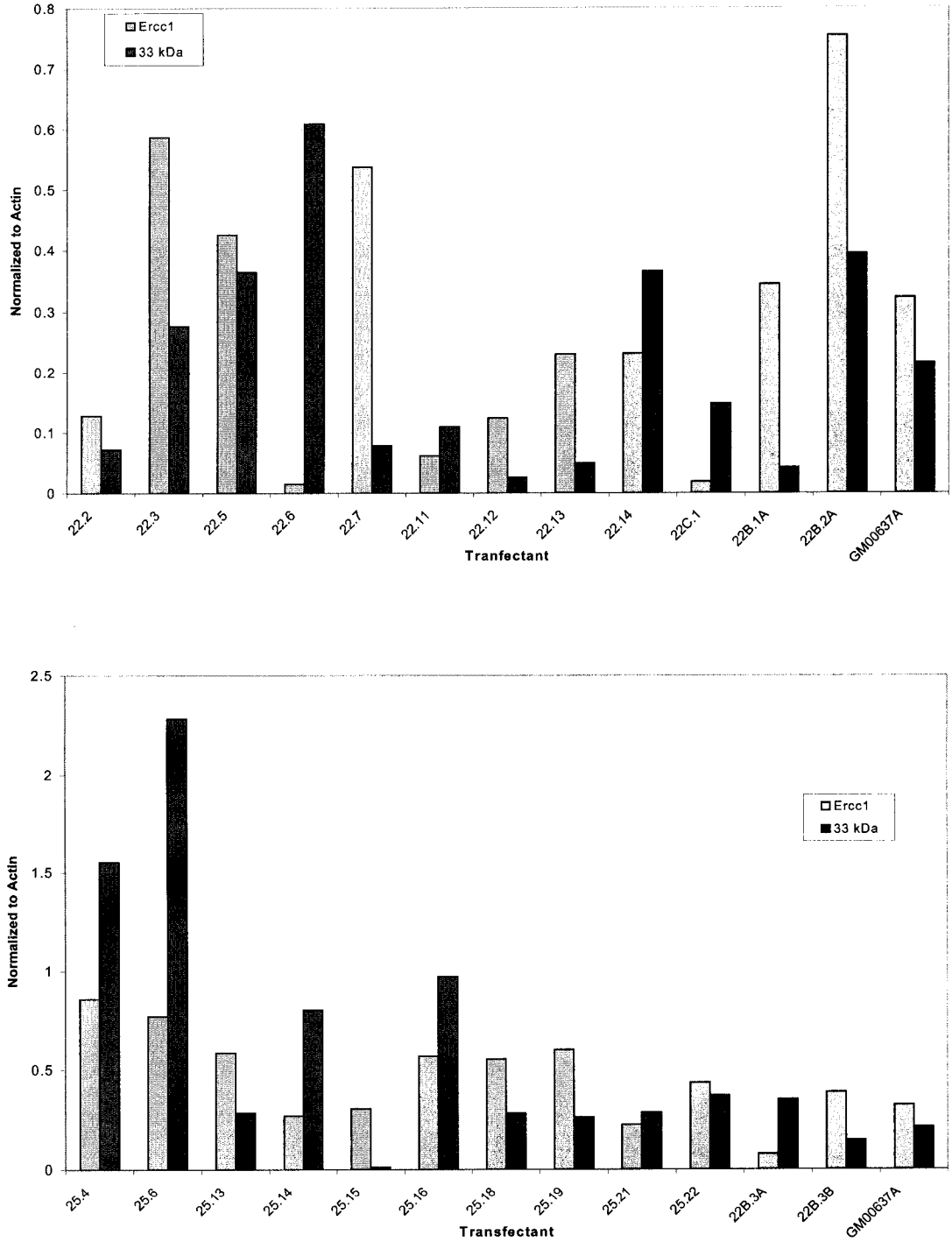

Figure 3-8. Analysis of Ercc1 and 33 kDa protein band values obtained by densitometry of Western blots of whole cell lysates from GM00637A transfectant cell lines. Protein band values were normalized to actin within each experiment. Graphs are the result of 3 separate experiments for each cell line.

3.4.2 Ercc1 protein levels in nuclear extracts

The expression of the Ercc1 protein in nuclear extracts was determined in all GM00637A transfectant cell lines, as shown in Figure 3-9. Protein bands detected in Western blots were quantitated by densitometry, and protein band intensities were normalized to actin within the same experiment and plotted in Excel (Figures 3-10). Control 22B.1A and 22B.2A cells were found to have a higher expression of the Ercc1 protein in the nucleus compared to GM00637A cells (Figure 3-10), whereas the control 22B.3A and 22B.3B cells were found to have a lower expression (Figure 3-10). The Ercc1 protein levels determined for the 22B.2A and 22B.3A cell lines in the nuclear and whole cell extracts were higher than the GM00637A cell line (see Table 3-1). However, the level of Ercc1 protein expression determined for the 22B.1A and 22B.3B cell lines in the nuclear extracts were higher and lower, respectively, than those determined in the whole cell extracts (see Table 3-1).

Table 3-1. Comparison of the relative UV-C and PM sensitivities of the control transfectant cell lines with the Ercc1 protein expression levels (in both nuclear and whole cell extracts) relative to the parental GM00637A cell line as detected by Western blotting and quantitated by densitometry.

Transfectant Cell Line	UV-C Sensitivity	PM Sensitivity	Ercc1 Protein Band Intensity	
			Whole cell extract	Nuclear extract
22B.1A	MR	N	N	H
22B.2A	HR	N	H	H
22B.3A	MR	MS	L	L
22B.3B	MR	N	N	L

The above table reflects a comparison of control transfectant cell lines to the parental GM00637A cell line. MR – modest resistance; HR – high resistance; N – approximately normal; MS – moderate sensitivity; H – high; L – low.

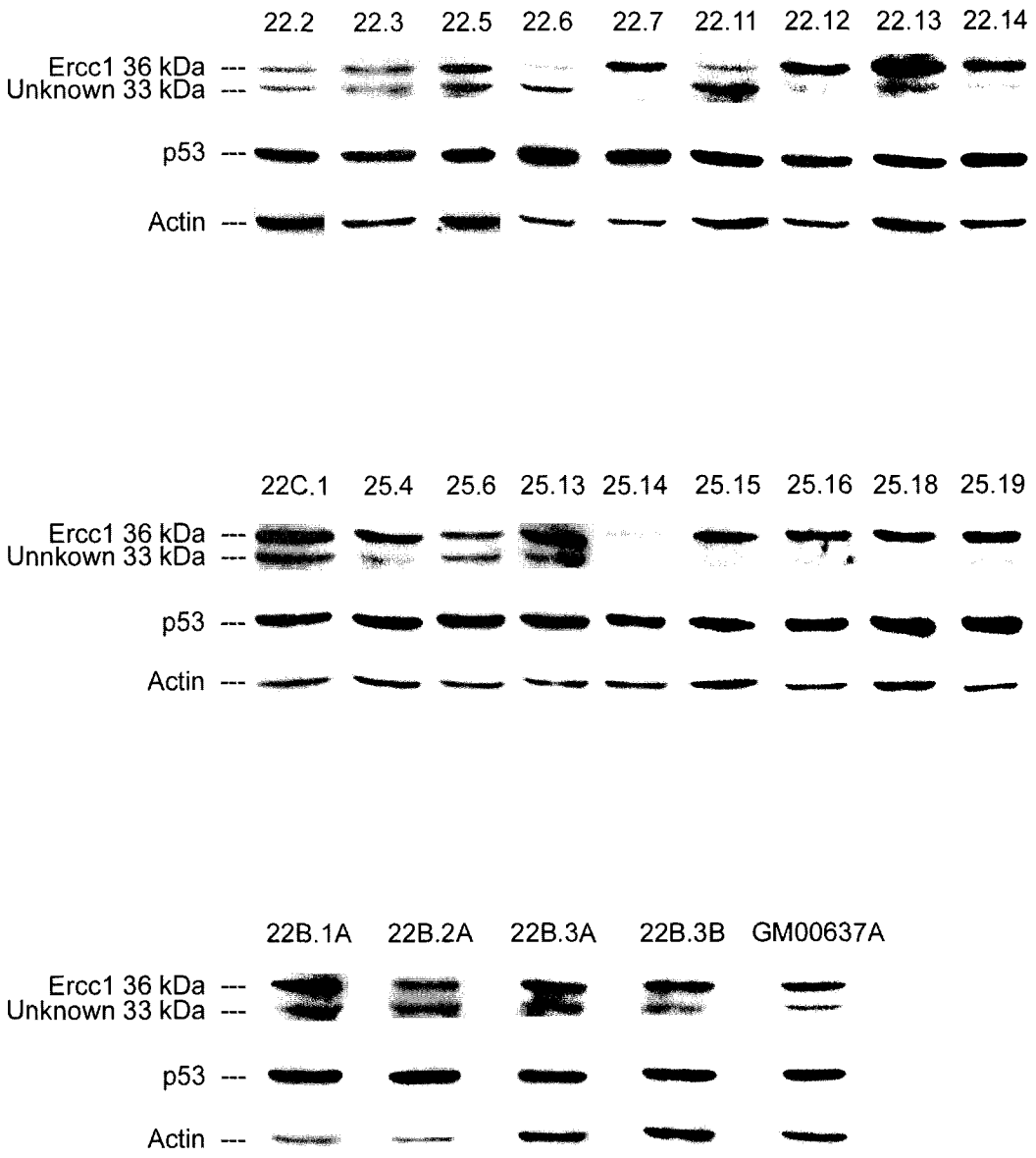

Figure 3-9. Western blot analysis of Ercc1 protein expression in nuclear extracts from GM00637A transfectant cell lines. Expression of p53 and actin were done as controls.

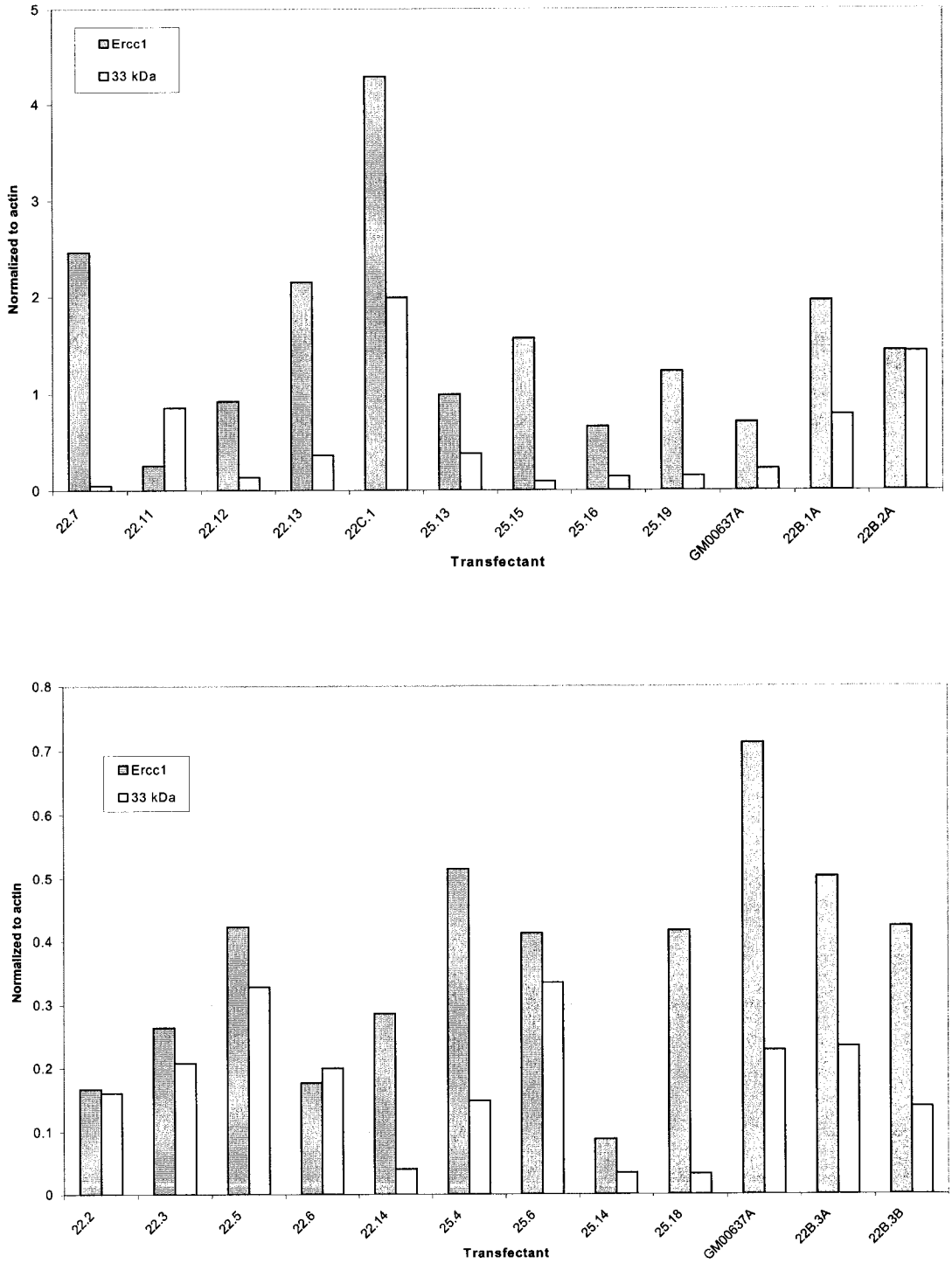

Figure 3-10. Analysis of Ercc1 and 33 kDa protein band values obtained by densitometry of Western blots of nuclear extracts from GM00637A transfectant cell lines. Protein band values were normalized to actin within each experiment. Graphs are the result of 3 separate experiments for each cell line.

The difference detected in expression levels between the nuclear and whole cell lysates of the 22B.1A and 22B.3B control cell lines, relative to the parental GM00637A cell line, could reflect differences in the amount of biologically important Ercc1 protein, as noted by Yu et al. (1998).

GM00637A cells transfected with the antisense-*ERCC1* cDNA determined to have a higher level of Ercc1 protein in the nuclear extract than the parental GM00637A cells were 22.7, 22.12, 22.13, 22C.1, 25.13, 25.15, and 25.19 (Figure 3-10). Transfectant cell lines determined to have a lower level of Ercc1 protein expression compared to GM00637A cells were 22.2, 22.3, 22.5, 22.6, 22.11, 22.14, 25.4, 25.6, 25.14, and 25.18 (Figures 3-10). The transfectant cell line 25.16 was found to have an Ercc1 protein level comparable to GM00637A cells.

3.4.3 Scatter plot analysis of Ercc1 protein expression levels relative to UV-C D_{90} and PM IC_{90} values

If the Ercc1 protein expression was being modulated through the activity of the antisense-*ERCC1* mRNA, a decrease in Ercc1 protein levels would be expected in transfectant cell lines to result in a corresponding increase in UV-C sensitivity and possibly an increase in PM sensitivity. Scatter plots were used to analyze the relationship of the UV-C D_{90} and PM IC_{90} values, determined in section 3.3.3, to the Ercc1 protein expression levels of the GM00637A transfectant cell lines (see Figures 3-11 and 3-12).

Analysis of the control transfectant cell lines revealed a possible correlation between the Ercc1 protein expression level (in both the nuclear and whole cell extracts) and UV-C resistance in the 22B.2A cell line (see Table 3-1 and Figure 3-11). The increase in the Ercc1 protein levels in nuclear or whole cell extracts of 22B.2A cells, however, was not associated with a significant alteration in PM sensitivity relative to the norm represented by GM00637A cells (see Table 3-1 and Figure 3-12). The 22B.3A control cells also appear to show a correlation between low Ercc1 protein expression (in the nuclear and whole cell extracts) and

A.

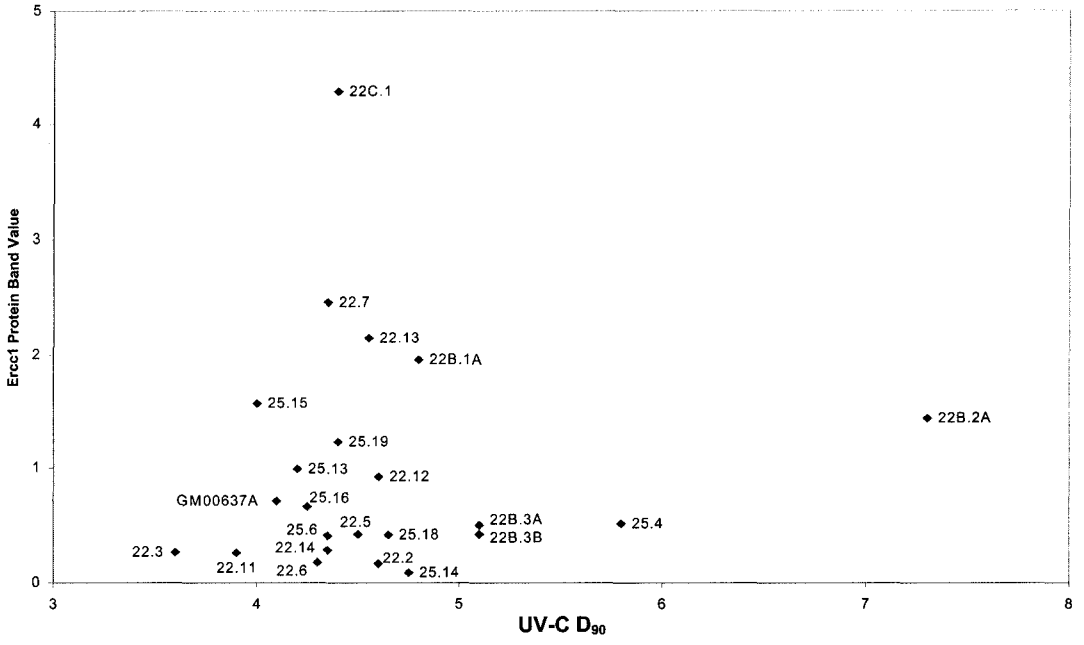

B.

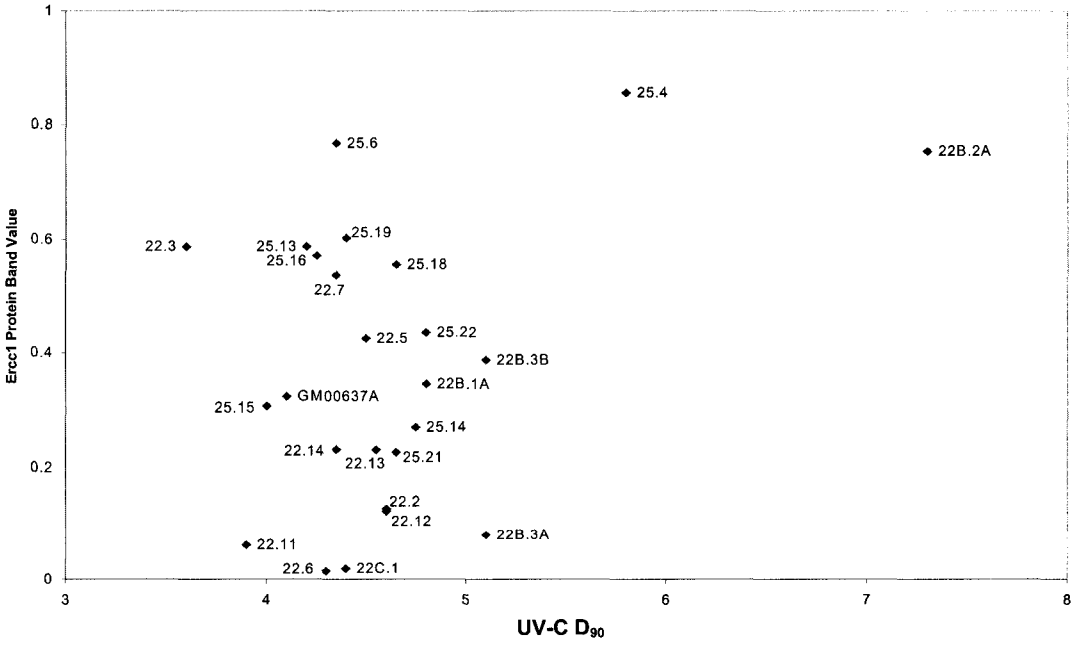

Figure 3-11. Scatter plot analysis of GM00637A transfectant Ercc1 protein band values (normalized to actin with in each experiment) from (A) nuclear extracts vs. the UV-C D_{90}, and (B) whole cell extracts vs. the UV-C D_{90} for each cell line.

A.

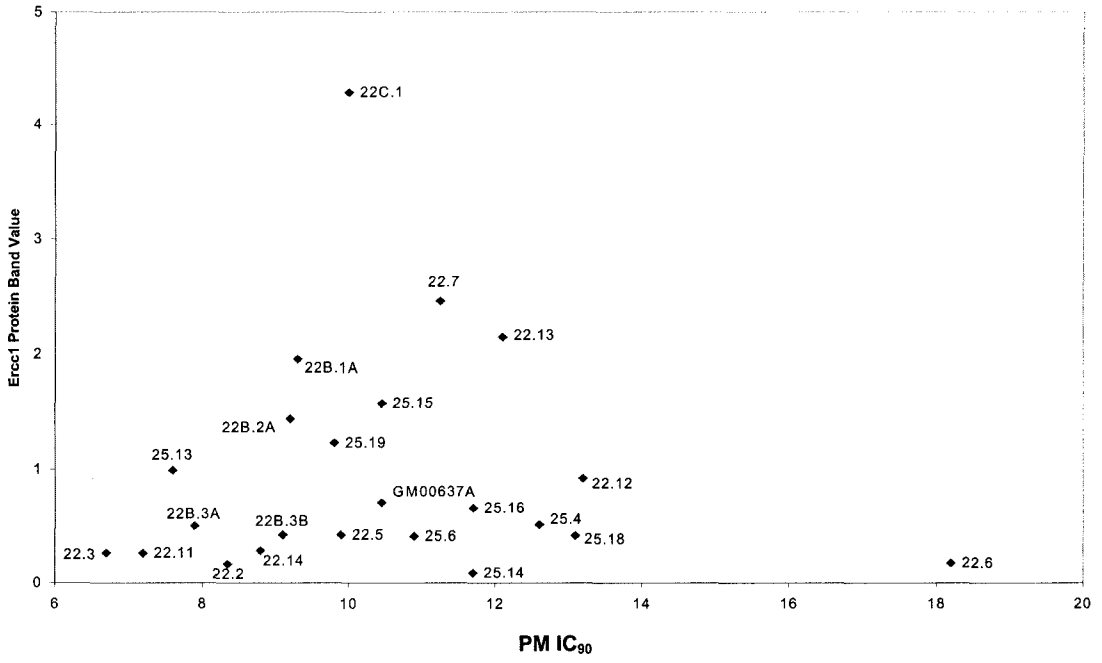

B.

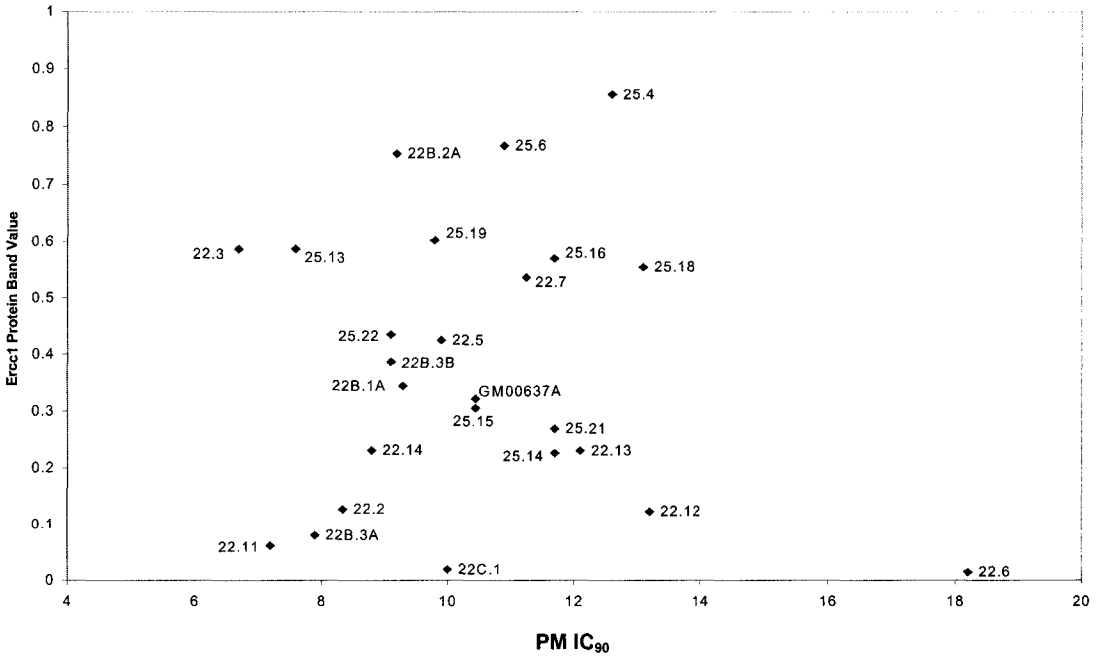

Figure 3-12. Scatter plot analysis of GM00637A transfectant Ercc1 protein band values (normalized to actin with in each experiment) from (A) nuclear extracts vs. the PM IC_{90}, and (B) whole cell extracts vs. the PM IC_{90} for each cell line.

a modest PM sensitivity, although these cells display moderate UV-C resistance (see Table 3-1 and Figures 3-11 and 3-12). The Ercc1 protein expression level in the nuclear and whole cell extracts of the other two control transfectant cell lines, however, does not appear to correlate with their respective UV-C and PM sensitivities (see Table 3-1 and Figures 3-11 and 3-12).

The UV-C sensitivity of transfectant cell lines 22.3 and 22.11 appears to correlate with low Ercc1 protein levels in nuclear extracts, however, this correlation did not extend to the whole cell extract (see Figure 3-11). A general lack of correlation between the Ercc1 protein levels, in both the nuclear and whole cell lysates, and UV-C sensitivity for the rest of the antisense transfectant cell lines can be seen in Figure 3-11. The same situation can be seen when the Ercc1 protein levels for the antisense transfectant cell lines are compared to PM sensitivity (see Figure 3-12). There appears to be a correlation between low Ercc1 protein expression levels in the nuclear extracts and high PM sensitivity for the transfectant cell lines 22.3 and 22.11, but no such correlation could be ascertained with whole cell extracts. Again, no general correlation was apparent between PM sensitivity and Ercc1 protein expression levels for the rest of the transfectant cell lines (see Figure 3-12).

3.4.4 Expression of the Ercc1-related 33 kDa protein

An unusual feature seen when using the Ercc1 monoclonal antibody from PharMingen was the appearance of a second, smaller, protein band at ~33 kDa (see Figures 3-7 and 3-9). Other researchers have also detected a smaller protein band when assessing Ercc1 protein expression. The smaller protein band was believed to be either an alternatively spliced variant or a degradation product of the Ercc1 protein (van Duin et al. 1986, Belt et al. 1991, Bramson and Panasci 1993, Yu et al. 1998, Goukassian et al. 2002). The possibility that the 33 kDa protein is an alternatively spliced variant of the Ercc1 protein could have an impact on the full-length, biologically active, Ercc1 protein expression, as suggested by Yu et

al. (1998). Thus, the expression of the 33 kDa protein in GM00637A cells and the transfectant cells was also examined.

The expression of the 33 kDa protein in Western blots of the whole cell extracts (Figure 3-7) and nuclear extracts (Figure 3-9) was quantitated by densitometry and normalized to actin within each experiment (see Figures 3-8 and 3-10). If the 33 kDa protein is an alternatively spliced variant of the Ercc1 protein that can inhibit DNA repair, as suggested by Yu et al. (1998), then some type of correlation between protein expression and UV-C or PM sensitivity might be expected. However, examination of the 33 kDa protein levels in the whole cell extracts, as well as the nuclear extracts, gave no apparent correlation with the UV-C or PM sensitivities determined in section 3.3 (see Appendix A, Figures A-5 to A-10).

If the 33 kDa protein is a degradation product of Ercc1, then the 33 kDa protein band detected in whole cell extracts (Figure 3-7) and nuclear extracts (Figure 3-9), may indicate a problem with the protein isolation procedure. This possibility is emphasized by the observed variation in the 33 kDa protein levels within a single transfectant cell line. An example would be the 25.18 cell line, where the whole cell lysate gives a definite 33 kDa band (Figure 3-7) but in the nuclear extract the 33 kDa protein band was barely detectable (Figure 3-9). It is unlikely that the Ercc1 protein is being degraded by proteases because stringent steps were taken to limit protein degradation by the addition of protease inhibitors. Sequencing of the 33 kDa protein would be required to determine whether it is either a related protein or a degradation fragment of the Ercc1 protein. If the 33 kDa protein was translated from an alternatively spliced variant of the *ERCC1* mRNA, the possibility of it acting as an inhibitor or regulator of DNA repair, as hypothesized by Yu et al. (1998), was not apparent from this study.

3.4.5 Expression of the p53 and actin proteins

The level of p53 protein in a normal non-transformed fibroblast cell line has been determined to be very low and, although the distribution of p53 can vary throughout the cell cycle, it is localized for the most part in the cytoplasm in the absence of genotoxic stress (Deppert and Haug 1986, Hess and Brandner 1997, Ozbun and Butel 1997, May and May 1999, Jiang et al. 2001). Transformation of a normal fibroblast cell line with SV40 results in an overall increase in the steady-state levels of the p53 protein due to the SV40 large T antigen binding to and sequestering the p53 protein within the nucleus (Deppert and Haug 1986, Hess and Brandner 1997, Ali and DeCaprio 2001).

As a loading control for Ercc1 immunoblotting, each blot was probed for p53 and actin proteins. Examination of whole cell extracts and nuclear extracts of GM00637A transfectant and the parental GM00637A cells, seen in Figures 3-7 and 3-9 reveals a very high level of p53 protein expression, which is as expected for an SV40-transformed cell line. The p53 protein expression was determined in the GM00637A transfectant cell lines as a positive control to confirm a high level of expression that would be expected to be similar between each cell line.

Actin was used as an internal loading control for all protein analyses. The level of actin protein in both the whole cell extracts and the nuclear extracts of all GM00637A transfectant cells, as well as the parental GM00637 cell line (see Figures 3-7 and 3-9) appears to be similar between each cell line.

3.5 Cyclohexamide time course assay

The inability to effect a decrease in Ercc1 protein levels with a corresponding increase in either UV-C/PM sensitivity in the GM00637A transfectant cells could be the result of a high degree of Ercc1 protein stability. In some CHO *ERCC1*$^{-}$ mutant cell lines and the XPF cell line XP2YO(SV), low levels of Ercc1 protein expression that result in residual NER

may be sufficient for normal ISC repair (van Vuuren et al. 1993, Brookman et al. 1996, Sijbers et al. 1996a, Yagi et al. 1997, 1998a, 1998b, Matsumura et al. 1998, Zhang et al. 2000, Gaillard and Wood 2001). If the Ercc1 protein is highly stable then this could directly influence NER and ISC repair. Such an increase in Ercc1 protein stability may be related to the SV40-transformation of the parental GM00637A cell line. Fanning and Knippers (1992) noted that transformation of a cell line with SV40 could affect a number of cellular proteins. To determine if the Ercc1 protein stability has been affected by SV40-transformation, the Ercc1 protein half-life was measured in both the SV40-transformed GM00637A and non-transformed GM38 human fibroblast cell lines using cyclohexamide. Cyclohexamide inhibits protein synthesis by binding the 60S subunit of the ribosome, thereby blocking the translocation step of translation (Kendrew and Lawrence 1994). The use of cyclohexamide to determine the rate of protein turnover has been found to give similar results to ^{35}S-methionine labeled proteins measured within a 4 h time course (Pan and Haines 1999).

3.5.1 GM38 time course : 0–48 h

The cyclohexamide time course assay using GM38 cells to determine the Ercc1 protein half-life is shown in Figure 3-13A. Nuclear extracts were analyzed for Ercc1, Xpf, p53 and actin protein expression by Western blotting. The protein band intensities were quantified by densitometry, normalized to actin, and then normalized to the initial band value (Figure 3-13B). As seen in Figure 3-13B, the Ercc1 protein expression significantly decreases to less than half its initial value by 2 h and there is little change at 4 h.

The 33 kDa protein detected in this assay does not appear to change appreciably, although it must be stressed that this is only a single experiment (see Figure 3-13).

The Xpf protein was also assessed for its half-life in GM38 cells. In Figure 3-13B, the Xpf protein expression can be seen to decrease to less than half of the initial value at 4 h.

The p53 protein was analyzed as a positive control because the protein half-life has been well documented (Reich et al. 1983, Caelles et al. 1994, Maki and Howley 1997, Ozbun

A.

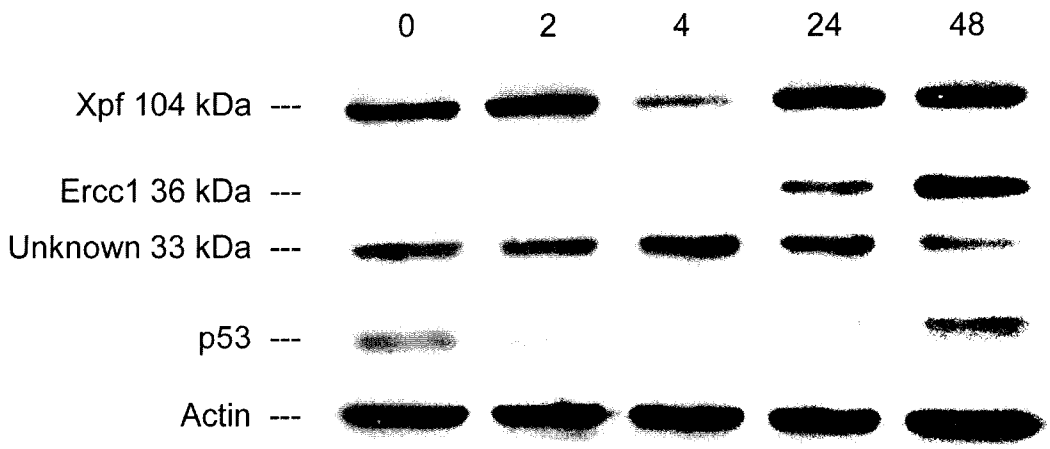

B.

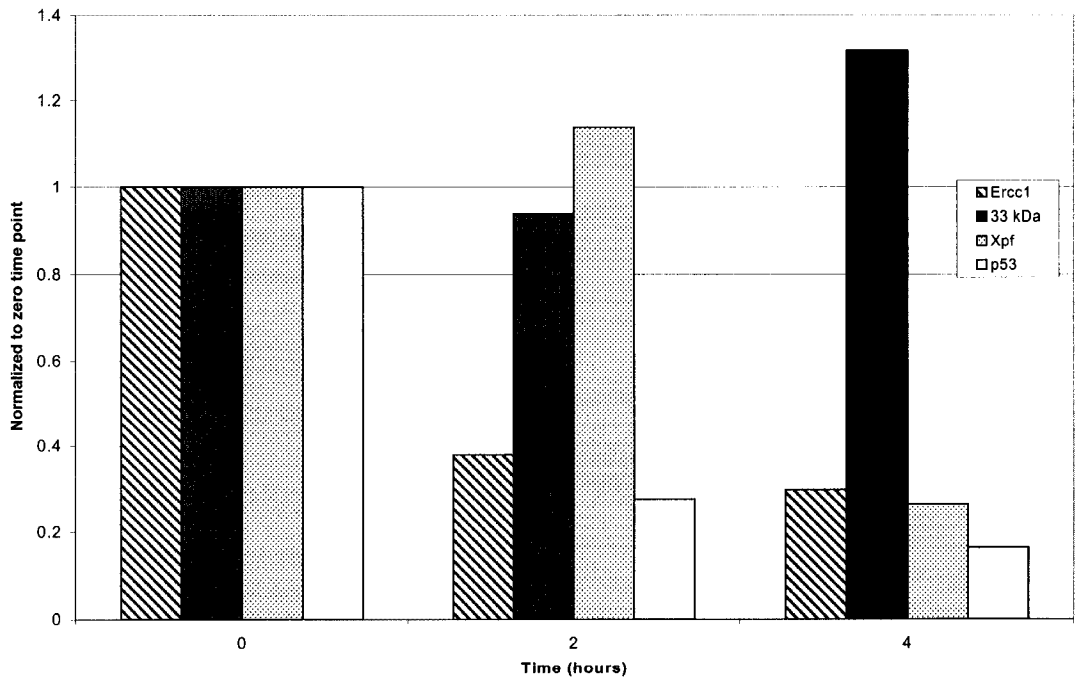

Figure 3-13. Cyclohexamide time course assay with GM38 nuclear extracts from 0-48 h. (A) Expression of Ercc1 and Xpf proteins detected by Western blotting. Expression of p53 and actin proteins were done as controls. (B) Analysis of protein band values for Ercc1, 33 kDa, Xpf, and p53. Time points were normalized to the zero time point after normalization to the actin protein within each sample. Only time points up to 4 h were plotted.

and Butel 1997). The half-life of the p53 protein has been determined to be 20–40 min in a normal non-transformed cell line (Ozbun and Butel 1997). As expected, p53 protein expression was seen to decrease to less than half the initial value at 2 h (the earliest time point studied) in GM38 cells (Figure 3-13B). This would also indicate that the concentration of 20 μg/ml cyclohexamide used for the time course assay was sufficient to allow measurement of protein half-life. A cyclohexamide concentration as low as 10 μg/ml has been previously shown to give ~95% inhibition of protein synthesis within 30 min as measured by ^{35}S-methionine incorporation into total cellular protein (Caelles et al. 1994).

A dramatic increase in protein levels was observed at 24 h and 48 h for all proteins except the 33 kDa protein, which appeared to decrease at 48 h (Figure 3-13A). The increase in specific protein levels at the later time points is probably an artifact of loading the gels on the basis of protein concentration, which will generate artifacts due to both enrichment and saturation. This experimental protocol should lead to the enrichment of proteins that are degraded slowly. Saturation would occur when proteins are no longer degraded because the proteases themselves may have a limited half-life or are limited in activity due to lack of cofactors. Thus an equilibrium would be achieved between the proteins being degraded and the proteases that degrade them.

3.5.2 GM00637A time course: 0–6 h

Since the Ercc1 protein half-life appeared to be between 0–2 h for GM38 cells (Figure 3-13B), the Ercc1 protein half-life within GM00637A cells was determined using a cyclohexamide time course assay over a period of 0–6 h (Figure 3-14A). Whole cell extracts were analyzed for Ercc1, Xpf, p53, and actin protein expression by Western blotting. Protein band intensities were quantified by densitometry, normalized to actin and then normalized to the initial band value (Figure 3-14B). The Ercc1 protein level drops slightly at 0.5 h, a level that remains relatively unchanged at 6 h (see Figure 3-14B).

A.

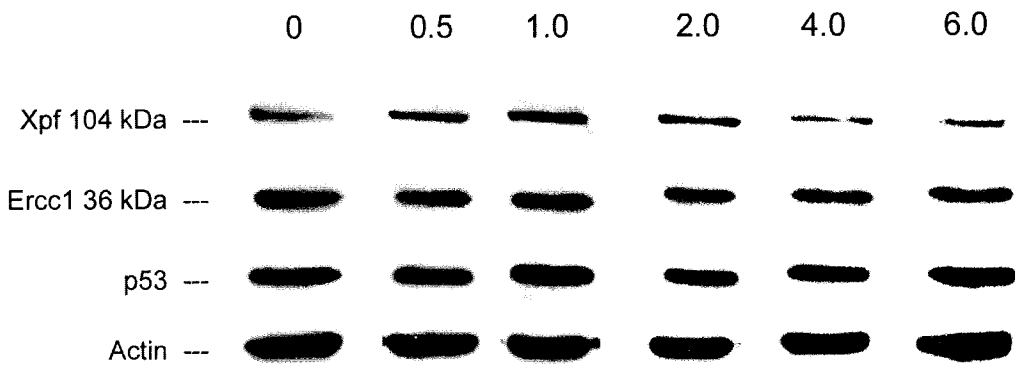

B.

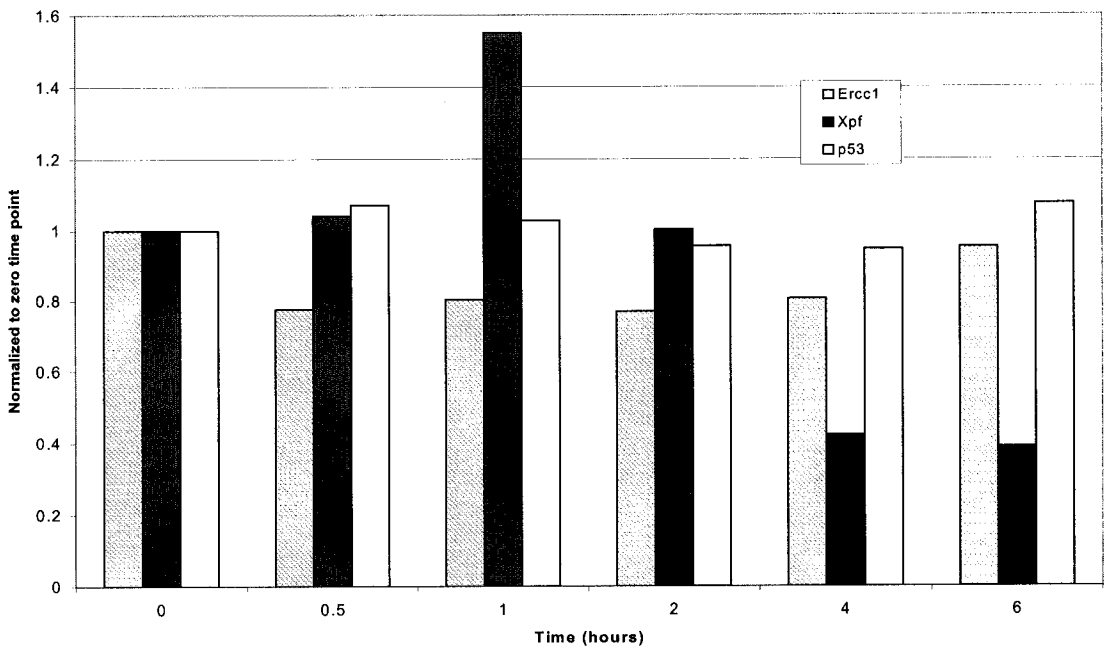

Figure 3-14. Cyclohexamide time course assay with GM00637A whole cell extracts from 0-6 h. (A) Expression of Ercc1 and Xpf proteins detected by Western blotting. Expression of p53 and actin proteins were done as controls. (B) Analysis of protein band values for Ercc1, Xpf, and p53. Time points were normalized to the zero time point after normalization to the actin protein within each sample. The graph represents 3 separate experiments.

The lack of a significant decrease to half the initial value for the Ercc1 protein in GM00637A cells in this assay would suggest an increase in the Ercc1 protein stability when compared to GM38 cells where the Ercc1 half-life is <2 h (see Figure 3-13B). Therefore, it would seem that SV40-transformation of GM00637A cells might impact the stability of the Ercc1 protein.

Analysis of Xpf protein expression in the whole cell extracts of GM00637A cells (see Figure 3-14B) reveals an increase at 1 h and then a decrease to less than half the zero time point at 4 h. The half-life of the Xpf protein in GM00637A cells (2-4 h) is very similar to the half-life (2-4 h) observed in the GM38 cell line (see Figure 3-13B). The consistent finding for the Xpf protein between the non-transformed GM38 cell line and the SV40-transformed GM00637A cell line would imply that the Xpf protein stability is unaffected by transformation with SV40 regardless of the increase seen in the Ercc1 protein stability.

Several researchers have observed that transformation of a cell line with SV40 can result in an increased stability of the p53 protein, resulting in a half-life that can exceed 22 h (Reich et al. 1983, Caelles et al. 1994, Hess and Brandner 1997). The p53 protein expression in the whole cell extracts as seen in Figure 3-14B, remained relatively unchanged over the 6 h time frame compared to the GM38 cell line ($t_{1/2}$=<2 h), which is as expected for an SV40-transformed cell line.

3.6 Genomic DNA – PCR

Stable expression of the pD3 vector or pD3αE1 construct within the GM00637A transfectant cell lines would be expected to result in transfectants that retain the G418 resistance gene of the pD3 vector given that the isolation of the cell lines was achieved using G418 selection medium. However, it cannot be automatically assumed that the rest of the pD3 vector or the antisense-*ERCC1* cDNA insert within the MCS of pD3 were also integrated into the genome of a particular transfectant cell line. In order to determine if the antisense-*ERCC1* cDNA insert was integrated into the genome of a transfectant cell line, PCR was

performed on genomic DNA. The PCR reaction involved the use of the T7 and Sp6 promoter primers that bind to the respective sequences that flank the MCS of the pD3 vector (see Figure 2-1C). PCR products were separated on agarose gels and the antisense-*ERCC1* cDNA insert was detected as a 775 bp band (Figure 3-15). The MCS, without the antisense-*ERCC1* cDNA, of the pD3 vector (control) would be detected as a 146 bp band in the control PCR of pD3/*Pvu* I (Figure 3-15); however, no band at 146 bp was detected within the control transfectant cell lines (22B.1A, 22B.2A, 22B.3A, and 22B.3B). This would suggest that the control transfectant cell lines have a stable integration of only the G418 resistance gene based on their ability to grow in G418 medium.

All transfectant cell lines containing the pD3αE1 construct show the presence of the 775 bp band (see Figure 3-15). Detection of the 775 bp band verifies that the antisense-*ERCC1* cDNA insert within the MCS, the T7 and Sp6 promoters that flank the MCS, and the G418 resistance gene of the pD3αE1 construct were integrated into the genome of the GM00637A cell line. These results do not, however, allow for the determination of the orientation of integration, location of integration, the number of copies of the vector that may have been integrated, or the level of antisense-*ERCC1* mRNA transcription.

3.7 Southern blotting

Verification by PCR that the antisense-*ERCC1* cDNA insert is present within the genomic DNA of the transfectant cell lines, other than the control transfectant cell lines, confirms that at least one copy of the antisense-*ERCC1* cDNA insert is present within their genome. The genomic DNA of each transfectant was analyzed by Southern blotting to determine the number of copies of the pD3αE1 construct that may have integrated (Figure 3-16). Since the vector randomly integrates, the number of copies that integrate within the genome can greatly affect the transfectant cell line depending on the integration site(s).

The genomic DNA from each of the transfectant cell lines was isolated and restricted with *Bam* HI. The *Bam* HI restriction enzyme results in a single cut within the MCS of the

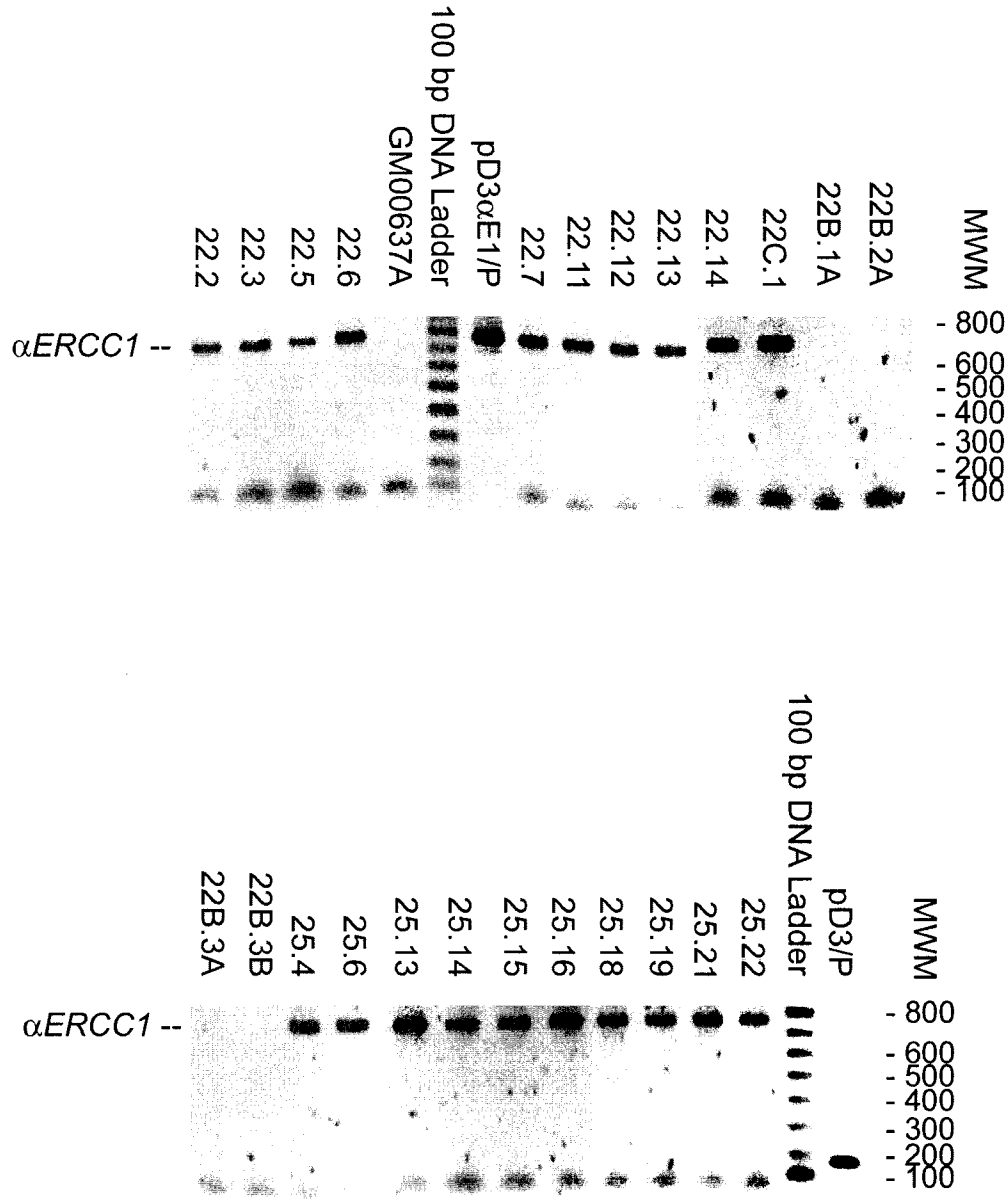

Figure 3-15. PCR amplification of antisense-*ERCC1* cDNA using genomic DNA from GM00637A transfectant cell lines. The T7 and Sp6 promoter primers were used in the PCR reaction and the α*ERCC1* cDNA insert was detected as a 775 bp band. Controls were the GM00637A cell line, pD3αE1/P construct and pD3/P vector. MWM – 100 bp molecular weight ladder (Amersham Pharmacia Biotech). Abbreviations are P – *Pvu* I and α*ERCC1* – antisense-*ERCC1* cDNA.

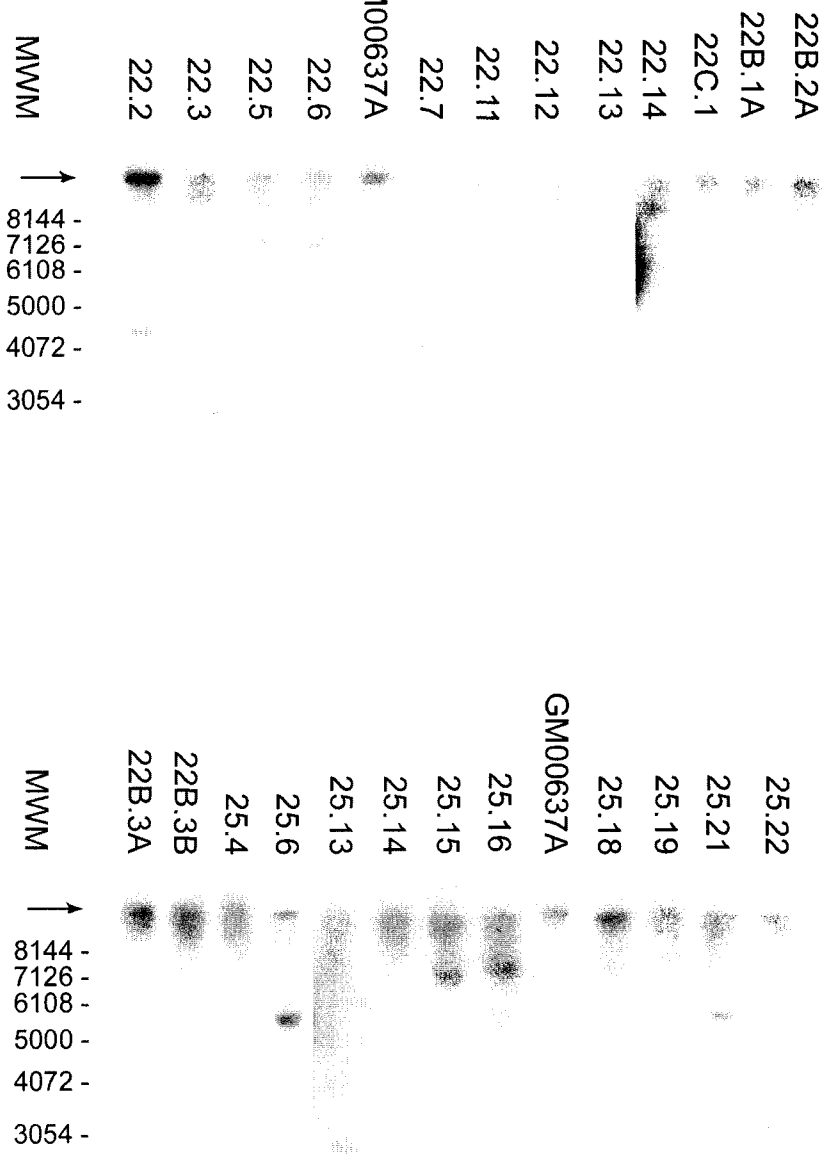

Figure 3-16. Southern blot analysis for antisense-*ERCC1* cDNA in genomic DNA restricted with *Bam* HI for GM00637A transfectant cell lines. Bands detected using an antisense-*ERCC1* probe made by random priming with the T7 promoter primer. MWM – 1 kb Plus DNA ladder (Life Technologies, Rockville, Maryland, USA). Arrow indicates the location of the >10 kb band.

pD3 vector on the 3′ end of the antisense-*ERCC1* cDNA insert (see Figure 2-1C). The restricted genomic DNA was run on an agarose gel, transferred to a Hybond-N+ nylon membrane, and blotted with a T7 probe generated by single strand synthesis with ^{32}P using *ERCC1* cDNA. As seen in Figure 3-16, a single band at >10 kb can be seen for GM00637A cells, indicating the presence of the endogenous *ERCC1* gene. The transfectant cell lines 22C.1 and 25.14, however, show **only** the >10 kb band which corresponds to the endogenous *ERCC1* gene. In these cases, the antisense-*ERCC1* cDNA is likely co-migrating with the endogenous *ERCC1* gene considering that PCR with genomic DNA in Figure 3-15 showed a band for the antisense-*ERCC1* cDNA insert in both of these cell lines as well. Therefore, based on these results, the cell lines 22C.1 and 25.14 may be considered to have at least one copy of the antisense-*ERCC1* cDNA insert. All other transfectant cell lines can be seen to have the >10 kb band as well as other smaller bands, which suggests the presence of more than one integrated copy of the vector construct in addition to any at >10 kb. It is possible that the pD3αE1 construct has integrated as a tandem repeat, and when cut with *Bam* HI this would be equivalent to ~6.0 kb. As seen in Figure 3-16, both the 25.21 and 25.6 cell lines have a band that corresponds to ~6.0 kb, which may indicate >1 copy of the pD3αE1 construct integrated into the GM00637A genome in this way. DNA bands smaller than ~6.0 kb may indicate partial integration of the pD3αE1 construct and could include the G418 resistance gene (based on selection with G418) and the antisense-*ERCC1* cDNA insert, the size of which would be between 3-5 kb. Unfortunately, use of a single restriction enzyme only enables detection of the antisense-*ERCC1* cDNA in conjunction with the genomic DNA it is associated with. Therefore, the >10 kb band detected in all transfectants could represent >1 copy of the antisense-*ERCC1* cDNA but without the use of a second restriction enzyme (that does not cut within the antisense-*ERCC1* cDNA) it is difficult to determine an actual number of integrated copies. The Southern blot in this case also does not allow for the determination of the vector integration sites within the GM00637A genome; or whether the vector has integrated with the CMV promoter intact, or in which direction the

vector has integrated into the genome. A possible method to determine the location of the integrated vector within a particular transfectant cell line would be the use of FISH (fluorescence in situ hybridization).

3.8 RT-PCR of antisense-*ERCC1* mRNA

RT-PCR was performed to determine if the antisense-*ERCC1* cDNA within each of the transfectant cell lines was expressed as mRNA. Total RNA was used in the reverse transcription reaction to produce single stranded DNA. The resulting single stranded DNA was in turn used in a PCR reaction with the T7 and Sp6 promoter primers that bind to the respective sequences that flank the MCS of the pD3 vector (see Figure 2-1C). The products of the PCR reaction were separated on an agarose gel, an example of which can be seen in Figure 3-17. All transfectant antisense and control cell lines can be seen in Figure 3-18. The antisense-*ERCC1* mRNA was detected as a 775 bp band and the β-*actin* mRNA control was detected as a 626 bp band. As expected, GM00637A and the empty vector control cell lines do not generate the 775 bp band, although the control transfectant cell line 22B.3B does show a band of ~100 bp which may indicate expression of the pD3 MCS. RT-PCR confirms the presence of the antisense-*ERCC1* mRNA expression in all of the transfectant cell lines as seen by the presence of the 775 bp band (see Figure 3-18). The exception is the 25.13 cell line in which the 775 bp band is absent; however, the lack of a 775 bp band in this case does not appear to be due to a lack of mRNA (in general) since the β-*actin* control resulted in a definite 626 bp band.

3.9 Actinomycin D time course assay

At the time the cyclohexamide time course assay was performed, it was unknown if the stability of either the *ERCC1* mRNA or Ercc1 protein had been altered in the SV40-transformed GM00637A cell line. As with protein stability, the stability of certain mRNA transcripts in SV40-transformed cells can also be affected (Fanning and Knippers 1992).

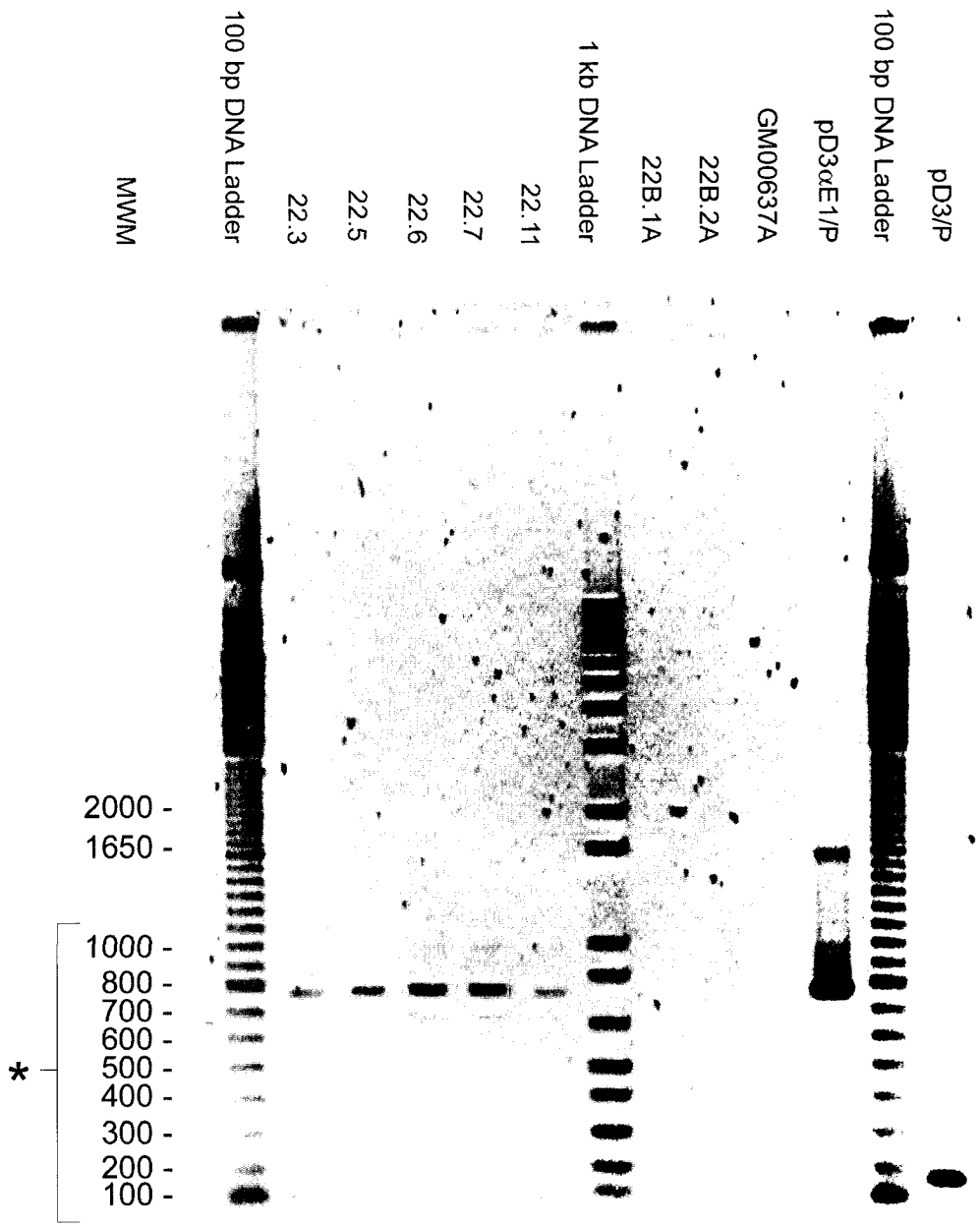

Figure 3-17. Example of a 0.8% agarose gel with RT-PCR reactions of total RNA from transfectant cell lines using the T7 and Sp6 promoter primers for detection of the antisense-*ERCC1* mRNA. Area of interest is the bottom third of the gel (*). MWM – 100 bp molecular weight ladder (Amersham Pharmacia Biotech).

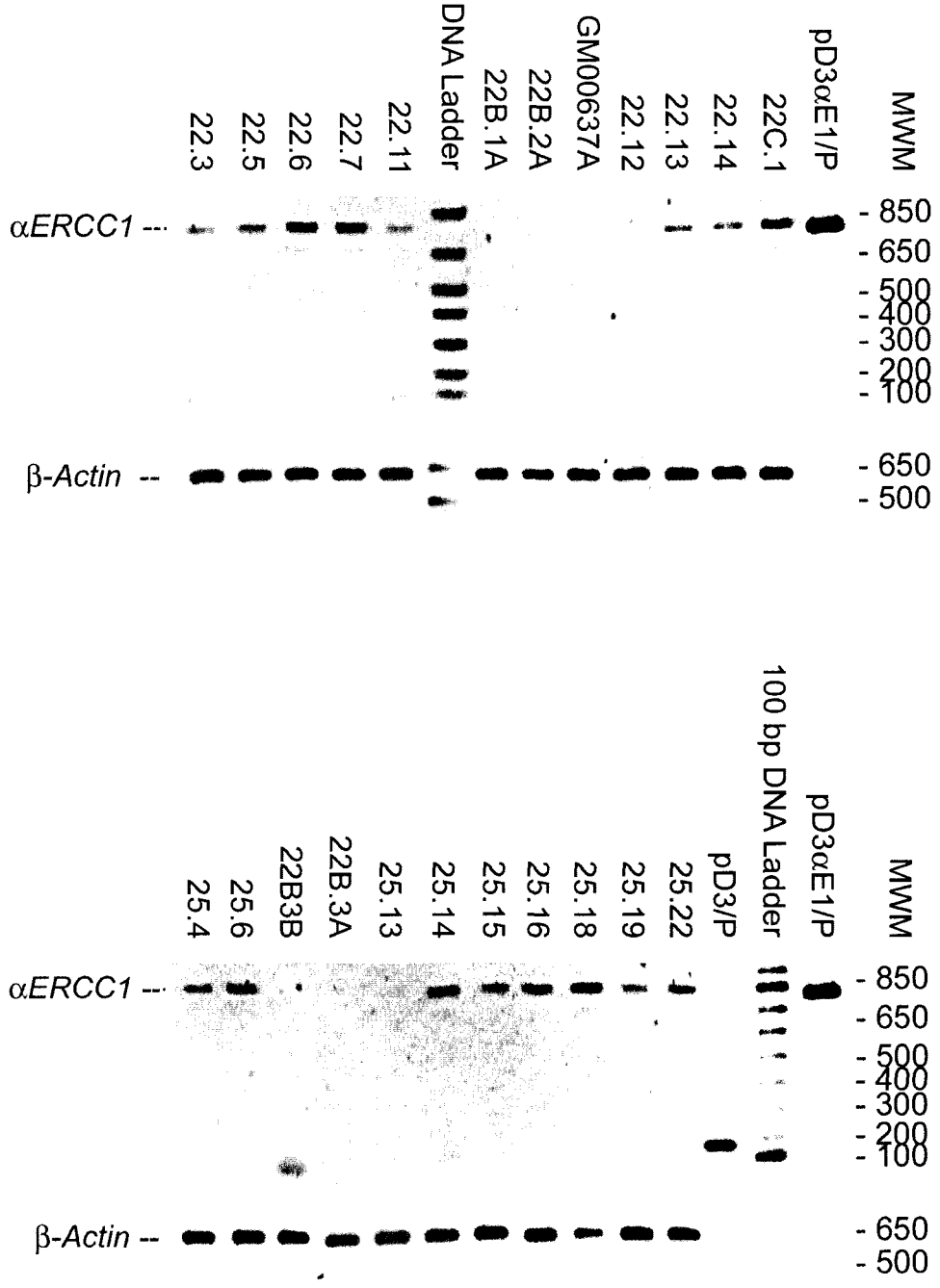

Figure 3-18. RT-PCR reactions for antisense-*ERCC1* mRNA in GM00637A transfectant cell lines using the T7 and Sp6 promoter primers. Antisense-*ERCC1* mRNA was detected as a 775 bp band. RT-PCR of total RNA for β-*actin* mRNA expression was done as a control. MWM – 100 bp molecular weight ladder (Amersham Pharmacia Biotech).

Fanning and Knippers (1992) noted that the SV40 large T antigen has an associated RNA helicase activity that may somehow be involved in translational regulation by resolving double-stranded regions in certain mRNA species. Reich et al. (1983) demonstrated in SV40-transformed mouse cells that high levels of p53 protein expression was due to high *p53* mRNA expression that resulted from the regulation of the rate of either mRNA transcription or turnover. Thus, it became relevant to determine the stability of the *ERCC1* mRNA in the SV40-transformed GM00637A cell line in conjunction with the cyclohexamide time course assay.

The *ERCC1* mRNA half-life was determined in non-transformed (GM38) and SV40-transformed (GM00637A) human fibroblast cell lines using actinomycin D in a time course assay. Actinomycin D inhibits transcription by forming a non-covalent complex with DNA by intercalation, thereby preventing the movement of the DNA-dependent RNA polymerase along the template by steric hindrance (Kendrew and Lawrence 1994). A concentration of 5 μg/ml actinomycin D has previously been shown to result in a 94% inhibition of RNA transcription (Chrzanowska-Lightowlers et al. 1994). In each of the time course assays total RNA was extracted, run on a denaturing gel, and transferred to a Hybond-N+ membrane. The *ERCC1* mRNA bands were detected using an *ERCC1*-specific cDNA probe, and quantified by densitometry. The band intensities were normalized to β-*actin* mRNA within each time point then normalized to the initial band value, and graphed in Excel.

3.9.1 GM38 time course of *ERCC*1 mRNA levels (0–24 h)

The Northern blot for the GM38 time course assay from 0-24 h can be seen in Figure 3-19A. The quantified *ERCC1* mRNA band intensities for the GM38 cell line, seen in Figure 3-20A, show the *ERCC1* mRNA decreases to less than half of the initial intensity at 2.0 h. There is a continual decrease in *ERCC1* mRNA expression to ~10% of the initial value at 4 h and to a barely detectable level at 24 h (Figures 3-19A and 3-20A). This was a somewhat unexpected result since Li et al. (1998) had previously reported the *ERCC1* mRNA half-life in

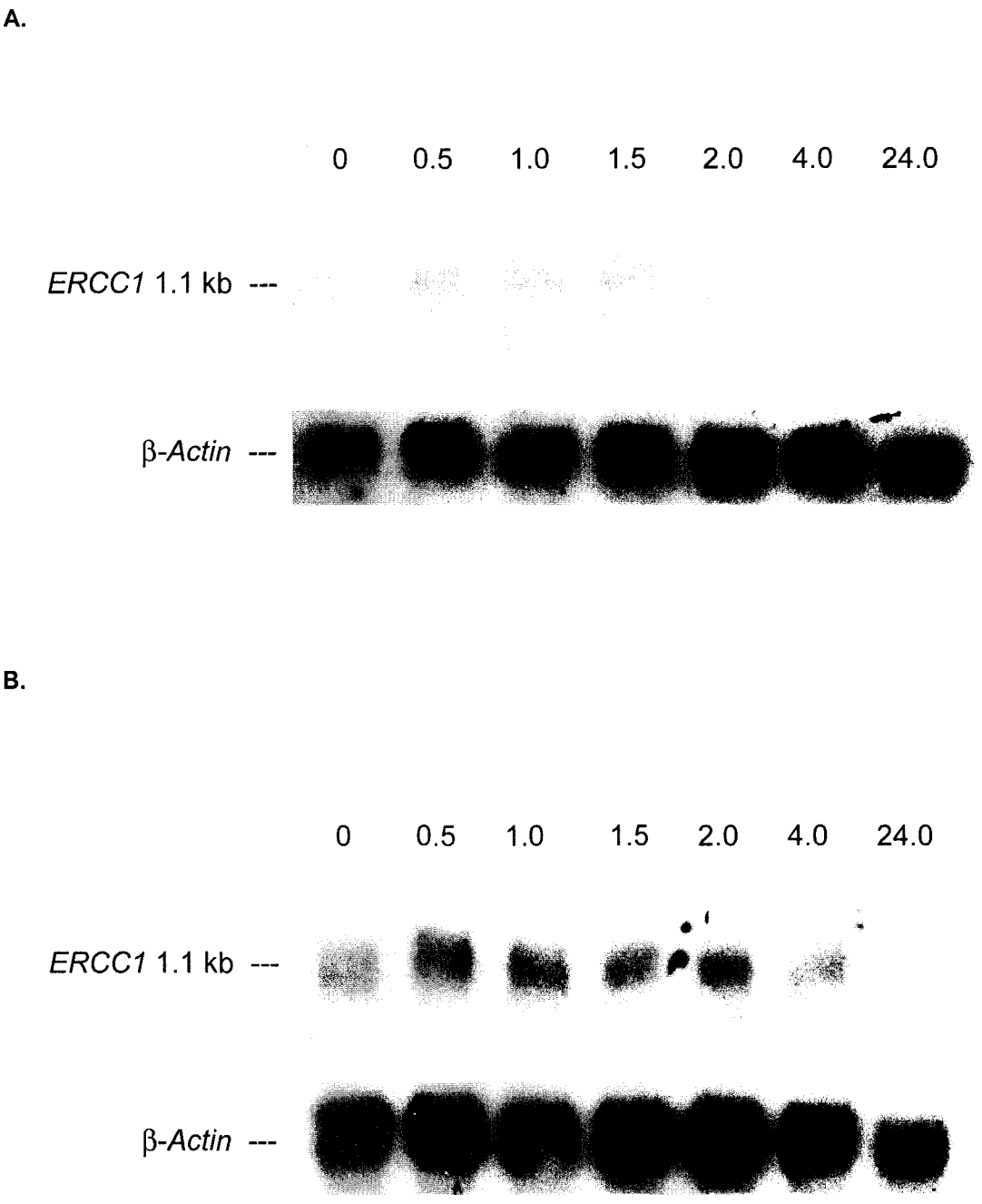

Figure 3-19. Northern blot analysis for *ERCC1* mRNA from actinomycin D time course assays with GM38 (A) and GM00637A (B) cells from 0-24 h. Expression of β-*actin* mRNA was measured as a control.

A.

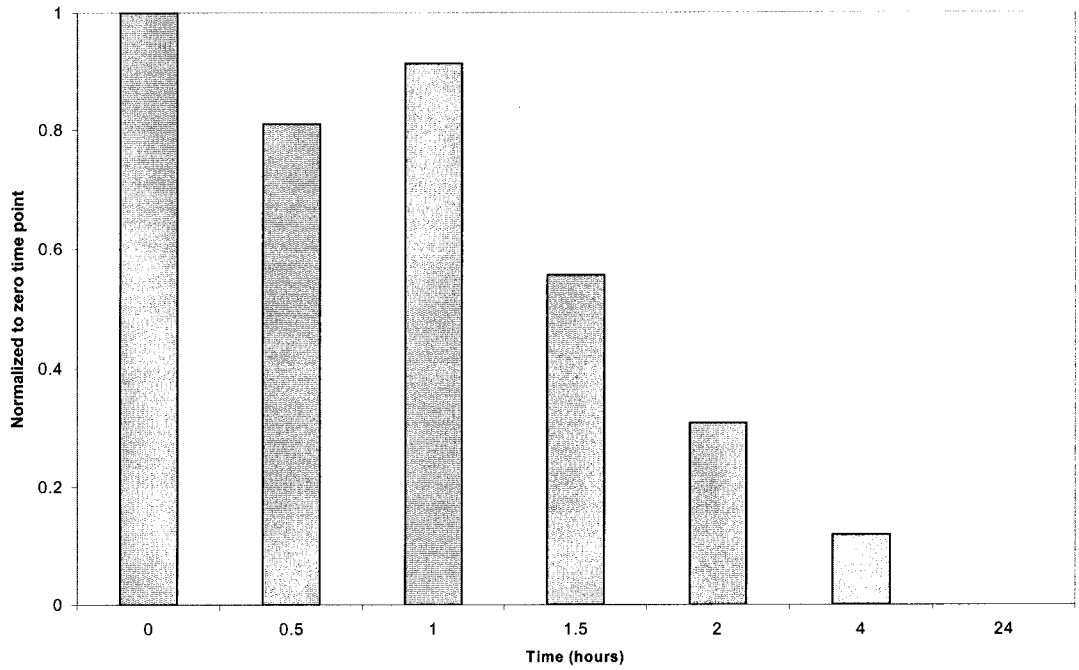

B.

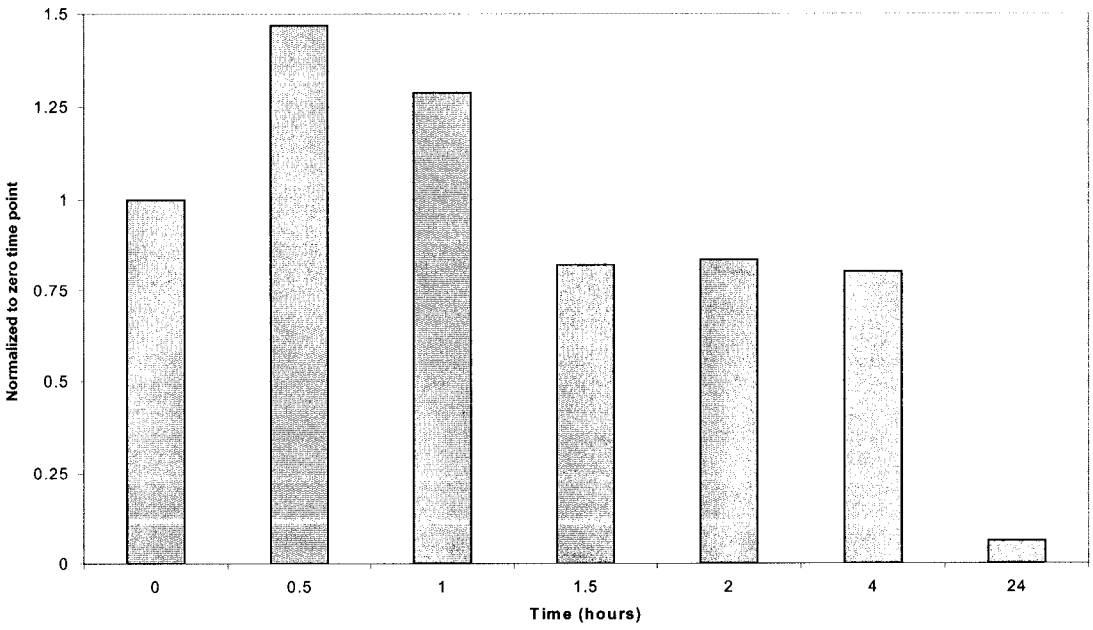

Figure 3-20. Analysis of *ERCC1* mRNA levels for actinomycin D time course assays with GM38 (A) and GM00637A (B) cell lines from 0-24 hours. Time points were normalized to the zero time point after normalization to the β-*actin* mRNA within each sample. Each graph represents one experiment.

human ovarian carcinoma cells to be much longer, on the order of 15 h.

3.9.2 GM00637A time course of *ERCC1* mRNA levels (0–24 h)

If cell transformation is an important determinant of *ERCC1* mRNA stability, then it is plausible that the SV40-transformed GM00637A cells could have *ERCC1* mRNA with an increased stability. Figure 3-19B shows a Northern blot for the actinomycin D time course assay over 0–24 h for GM00637A cells. When the band intensities were quantified by densitometry and graphed (Figure 3-20B), the *ERCC1* mRNA shows a large increase at 0.5 h with a gradual decrease at 1.5 h, after which levels remain relatively unchanged until a dramatic decrease at 24 h. The initial increase in the *ERCC1* (1.1 kb) transcript could be the result of post-transcriptional modification of larger *ERCC1* transcripts (3.8 and 3.4 Kb) that are known to exist in transformed (HeLa) and normal cells (van Duin et al. 1986). The increased half-life seen with the *ERCC1* mRNA from the GM00637A cells was as expected, and seems to indicate that the SV40-transformation of this cell line may indeed have a major effect on *ERCC1* mRNA stability when compared to the GM38 cell line.

3.9.3 GM00637A Time Course of *ERCC1* mRNA Levels (0–12 h)

To further define the *ERCC1* mRNA half-life in the GM00637A cell line, a 0–12 h time course assay was performed (Figure 3-21). The *ERCC1* and β-*actin* mRNA bands detected in Northern blots (Figure 3-21) were quantitated by densitometry and the band intensities were graphed separately as seen in Figure 3-22. The β-*actin* mRNA was originally detected as a control against which the *ERCC1* mRNA could be normalized, however, as seen in Figures 3-21 and 3-22B, there is an obvious decrease in the level of β-*actin* mRNA over the 12 h time period. The β-*actin* mRNA expression becomes approximately half the initial value at 8 h. Comparison of the β-*actin* mRNA half-life with other published values is not particularly informative since there is the complication of dependence on cell type and intracellular concentrations of polymerized vs. heteromeric proteins (Chrzanowska-

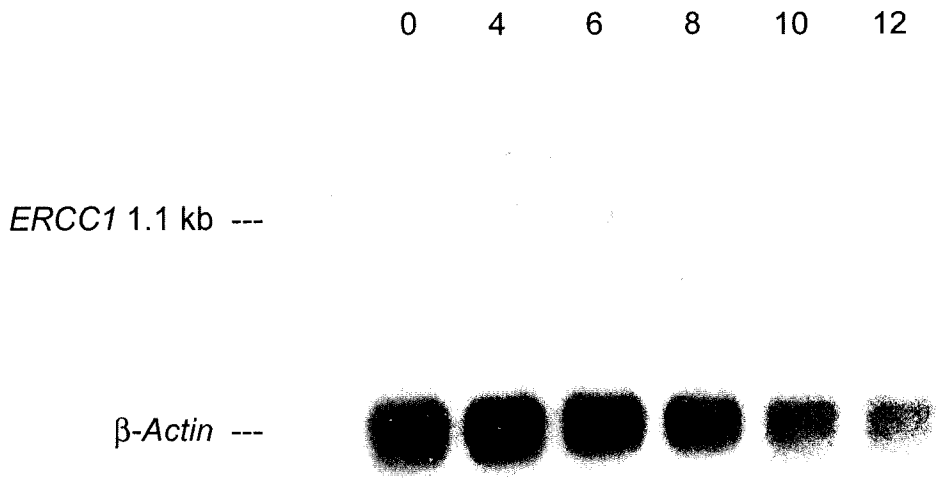

Figure 3-21. Northern blot for *ERCC1* mRNA from an actinomycin D time course assay with GM00637A cells from 0-12 h. Expression of *ERCC1* mRNA was detected by Northern blotting. Expression of β-*actin* mRNA was done as a control.

Lightowlers et al. 1994).

The level of *ERCC1* mRNA expression can be seen in Figure 3-22A to decrease to less than half the initial value at 8h and remains unchanged at 12 h. From the data obtained, the apparent *ERCC1* mRNA half-life in GM00637A cells is between 6 h and 8 h, indicating that the *ERCC1* mRNA is very stable when compared to this mRNA in GM38 cells ($t_{1/2}$ = 1.5-2.0 h). The increase in *ERCC1* mRNA stability seen in the GM00637A cell line in this study, and the *ERCC1* mRNA half-life ($t_{1/2}$ = 15 h) reported by Li et al. (1998), would imply that the transformation state of a cell can have a major impact on *ERCC1* mRNA stability, and possibly on Ercc1 protein levels. When comparing the GM00637A and GM38 cell lines, it is important to remember that they are not isogenic. That is, the GM00637A cell line is **not** the SV40-transformed product of the GM38 cell line. In order to determine the impact of SV40-transformation on *ERCC1* mRNA stability it would be prudent to use related cell lines, i.e., a

A.

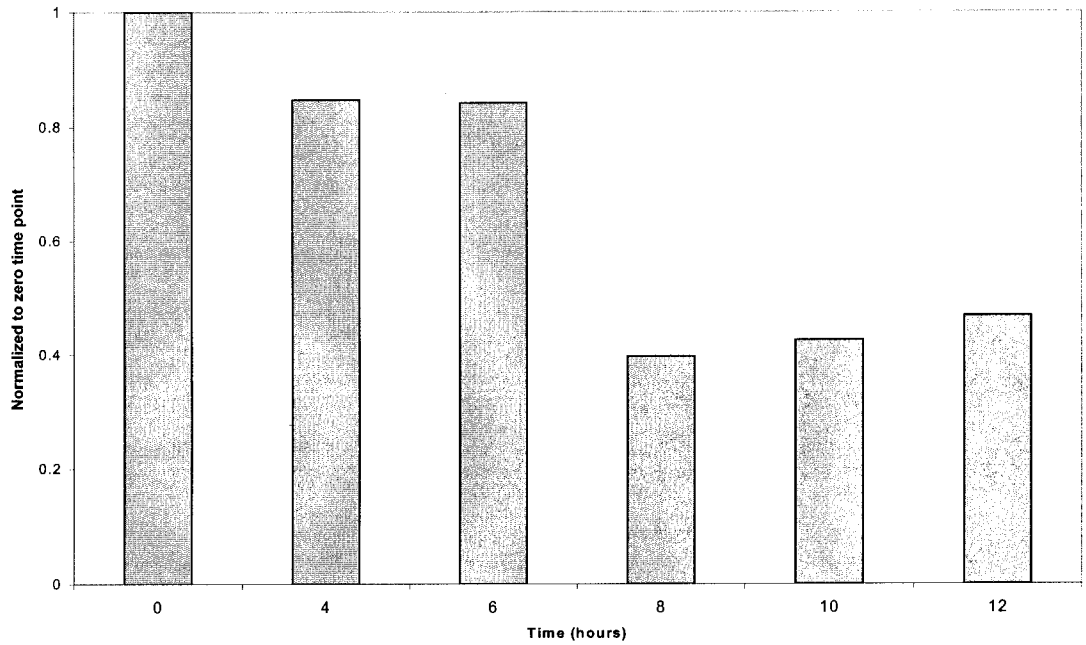

B.

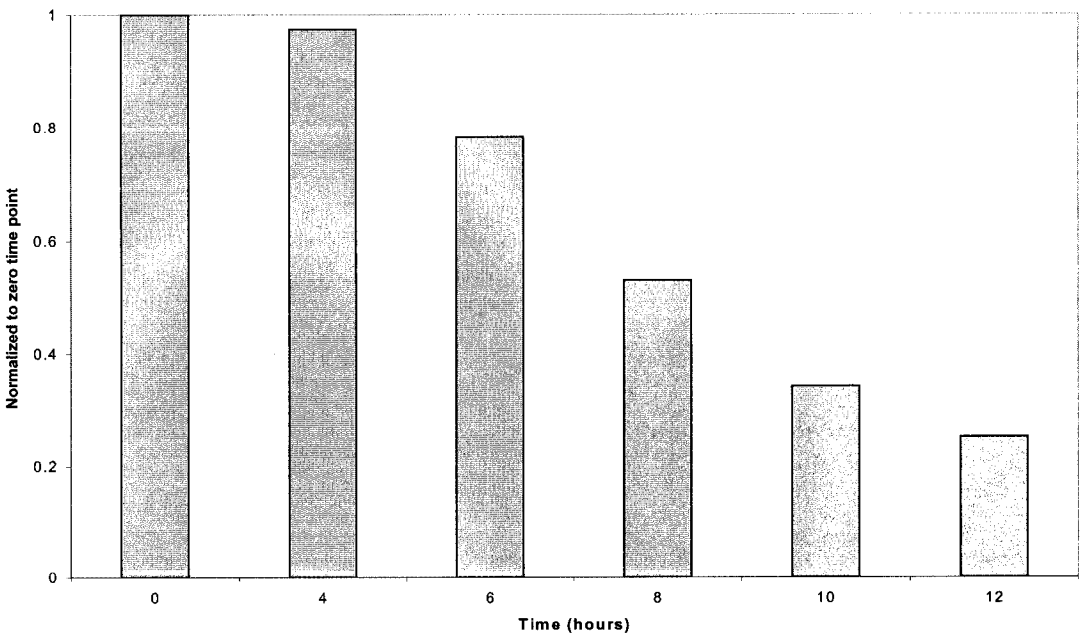

Figure 3-22. Analysis of *ERCC1* mRNA (A) and β-*actin* mRNA (B) levels for an actinomycin D time course assay with GM00637A cells from 0-12 h. Time points were normalized to the zero time point and represent one experiment.

normal non-transformed cell line such as GM38 and its SV40-transformed counterpart.

It should also be noted that the use of actinomycin D has been reported to stabilize mRNA and, as a result, the mRNA half-life can be almost double the actual mRNA half-life (Johnson et al. 1991). Therefore, to obtain a more accurate determination of the *ERCC1* mRNA half-life within transformed vs. non-transformed cell lines, [^{3}H]uridine may be a better choice since it has been demonstrated to give no apparent effect on mRNA stability and it can be used to measure very long-lived transcripts (Johnson et al. 1991).

CHAPTER 4: DISCUSSION

4.1 Sensitivity of human xeroderma pigmentosum cell lines to phosphoramide mustard

In the present study the sensitivity of human NER-deficient cell lines XPF (XP2YO(SV)) and XPA (XP12T703) to PM-induced DNA lesions was determined in order to assess the possible role of the Xpf and Xpa proteins in ISC repair. The comparatively normal sensitivity of the XPA cell line to PM would suggest that the Xpa protein is not required for recognition or processing of PM-induced ISCs. Mimaki et al. (1996) observed that unless an XPA cell line is homozygous for a mutation that ultimately does not generate the full length/wild type Xpa protein, a truncated protein could still have some DNA-binding activity and possibly DNA repair function. This is emphasized by the recent findings of Muotri et al. (2002), who found that even low Xpa protein expression was sufficient for total complementation of cellular UV sensitivity and DNA repair activity in human XPA cells. Initially, XP cells were grouped by the extent of their defect in NER when exposed to UV, with XPA cells being the most defective (Freidberg et al. 1995). The human XP12T703 cells were derived from a patient with the classical XPA phenotype that is typified by severe skin symptoms and neurological abnormalities (Satokata et al. 1992). Molecular characterization has determined that the XP12T703 cells are homozygous for a mutation in exon 5 (which encodes the DNA-binding domain) of the *XPA* gene that alters the Arg207 codon to a nonsense codon (R207stop) (Satokata et al. 1992, States et al. 1998). This mutation results in decreased or undetectable levels of *XPA* mRNA and undetectable Xpa protein, effectively making this cell line a human *XPA* null mutant (Tanaka et al. 1990, Satokata et al. 1992, Kobayashi et al. 1998, Mellon et al. 2002). Thus, the lack of sensitivity of these cells to PM observed in this study would indeed suggest that the Xpa protein is not required in the major repair pathway of PM-induced DNA damage. Based on previous findings that XP12T703 cells **are** sensitive to MMC, this observation would suggest a fundamental difference in the

mechanism of repair of MMC-induced DNA crosslinks compared to PM-induced DNA crosslinks (O'Driscoll et al. 1999).

Although NER has been determined to play a minor role in ISC repair in human cells, the major pathway for ISC repair is considered to be HR (Chaney and Sancar 1996, Wang et al. 2001, Dronkert and Kanaar 2001). HR is thought to require some activity of the Ercc1 and Xpf proteins, based on the severe sensitivity demonstrated by CHO mutants within these complementation groups (CG1 and CG4, respectively) to the ISC-inducing agent MMC (Busch et al. 1980, Thompson et al. 1980, 1982, Hoy et al. 1985). However, when the human XPF (XP2YO(SV)) cell line was analyzed for its response to PM, only moderate sensitivity (~1.75 fold) was observed. The discrepancy in PM sensitivity seen between the human XP2YO(SV) and rodent UV41 cell lines may be related to the differing backgrounds of these cell lines, as discussed below.

The human XPF cell line was isolated from an individual who displayed the clinical phenotype of XP, with subsequent classification into CG4 by somatic cell hybridization. Molecular characterization of XP2YO cells, the parental cell line to XP2YO(SV) cells, revealed that both of the *XPF* alleles had point mutations in the proposed Ercc1 protein-binding domain (Matsumura et al.1998). These mutations not only interrupt the binding of Xpf to Ercc1 but also result in Xpf protein instability, leading ultimately to its degradation (Matsumura et al.1998). Although XP2YO(SV) cells have mutations that do not result in detectable Xpf protein when examined by Western blotting, even though *XPF* mRNA expression is normal, the Xpf protein could still be produced below levels detectable by Western blotting, resulting in the mild sensitivity to PM (Yagi et al. 1998a, van Duin et al. 1989b). This is supported by the observation that XP2YO(SV) cells retain a very low ability to perform NER and this may be sufficient to cope with a low steady-state of DNA-damage (Weeda et al. 1997). A byproduct of the loss of the Xpf protein is the instability induced upon its binding partner, the Ercc1 protein; thus, Western blotting reveals little evidence of this

protein as well (Biggerstaff et al. 1993, van Vuuren et al. 1993, Sijbers et al. 1996a, 1998, Yagi et al. 1997, 1998a, 1998b).

The CHO UV41 (*XPF*$^-$) cell line, in contrast, is the result of extreme *in vitro* mutagenesis of the wild-type AA8 cell line followed by the selection of individual mutant cells based on UV sensitivity (Thompson et al. 1982). These cells are only required to survive as discrete cells, rather than as part of a complex organism. The use of chemical mutagens for conventional mutagenesis produces CHO mutants with some heterophenotypes with respect to NER deficiency or cytotoxic and mutational responses (Rolig et al. 1998). This was emphasized by the isolation of an *XPF*$^-$ CHO CG4 mutant (UV140) that, in marked contrast to UV41, exhibited only moderate UV sensitivity and a very mild sensitivity to the cross-linking agent MMC (Busch et al. 1997). Although CHO UV140 cells differ from human XP2YO(SV) cells in their response to UV and MMC (Busch et al. 1997), cell-free assays for NER and CRS (cross-link induced-repair synthesis) activity have shown these two cell lines to be similar (Zhang et al. 2000). Severe CHO mutant cell lines that have been isolated within the same complementation group (CG4) have been shown to exhibit similar phenotypes to each other when treated with UV or the ISC-inducing agents cisplatin or MMC (Hoy et al. 1985, Friedberg et al. 1995, Andersson et al. 1996). The CHO UV41 (*XPF*$^-$) and UV20 (*ERCC1*$^-$) cell lines, which are in CGs 4 and 1, respectively, have also been shown to have similar phenotypes with respect to their extreme UV and MMC sensitivity (Busch et al. 1980, Thompson et al. 1980, 1982, Hoy et al. 1985). This similarity in phenotype would be expected considering that the Xpf and Ercc1 proteins associate to give a dimeric endonuclease and that the absence of either protein results in instability in the binding partner (Biggerstaff et al. 1993, van Vuuren et al. 1993, Sijbers et al. 1996a, 1998, Yagi et al. 1997, 1998a, 1998b).

The role of both the Ercc1 and Xpf proteins in HR would suggest that a complete deficiency in either protein might be developmentally lethal, especially as embryonic lethality is seen with other HR proteins, such as Rad51 (McWhir et al. 1993). However, *ERCC1*

knockout mice can develop to term although they display severe growth retardation and a limited life span (McWhir et al. 1993, Weeda et al. 1997). The XP2YO(SV) cell line has been determined to be relatively defective in NER, but proficient in the CRS assay, indicating that the essential recombination pathway remains intact (Zhang et al. 2000). However, unlike the XP2YO(SV) cell line, the CHO UV41 cell line is deficient in both the NER and CRS assays (Zhang et al. 2000). This would indicate that the UV41 cells are deficient in the HR pathway and further that, because knockout mice for HR proteins are embryonic lethal, a combination of an NER and HR deficiency is not likely to be achieved in a knockout mouse. Thus the extreme CHO mutants represent a severe HR deficiency that would not be seen in a system requiring embryonic development. This would suggest that in human cells an effective method that results in the elimination of either *ERCC1* or *XPF* gene expression from both alleles is required in order to determine their role in ISC repair. Alternatively, there may be a fundamental difference between human and rodent cells in this regard, that lead to a premise that formed the initial rational for undertaking this study.

4.2 Transfection of the human fibroblast cell line GM00637A with antisense-*ERCC1* cDNA

At present, no human disease has been associated with an *ERCC1* deficiency; thus, no human cell line has been isolated where the Ercc1 protein is deficient in association with a genetic mutation. In an attempt to generate an *ERCC1* deficient human cell line, antisense-*ERCC1* cDNA was inserted into a plasmid vector. The resulting vector construct (pD3αE1) was used to transfect the SV40-transformed human fibroblast cell line GM00637A. Subsequent sub-cloning of G418 resistant colonies resulted in the recovery of a number of transfectants. These transfectants were analyzed for UV-C sensitivity to determine if they displayed the expected NER-deficient phenotype that would indicate whether the Ercc1 protein is being affected.

Many of the empty vector control transfectants displayed an inherently UV-C resistant phenotype, suggesting that the vector alone or possibly the integration sites(s) of the plasmid vector were somehow influencing the response to UV-C injury. The majority of the antisense transfectant cell lines (with the antisense-*ERCC1* cDNA stably integrated within their genome) also had an UV-C resistant phenotype when compared to the parental GM00637A cell line. Only two of the antisense transfectant cell lines were even moderately UV-C sensitive – 22.3 and 22.11. The determination of PM sensitivity indicated primarily a moderate PM sensitivity for all control transfectants. However, transfectants with the antisense-*ERCC1* cDNA displayed a wide range of PM sensitivity, with the 22.3 and 22.11 cell lines being the most sensitive to PM. When the antisense transfectant cell lines were compared to an average of the transfectant control cell lines, there is a predominant UV-C sensitivity, with the majority of the antisense transfectant cell lines also displaying resistance to PM.

Analysis of Ercc1 protein levels in the antisense transfectant cell lines, however, did not reveal a correlation between this parameter and UV-C/PM sensitivity. The lack of consistency within the controls, and ultimately the transfectants with the antisense-*ERCC1* cDNA, suggests that the impact of the random integration of the plasmid vector will confound the interpretation of the observed results.

The detection of a second protein band with the anti-Ercc1 monoclonal antibody at ~33 kDa hinted at the possibility of a regulatory spliced variant of the Ercc1 protein, as noted by other researchers (van Duin et al. 1986, Belt et al. 1991, Bramson and Panasci 1993, Yu et al. 1998, Goukassian et al. 2002). However, no correlation between the 33 kDa protein levels detected by Western blotting and UV-C/PM sensitivity could be determined. The possibility that the 33 kDa protein was a degradation product could not be discounted based on the observed data, and further examination of this protein would be required to resolve this question.

Each transfectant cell line was examined to determine if the antisense-*ERCC1* cDNA had integrated into the genomic DNA. PCR revealed a 775 bp band corresponding to the antisense-*ERCC1* cDNA in all transfectants (except the controls, as expected). An attempt to determine the number of integrated copies of the antisense-*ERCC1* cDNA was also done for each of the transfectant cell lines however, determination of an exact number was limited by the use of only one restriction enzyme. The result was Southern blots that could only confirm the presence of one or more copies of the antisense-*ERCC1* cDNA integrating into the genome of the transfectant cells. An exact number of integrated copies would require the use of a second restriction enzyme or an alternative technique such as FISH. A relationship between the number of integrated copies of the antisense-*ERCC1* cDNA and PM/UV-C sensitivity for each of the transfectant cell lines, therefore, could not be determined.

In order to determine if the antisense-*ERCC1* cDNA was expressed as mRNA in each of the transfectant cell lines, RT-PCR was performed. Analysis of each of the transfectant cell lines revealed that all had the 775 bp band, except for sub-clone 25.13 (and the transfectant control cell lines, as expected). However, since the RT-PCR assay only detects the presence of the antisense-ERCC1 mRNA and is not quantitative, a comparison of the antisense-ERCC1 mRNA expression to the UV-C/PM sensitivity of each transfectant cell line also could not be determined.

The highly variable results in Ercc1 protein expression observed among the transfectant cell lines would point to secondary effects that may be directly attributed to the random integration of the vector construct or the transfection and/or selection of the resulting clones.

4.3 Determination of the Ercc1 protein and *ERCC1* mRNA half-lives in GM38 and GM00637A cells

The lack of UV-C/PM sensitivity in the transfectant cell lines led to the hypothesis that the SV40-transformed normal human fibroblast cell line GM00637A (GM54 being the parental

cell line to GM00637A) may have an altered Ercc1 protein or even *ERCC1* mRNA expression related to the SV40-transformation itself. SV40-transformation of a cell line is known to have a range of effects on a cell, such as p53 sequestration within the nucleus (Deppert and Haug 1986, Fanning and Knippers 1992, Hess and Brandner 1997, Ali and DeCaprio 2001). New roles for the SV40 large T antigen are being discovered, and not all of its functions are known.

The Ercc1 protein half-life was determined within the GM38 and GM00637A cell lines to be <2 h and >6 h, respectively, using a cyclohexamide time course assay. The increase in the Ercc1 protein half-life noted in the GM00637A cells compared to the GM38 cells would suggest that the SV40-transformation event does indeed have some influence on Ercc1 protein stability. The Ercc1 protein half-life in primary human fibroblasts has been previously reported to be < 1 h (van Vuuren et al. 1993, Sijbers et al. 1996a). However, the half-life observed in those studies was determined by microinjection of excess purified human Ercc1 protein into the nucleus and, as previously noted, the Ercc1 protein is unstable in the absence of the Xpf protein (van Duin et al. 1988, Sijbers et al. 1996a, de Laat et al. 1998). The increased stability of the Ercc1 protein in GM00637A cells would suggest that this cell line would not be ideal for down-regulation of the Ercc1 protein expression via antisense-*ERCC1* cDNA.

In parallel to the cyclohexamide time course assay, the *ERCC1* mRNA half-life was determined using actinomycin D in both GM38 and GM00637A cells. An interesting observation was an increase in the *ERCC1* mRNA half-life in GM00637A cells (6-8 h) compared GM38 cell line (1.5-2 h). Thus, the *ERCC1* mRNA is also more stable in the SV40-transformed GM00637A cell line. The similarity between the *ERCC1* mRNA half-life of 15 h determined by Li et al. (1998) in human ovarian carcinoma cells and that of the GM00637A cells in this study, when compared to the GM38 cell line, would indicate that cellular transformation, whether as a cancer cell or viral infection, can somehow lead to

increased stability of the *ERCC1* mRNA. On reflection, a better choice would have been the use of a primary cell line such as GM38 in which to modulate the Ercc1 protein expression.

The determination of the Ercc1 protein and *ERCC1* mRNA half-life values in the GM38 and GM00637A cell lines was not the initial impetus of this study, but rather evolved from trying to understand the ineffectiveness of the antisense-*ERCC1* cDNA in these cells. The results from these experiments, however, would imply that transformation of a cell line could have a dramatic impact on the level of the Ercc1 protein and *ERCC1* mRNA expression. In turn, this could have important implications with regards to the use of transformed cells in determining the role of the Ercc1 protein (or even the Xpf protein) in human ISC repair.

4.4 Determination of Xpf and p53 protein half-lives in GM38 and GM00637A cell lines

Assessment of the Xpf protein half-life as being between 2-4 hours, using cyclohexamide, in both the GM38 and GM00637A cell lines indicated that Xpf protein stability, unlike Ercc1, appears to be unaffected by SV40-transformation. This is an interesting finding considering that both the Xpf and Ercc1 proteins have been determined to be unstable in each others' absence (Biggerstaff et al. 1993, van Vuuren et al. 1993, Sijbers et al. 1996a, 1998, Yagi et al. 1997, 1998a, 1998b). Because of their functional association, it might be expected that the degradation of these proteins might have similar kinetics. However, an ~2 fold difference was observed between the Xpf and Ercc1 protein half-lives, which may be the result of differences in domains responsible for protein destabilization and the location of such domains (Tsurumi et al. 1995). Thus, the Xpf protein in the absence of the Ercc1 protein may have a domain(s) that confer some minor stability before being degraded.

The p53 protein was used as a control when Western blots were used to identify the presence of the Ercc1 protein in each of the transfectants. The level of p53 protein

expression is known to be relatively high in SV40-transformed cell lines due to the SV40 large T antigen binding to and sequestering the p53 in the nucleus, as noted previously in section 4.3 (Deppert and Haug 1986, Hess and Brandner 1997, Ali and DeCaprio 2001). In all of the GM00637A transfectant cell lines, as well as in the GM00637A cell line itself, the p53 protein was expressed at very high levels, as expected. The p53 protein was also used as a control in the cyclohexamide time course assay because its half-life has been determined previously in both normal (non-transformed) and transformed cell lines (Reich et al. 1983, Caelles et al. 1994, Maki and Howley 1997, Ozbun and Butel 1997). As expected, the half-life of the p53 protein was found to be less than 2 h (the shortest time point studied) in GM38 cells. The increased stability of the p53 protein brought about by the SV40-transformation of the GM00637A cells was manifested by a half-life that exceeded 6 h, also as expected.

4.5 Antisense-*ERCC1* mRNA effects in other studies

Although the antisense-*ERCC1* mRNA approach used in this study did not appear to greatly affect the sense-*ERCC1* mRNA or Ercc1 protein expression in the majority of transfectants, two other studies using antisense-*ERCC1* mRNA were able to isolate sub-clones displaying a significant decrease in sense-*ERCC1* mRNA and Ercc1 protein expression (Yang et al. 2000, Selvakumaran et al. 2003). These studies were able to show a correlation between an increase in cisplatin sensitivity and a decrease in *ERCC1* mRNA/Ercc1 protein expression (Yang et al. 2000, Selvakumaran et al. 2003). However, these authors used cancer cell lines, either human colon or ovarian carcinoma cells, whereas in this study non-cancerous cell lines were used. There are several possible reasons for the differences in results. First, it is possible that the level of the Ercc1 protein could have a greater impact on cisplatin sensitivity as opposed to PM sensitivity. Second, down-regulation of the *ERCC1* mRNA and Ercc1 protein observed by Yang et al. (2000) and Selvakumaran et al. (2003) may influence the chemotherapeutic response of malignant cells but not of non-

malignant cells. Another possibility is that changes in proteins that influence Ercc1 expression/activity may be associated with the transformation of a normal cell into a cancer cell. In particular, signal transduction pathways that regulate the expression of select proteins upon exposure to genotoxic stress could have an influence on the expression of *ERCC1* mRNA or the Ercc1 protein. Likely candidates for regulating *ERCC1* mRNA expression, for example, are the oncogenes c-*FOS* and c-*JUN* that together form the transcription factor AP-1 (Friedberg et al. 1995). The identification of an AP-1-like site in the promoter region of the *ERCC1* gene makes it a likely target for transcriptional modulation by AP-1 as observed by Li et al. (1998). The lack of consistency in correlating Ercc1 protein expression with drug sensitivity in the existing literature would favor the theory that transcriptional/translational modulation of the *ERCC1* gene may be a byproduct of another de-regulated pathway. However, the *ERCC1* mRNA for instance could be used as a surrogate indicator for chemotherapeutic response, as seen in many human ovarian cancers where *ERCC1* mRNA expression has been correlated with cisplatin sensitivity.

The results reported in this thesis demonstrate that modulation of the *ERCC1* mRNA and Ercc1 protein was not achieved in the human GM00637A fibroblast cell line transfected with antisense-*ERCC1* cDNA and thus, no extreme sensitivity to either UV-C or PM was observed. The unexpected effect of integrated vector alone on UV-C sensitivity would suggest the integration site may be important and may affect other systems. To avoid this problem a stable episomal vector (i.e. pCEP4) transfected into a primary cell line might be more effective in avoiding potential problems with integration. However, from the results obtained in this study, and the previously published reports with XP2YO(SV), the likelihood of decreasing the expression of the Ercc1 protein to the point where there is a significant effect on ISC repair may not be achieved with the present methods available given that very little Ercc1-Xpf appears to be required for ISC repair.

The findings with the non-cancerous cell line GM38, in conjunction with those reported by others for cancer cells (Yang et al. 2000, Selvakumaran et al. 2003), warrant

further studies to determine, under the same experimental conditions, whether down-regulation of the Ercc1 protein can selectively sensitize cancer cells to a particular chemotherapeutic agent. These studies would enable the identification of chemotherapeutic strategies that are more effective on certain types of cancer cells to chemotherapeutic agents.

CHAPTER 5: BIBLIOGRAPHY

Ali, S. H., and J. A. DeCaprio (2001). Cellular transformation by SV40 large T antigen: interaction with host proteins. Review. Cancer Biology, 11:15-22.

Adelman, J. P., C. T. Bond, J. Douglass, and E. Herbert (1987). Two mammalian genes transcribed from opposite strands of the same DNA locus. Science, 235:1514-1517.

Andersson, B. S., T. Sadeghi, M. J. Siciliano, R. Legerski, and D. Murray (1996). Nucleotide excision repair genes as determinants of cellular sensitivity to cyclophosphamide analogs. Cancer Chemotherapy and Pharmacology, 38:406-416.

Bauer, G. B., and L. F. Povirk (1997). Specificity and kinetics of interstrand and intrastrand bifunctional alkylation by nitrogen mustards at a G-G-C sequence. Nucleic Acids Research, 25(6):1211-1218.

Belt, P. B. G. M., M. F. van Oosterwijk, H. Odijk, J. H. J. Hoeijmakers, and C. Backendorf (1991). Induction of a mutant phenotype in human repair proficient cells after overexpression of a mutated human DNA repair gene. Nucelic Acids Research, 19 (20):5633-5637.

Bessho, T., A. Sancar, L. H. Thompson, and M. P. Thelen (1997). Reconstitution of human excision nuclease with recombinant XPF-ERCC1 complex. Journal of Biological Chemistry, 272(6):3833-3837.

Biggerstaff, M., D. E. Szymkowski, and R. D. Wood (1993). Co-correction of the ERCC1, ERCC4 and xeroderma pigmentosum group F DNA repair defects in vitro. The EMBO Journal, 12(9):3685-3692.

Bramson, J., and L. C. Panasci (1993). Effect of ERCC-1 overexpression on sensitivity of Chinese hamster ovary cells to DNA damaging agents. Cancer Research, 53:3237-3240.

Britten, R. A., D. Liu, A. Tessier, M. J. Hutchison, and D. Murray (2000). *ERCC1* expression as a molecular marker of cisplatin resistance in human cervical tumor cells. International Journal of Cancer, 89:453-457.

Brook, J. D., D. J. Shaw, A. L. Meredith, M. Worwood, J. Cowell, J. Scott, T. J. Knott, M. Litt, L. Bufton, and P. S. Harper (1985). A somatic cell hybrid panel for chromosome 19 localization of known genes and RFLP's and orientation of the linkage group. Cytogen. Cell Gen., 40:590-591.

Brookman, K. W., J. E. Lamerdin, M. P. Thelen, M. Hwang, J. T. Reardon, A. Sancar, Z-Q. Zhou, C. A. Walter, C. N. Parris, and L. H. Thompson (1996). *ERCC4* (*XPF*) encodes a human nucleotide excision repair protein with eukaryotic recombination homologs. Molecular and Cellular Biology, 16(11):6553-6562.

Busch, D. B., J. E. Cleaver, and D. A. Glaser (1980). Large-scale isolation of UV-sensitive clones of CHO cells. Somatic Cell Genetics, 6(3):407-418.

Busch, D. B., H. van Vuuren, J. de Wit, A. Collins, M. Z. Zdzienicka, D. L. Mitchell, K. W. Brookman, M. Stefanini, R. Riboni, L. H. Thompson, R. B. Albert, A. J. van Gool, and J. Hoeijmakers (1997). Phenotypic heterogeneity in nucleotide excision repair mutants of rodent complementation groups 1 and 4. Mutation Research, 383:91-106.

Caelles, C., A. Helmberg, and M. Karin (1994). p53-dependent apoptosis in the absence of transcriptional activation of p53-target genes. Nature, 370:220-223.

Chabner, B. A., C. J. Allegra, G. A. Curt and P. Calabresi. (1996). Chapter 51: Antineoplastic agents. *In* Goodman and Gilman's The Pharmacological Basis of Therapeutics. 9th Edition. pp. 1233-1287.

Chaney, S. G., and A. Sancar (1996). DNA repair: enzymatic mechanisms and relevance to drug response. Review. Journal of the National Cancer Institute, 88 (19):1346-1360.

Chen, C-N., T. Malone, S. K. Beckendorf, and R. L. Davis (1987). At least two genes reside within a large intron of *dunce* gene of *Drosophila*. Nature, 329:721-724.

Chen, P., J. Wiencke, K. Aldape, A. Kesler-Diaz, R. Miike, K. Kelsey, M. Lee, J. Liu, and M. Wrensch (2000). Association of an *ERCC1* polymorphism with adult-onset glioma. Cancer Epidemiology, Biomarkers and Prevention, 9(8):843-847.

Chen, Y., and A. Y. Sun (1998). Activation of transcription factor AP-1 by extracellular ATP in PC12 cells. Neurochemical Research, 23(4):543-550.

Cheng, L., Y. Guan, L. Li, R. J. Legerski, J. Einspahr, J. Bangert, D. S. Alberts, and Q. Wei (1999). Expression in normal human tissues of five nucleotide excision repair genes measured simultaneously by multiplex reverse transcription-polymerase chain reaction. Cancer Epidemiology, Biomarkers and Prevention, 8:801-807.

Cheng, L., E. M. Sturgis, S. A. Eicher, M. R. Spitz, and Q. Wei (2002). Expression of nucleotide excision repair genes and the risk for squamous cell carcinoma of the head and neck. Cancer, 94(2):393-397.

Codegoni, A. M., M. Broggini, M. R. Pitelli, M. Pantarotto, V. Torri, C. Mangioni, and M. D'Incalci (1997). Expression of genes of potential importance in the response to chemotherapy and DNA repair in patients with ovarian cancer. Gynecologic Oncology, 65:130-137.

Colvin, D. M. (2000). Alkylating agents and platinum antitumor compounds. *In* Cancer Medicine, 5th Edition. Eds. Holland and Frei. American Cancer Society, pp. 648-669.

Chrzanowska-Lightowlers, Z. M. A., T. Preiss, and R. N. Lightowlers (1994). Inhibition of mitochondrial protein synthesis promotes increased stability of nuclear-encoded respiratory gene transcripts. The Journal of Biological Chemistry, 269(44):27322-27328.

Current Protocols in Molecular Biology Edition Vol. 1 (1993). Eds. F. M. Ausubel, R. Brent, R. E. Kingston, D. D. Moore, J. G. Seidman, J. A. Smith, and K. Struhl. Greene Publishing Associates and John Wiley and Sons Inc., USA. pp. 2.1.1-2.1.3.

Dabholkar, M., F. Bostick-Bruton, C. Weber, V. A. Bohr, C. Egwuagu, and E. Reed (1992). ERCC1 and ERCC2 expression in malignant tissues from ovarian cancer patients. Journal of the National Institute of Cancer, 84(19):1512-1517.

Dabholkar, M., F. Bostick-Bruton, C. Weber, C. Egwuagu, V. A. Bohr, and E. Reed (1993). Expression of excision repair genes in non-malignant bone marrow from cancer patients. Mutation Research, 293:151-160.

Dabholkar, M., J. Vionnet, F. Bostick-Bruton, J. J. Yu, and E. Reed (1994). Messenger RNA levels of XPAC and ERCC1 in ovarian cancer tissue correlate with response to platinum-based chemotherapy. Journal of Clinical Investigation, 94:703-708.

Dabholkar, M., J. Vionnet, R. J. Parker, F. Bostick-Bruton, A. Dobbins, and E. Reed (1995a). Expression of an alternatively spliced ERCC1 mRNA species, is related to reduced DNA repair efficiency in human T lymphocytes. Oncology Reports, 2:209-214.

Dabholkar, M. D., M. S. Berger, J. A. Vionnet, C. Egwuagu, J. R. Silber, J. J. Yu, and E. Reed (1995b). Malignant and nonmalignant brain tissues differ in their messenger RNA expression patterns for ERCC1 and ERCC2. Cancer Research, 55:1261-1266.

Damia, G., L. Imperatori, M. Stefanini, and M. D'Incalci (1996). Sensitivity of CHO mutant cell lines with specific defects in nucleotide excision repair to different anti-cancer agents. International Journal of Cancer, 66:779-783.

De Laat, W. L., A. M. Sijbers, H. Odijk, N. G. J. Jaspers, and J. H. J. Hoeijmakers (1998). Mapping of interaction domains between human repair proteins ERCC1 and XPF. Nucleic Acids Research, 26(18):4146-4152.

Deppert, W., and M. Haug (1986). Evidence for free and metabolically stable p53 protein in nuclear subfractions of Simian Virus 40-transformed cells. Molecular and Cellular Biology, 6(6):2233-2240.

Dronkert, M. L. G., and R. Kanaar (2001). Repair of DNA interstrand cross-links. Minireview. Mutation Research, 486:217-247.

Fanning, E., and R. Knippers (1992). Structure and function of Simian Virus 40 large tumor antigen. Review. *In* Annual Review of Biochemistry, 61:55-85.

Feinberg, A. P., and B. Vogelstein (1983). A technique for radiolabeling DNA restriction endonuclease fragments to high specific activity. Analytical Biochemistry, 132:6-13.

Feinberg, A. P., and B. Vogelstein (1984). Addendum to "A technique for radiolableling DNA restriction endonuclease fragments to high specific activity". Analytical Biochemistry, 137:266-267.

Fink, D., S. Aebi, and S. B. Howell (1998). The role of DNA mismatch repair in drug resistance. Clinical Cancer Research, 4:1-6.

Flowers, J. L., S. M. Ludeman, M. P. Gamcsik, O. M. Colvin, K.-L. Shao, J. H. Boal, J. B. Springer, and D. J. Adams (2000). Evidence for a role of chloroethylaziridine in the cytotoxicity of cyclophosphamide. Cancer Chemotherapy and Pharmacology, 45:335-344.

Friedberg, E. C., G. C. Walker, W. Siede (1995). Chapter 14: Human hereditary diseases with defective processing of DNA damage. *In* DNA Repair and Mutagenesis. ASM Press, Washington, D.C. pp. 637.

Friedberg, E. C. (2001). How nucleotide excision repair protects against cancer. Review. Nature Reviews Cancer, 1:22-33.

Gamcsik, M. P., M. E. Dolan, B. S. Andersson, and D. Murray (1999). Mechanisms of resistance to the toxicity of cyclophosphamide. Current Pharmaceutical Design, 5:587-605.

Gaillard, P-H. L., and R. D. Wood (2001). Activity of individual ERCC1 and XPF subunits in DNA nucleotide excision repair. Nucleic Acids Research, 29(4):872-879.

Goode, E. L., C. M. Ulrich, and J. D. Potter (2002). Polymorphisms in DNA repair genes and associations with cancer risk. Cancer Epidemiology, Biomarkers and Prevention, 11(12):1513-1530.

Goukassian, D. A., S. Bagheri, L. El-Keeb, M. S. Eller, and B. A. Gilchrest (2002). DNA oligonucleotide treatment corrects the age-associated decline in DNA repair capacity. FASEB Journal, 16:754-756

Hanawalt, P. C. (2001a). Controlling the efficiency of excision repair. Review. Mutation Research, 485:3-13.

Hanawalt, P. C. (2001b). Revisiting the rodent repairadox. Environmental and Molecular Mutagenesis, 38:89-96.

Henikoff, S., M. A. Keene, K. Fechtel, and J. W. Fristrom (1986). Gene within a gene: nested Drosophila genes encode unrelated proteins on opposite DNA strands. Cell, 44:33-42.

Hess, R. D., and G. Brandner (1997). DNA-damage-inducible p53 activity in SV40-transformed cells. Oncogene, 15:2501-2504.

Houtsmuller, A. B., S. Rademakers, A. L. Nigg, D. Hoogstraten, J. H. J. Hoeijmakers, and W. Vermeulen (1999). Action of DNA repair endonuclease ERCC1/XPF in living cells. Science, 284:958-961.

Hoy, C. A., L. H. Thompson, C. L. Mooney, and E. P. Salazar (1985). Defective DNA cross-link removal in Chinese hamster cell mutants hypersensitive to bifunctional alkylating agents. Cancer Research, 45:1737-1743.

Jiang, M., T. Axe, R. Holgate, C. P. Rubbi, A. L. Okorokov, T. Mee, and J. Milner (2001). p53 binds the nuclear matrix in normal cells: binding involves the proline-rich domain of p53 and increases following genotoxic stress. Oncogene, 20:5449-5458.

Johnson, T. R., S. D. Rudin, B. K. Blossey, J. Ilan, and J. Ilan (1991). Newly synthesized RNA: simultaneous measurement in intact cells of transcription rates and RNA stability of insulin-like growth factor I, actin, and albumin in growth hormone-stimulated hepatocytes. Proceedings of the National Institute of Science, 88:5287-5291.

Kendrew, Sir J., and E. Lawrence (1994). The Encyclopedia of Molecular Biology. Blackwell Science Ltd, Alden Press, Great Britain. pp.14 and 240.

Kobayashi, T., S. Takeuchi, M. Saijo, Y. Nakatsu, H. Morioka, E. Otsuka, M. Wakasugi, O. Nikaido, and K. Tanaka (1998). Mutation analysis of a function of xeroderma pigmentosum group A (XPA) protein in strand-specific DNA repair. Nucleic Acids Research, 26 (20):4662-4668.

Kuraoka, I., W. R. Kobertz, R. R. Ariza, M. Biggerstaff, J. M. Essigmann, and R. D. Wood (2000). Repair of an interstrand DNA cross-link initiated by ERCC1-XPF repair/recombination nuclease. The Journal of Biological Chemistry, 275 (34):26632-26636.

Lee-Kwon, W., D. Park, and M. Bernier (1998). Involvement of the Ras/extracellular signal-regulated kinase signalling pathway in the regulation of ERCC-1 mRNA levels by insulin. Biochemistry Journal, 331:591-597.

Legerski, R. J., and C. Richie (2002). Mechanisms of repair of interstrand crosslinks in DNA. Review. Cancer Treatment Research, 112:109-128.

Li, L., S. J. Elledge, C. A. Peterson, E. S. Bales, and R. J. Legerski (1994). Specific association between the human DNA repair proteins XPA and ERCC1. Proceedings of the National Academy of Science, 91:5012-5016.

Li, Q., K. Gardner, L. Zhang, B. Tsang, F. Bostick-Bruton, and E. Reed (1998). Cisplatin induction of *ERCC-1* mRNA expression in A2780/CP70 human ovarian cancer cells. The Journal of Biological Chemistry, 273(36):23419-23425.

Li, Q., B. Tsang, F. Bostick-Bruton, and E. Reed (1999a). Modulation of excision repair cross complementation group 1 (ERCC-1) mRNA expression by pharmacological agents in human ovarian carcinoma cells. Biochemical Pharmacology, 57:347-353.

Li, Q., L. Zhang, B. Tsang, K. Gardner, F. Bostick-Bruton, and E. Reed (1999b). Phorbol ester exposure activates an AP-1-mediated increase in ERCC-1 messenger RNA expression in human ovarian tumor cells. Cellular and Molecular Life Sciences, 55:456-466.

Li, Q., J. J. Yu, C. Mu, M. K. Yunmbam, D. Slavsky, C. L. Cross, F. Bostick-Bruton, and E. Reed (2000a). Association between the level of ERCC-1 expression and the repair of cisplatin-induced DNA damage in human ovarian cancer cells. Anticancer Research, 20:645-652.

Li, V-S., M. Reed, Y. Zheng, H. Kohn, and M-S. Tang (2000b). C5 cytosine methylation at CpG sites enhances sequence selectivity of mitomycin C-DNA bonding. Biochemistry, 39:2612-2618.

Liang, B. C., D. A. Ross, and E. Reed (1995). Genomic copy number changes of DNA repair genes *ERCC1* and *ERCC2* in human gliomas. Journal of Neuro-Oncology, 26:17-23.

Lin, Y-W., M. Kubota, S. Koishi, M. Sawada, I. Usami, K-I. Watanabe, and Y. Akiyama (1998). Analysis of mutations at the DNA repair genes in acute childhood leukaemia. British Journal of Haematology, 103:462-466.

Lord, R. V. N., J. Brabender, D. Gandara, V. Alberola, C. Camps, M. Domine, F. Cardenal, J. M. Sanchez, P. H. Gumerlock, M. Taron, J. J. Sanchez, K. D. Danenberg. P. V. Danenberg, and R. Rosell (2002). Low *ERCC1* expression correlates with prolonged survival after cisplatin plus gemcitabine chemotherapy in non-small cell lung cancer. Clinical Cancer Research, 8:2286-2291.

Ludeman, S. M. (1999). The chemistry of the metabolites of cyclophosphamide. Current Pharmaceutical Design, 5:627-643.

Maki, C. G., and P. M. Howley (1997). Ubiquitination of p53 and p21 is differentially affected by ionizing and UV radiation. Molecular and Cellular Biology, 17(1):355-363.

Masutani, C., R. Kusumoto, S. Iwai, and F. Hanaoka (2000). Mechanisms of accurate translesion synthesis by human DNA polymerase η. The EMBO Journal, 19(12):3100-3109.

Matsumura, Y., C. Nishigori, T. Yagi, S. Imamura, and H. Takebe (1998). Characterization of molecular defects in xeroderma pigmentosum group F in relation to its clinically mild symptoms. Human Molecular Genetics, 7(6):969-974.

Matsunaga, T., C-H. Park, T. Bessho, D. Mu, and A. Sancar (1996). Replication protein A confers structure-specific endonuclease activities to the XPF-ERCC1 and XPG subunits of human DNA repair excision nuclease. Journal of Biological Chemistry, 271(19):11047-11050.

May, P, and E. May (1999). Twenty years of p53 research: structural and functional aspects of the p53 protein. Oncogene, 18:7621-7636.

McHugh, P. J., V. J. Spanswick, and J. A. Hartley (2001). Repair of DNA interstrand crosslinks: molecular mechanisms and clinical relevance. Review. The Lancet Oncology, 2:483-490.

McWhir, J., J. Selfridge, D. J. Harrison, S. Squires, and D. W. Melton (1993). Mice with DNA repair gene (ERCC-1) deficiency have elevated levels of p53, liver nuclear abnormalities and die before weaning. Nature Genetics, 5:217-224.

Mellon, I., T. Hock, R. Reid, P. C. Porter, and J. C. States (2002). Polymorphisms in the human xeroderma pigmentosum group A gene and their impact on cell survival and nucleotide excision repair. DNA Repair, 1:531-546.

Merino, E., P. Balbas, J. L. Puente, and F. Bolivar (1994). Antisense overlapping open reading frames in genes from bacteria to humans. Nucleic Acids Research, 22(10):1903-1908.

Metzger, R., C. G. Leichman, K. D. Danenberg, P. V. Danenberg, H-J. Lenz, K. Hayashi, S. Groshen, D. Salonga, H. Cohen, L. Laine, P. Crookes, H. Silberman, J. Baranda, B. Konda, and L. Leichman (1998). *ERCC1* mRNA levels complement thymidylate synthase mRNA levels in predicting response and survival for gastric cancer patients receiving combination cisplatin and fluorouracil chemotherapy. Journal of Clinical Oncology, 16(1):309-316.

Mimaki, T., M. Nitta, M. Saijo, N. Tachi, R. Minami, and K. Tanaka (1996). Truncated XPA protein detected in atypical group A xeroderma pigmentosum. Acta Paediatr, 85:511-513.

Miyakoshi, J., D. A. Scudiero, J. Allalunis-Turner, and R. S. Day III (1991). The sensitivities of SV40-transformed human fibroblasts to monofunctional and DNA-crosslinking alkylating agents. Mutation Research, 254:55-64.

Mu, D., T. Bessho, L. V. Nechev, D. J. Chen, T. M. Harris, J. E. Hearst, and A. Sancar (2000). DNA interstrand cross-links induce futile repair synthesis in mammalian cell extracts. Molecular and Cellular Biology, 20(7):2446-2454.

Muotri, A. R., M. C. N. Marchetto, M. F. Suzuki, K. Okazaki, C. F. P. Lotfi, G. Brumatti, G. P. Amarante-Mendes, and C. F. M. Menck (2002). Low amounts of the DNA repair XPA protein are sufficient to recover UV-resistance. Carcinogenesis, 23(6);1039-1046.

Murray, D. (2002) DNA repair in resistance to bifunctional alkylating and platinating agents. Review. Cancer Treatment Research, 112:129-160.

Murray, D., L. Vallee-Lucic, E. Rosenberg, and B. Andersson (2002). Sensitivity of nucleotide excsion repair-deficient human cells to ionizing radiation and cyclophosphamide. Anticancer Research, 22:21-26.

Nakane, H., S. Takeuchi, S. Yuba, M. Saijo, Y. Nakatsu, H. Murai, Y. Nakatsuru, T. Ishikawa, S. Hirota, Y. Kitamura, Y. Kato, Y. Tsunoda, H. Miyauchi, T. Horio, T. Tokunaga, T. Matsunaga, O. Nikaido, Y. Nishimune, Y. Okada, and K. Tanaka (1995). High incidence of ultraviolet-B- or chemical-carcinogen-induced skin tumours in mice lacking the xeroderma pimentosum group A gene. Nature, 377:165-168.

Nepveu, A., and K. B. Marcu (1986). Intragenic pausing and anti-sense transcription within the murine *c-myc* locus. The EMBO Journal, 5(11):2859-2865.

Niedner, H., R. Christen, X. Lin, A. Kondo, and S. B. Howell (2001). Identification of genes that mediate sensitivity to cisplatin. Minireview. Molecular Pharmacology, 60(6):1153-1160.

O'Driscoll, M., S. Martinelli, C. Ciotta, and P, Karran (1999). Combined mismatch and nucleotide excision repair defects in a human cell line: mismatch repair processes methylation but not UV- or ionizing radiation-induced DNA damage. Carcinogenesis, 20(5):799-804.

Ozbun, M. A., and J. S. Butel (1997). p53 tumor suppressor gene: structure and function. *In* Encyclopedia of Cancer Volume II., 1240-1257.

Palom, Y., G. S. Kumar, L-Q. Tang, M. M. Paz, S. M. Musser, S. Rockwell, and M. Tomasz (2002). Relative toxicities of DNA cross-links and monoadducts: new insights from studies of decarbamoyl mitomycin C and mitomycin C. Chemical Research and Toxicology, 15:1398-1406.

Pan, Y., and D. S. Haines (1999). The pathway regulating MDM2 protein degradation can be altered in human leukemic cells. Cancer Research, 59:2064-2067.

Perfetti, R., W. Lee-Kwon, C. Montrose-Rafizadeh, and M. Bernier (1997). Overexpression and activation of the insulin receptor enhances expression of ERCC-1 messenger ribonucleic acid in cultured cells. Endocrinology, 138(5):1829-1835.

Protic-Sabljic, M., D. Whyte, J. Fagan, B. H. Howard, C. M. Gorman, R. Padmanabhan, and K. H. Kraemer (1985). Quantification of expression of linked cloned genes in a simian virus 40-transformed xeroderma pigmentosum cell line. Molecular and Cellular Biology, 5(7):1685-1693.

Raff, T., M. van der Giet, D. Endemann, T. Wiederholt, and M. Paul (1997). Design and testing of β-actin primers for RT-PCR that do not co-amplify processed pseudogenes. BioTechniques, 23(3):456-460.

Reed, E., M. Dabholkar, K. Thornton, C. Thompson, J. J. Yu, and F. Bostick-Bruton (2000). Evidence for 'order' in the appearance of mRNAs of nucleotide excision repair genes, in human ovarian cancer tissues. Oncology Reports, 7(5):1123-1128.

Reich, N. C., M. Oren, and A. J. Levine (1983). Two distinct mechanisms regulate the levels of a cellular tumor antigen, p53. Molecular and Cellular Biology, 3(12):2143-2150.

Rink, S. M., R. Lipman, S. C. Alley, P. B. Hopkins, and M. Tomasz (1996). Bending of DNA by the mitomycin C-induced, GpG intrastrand cross-link. Chemical Research and Toxicology, 9:382-389.

Rolig, R. L., M. P. Lowery, G. M. Adair, and R. S. Nairn (1998). Characterization and analysis of Chinese hamster ovary cell ERCC1 mutant alleles. Mutagenesis, 13(4):357-365.
Sambrook, J., E. Fritsch, and T. Maniatis (1989). Molecular cloning: A laboratory manual. Cold Spring Harbor Laboratory Press, Cold Spring Harbor New York. pp. 7.46-7.50, 9.38-9.40 and 9.44.

Satokata, I., K. Tanaka, N. Miura, M Narita, T. Mimaki, Y. Satoh, S. Kondo, and Y. Okada (1992). Three nonsense mutations responsible for group A xeroderma pigmentosum. Mutation Research, 273:193-202.

Selvakumaran, M., D. A. Pisarcik, R. Bao, A. T. Yeung, and T. C. Hamilton (2003). Enhanced cisplatin cytotoxicity by disturbing the nucleotide excision repair pathway in ovarian cancer cell lines. Cancer Research, 63:1311-1316.

Shen, M. R., I. M. Jones, and H. Mohrenweiser (1998). Nonconservative amino acid substitution variants exist at polymorphic frequency in DNA repair genes in healthy humans. Cancer Research, 58:604-608.

Shirota, Y., J. Stoehlmacher, J. Brabender, Y-P. Xiong, H. Uetake, K. D. Danenberg, S. Groshen, D. D. Tsao-Wei, P. V. Danenberg, and H-J. Lenz (2001). *ERCC1* and thymidylate synthase mRNA levels predict survival for colorectal cancer patients receiving combination oxaliplatin and fluorouracil chemotherapy. Journal of Clinical Oncology, 19(23):4298-4304.

Siddik, Z. H. (2002). Biochemical and molecular mechanisms of cisplatin resistance. Cancer Treatment and Research, 112:263-284.

Sijbers, A. M., P. J. van der Spek, H. Odijk, J. van den Berg, M. van Duin, A. Westerveld, N. G. J. Jaspers, D. Bootsma and J. H. J. Hoeijmakers (1996a). Mutational analysis of the human nucleotide excision repair gene *ERCC1*. Nucleic Acids Research, 24(17):3370-3380.

Sijbers, A. M., W. L. de Laat, R. R. Ariza, M. Biggerstaff, Y-F. Wei, J. G. Moggs, K. C. Carter, B. K. Shell, E. Evans, M. C. de Jong, S. Rademakers, J. de Rooij, N. G. J. Jaspers, J. H. J. Hoeijmakers, and R. D. Wood (1996b). Xeroderma pigmentosum group F caused by a defect in a structure-specific DNA repair endonuclease. Cell, 86:811-822.

Sijbers, A. M., P. C. van Voorst Vader, J. W. Snoek, A. Raams, N. G. J. Jaspers, and W. J. Kleijer (1998). Homozygous R788W point mutation in the *XPF* gene of a patient with xeroderma pigmentosum and late-onset neurologic disease. The Journal of Investigative Dermatology, 110(5):832-836.

De Silva, I. U., P. J. McHugh, P. H. Clingen, and J. A. Hartley (2000). Defining the roles of nucleotide excision repair and recombination in the repair of DNA interstrand cross-links in mammalian cells. Molecular and Cellular Biology, 20(21):7980-7990.

De Silva, I. U., P. J. McHugh, P. H. Clingen, and J. A. Hartley (2002). Defects in interstrand cross-link uncoupling do not account for the extreme sensitivity of ERCC1 and XPF cells to cisplatin. Nucleic Acids Research, 30(17):3848-3856.

Sorenson, C.M., and A. Eastman (1988). Influence of *cis*-diamminedichloroplatinum(II) on DNA synthesis and cell cycle progression in excision repair proficient and deficient Chinese hamster ovary cells. Cancer Research, 48:6703-6707.

Spencer, C. A., R. D. Gietz, and R. B. Hodgetts (1986). Overlapping transcription units in the dopa decarboxylase region of *Drosophila*. Nature, 322:279-281.

States, J. C., E. R. McDuffie, S. P. Myrand, M. McDowell, and J. E. Cleaver (1998). Distribution of mutations in the human xeroderma pigmentosum group A gene and their relationships to the functional regions of the DNA damage recognition protein. Human Mutation, 12:103-113.

Tanaka, K., N. Miura, I. Satokata, I. Miyamoto, M. C. Yoshida, Y. Satoh, S. Kondo, A. Yasui, H. Okayama, and Y. Okada (1990). Analysis of a human DNA excision repair gene involved in group A xeroderma pigmentosum and containing a zinc-finger domain. Nature, 348:73-76.

Thompson, L. H., J. S. Rubin, J. E. Cleaver, G. F. Whitmore, and K. Brookman (1980). A screening method for isolating DNA repair-deficient mutants of CHO cells. Somatic Cell Genetics, 6(3):391-405.

Thompson, L. H., K. W. Brookman, L. E. Dillehay, C. L. Mooney, and A. V. Carrano (1982). Hypersensitivity to mutation and sister-chromatid-exchange induction in CHO cell mutants defective in incising DNA containing UV lesions. Somatic Cell Genetics, 8(6):759-773.

Thompson, L. H. (1996). Evidence that mammalian cells possess homologous recombinational repair pathways. Minireview. Mutation Research, 363:77-88.

Thompson, L. H., and D. Schild (2001). Homologous recombinational repair of DNA ensures mammalian chromosome stability. Mutation Research/Fundamental and Molecular Mechanisms of Mutagenesis, 477(1-2):131-153.

Tsurumi, C., N. Ishida, T. Tamura, A. Kakizuka, E. Nishida, E. Okumura, T. Kishimoto, M. Inagaki, K. Okazaki, N. Sagata, A. Ichihara, and K. Tanaka (1995). Degradation of c-Fos by the 26S proteasome is accelerated by c-Jun and multiple protein kinases. Molecular and Cellular Biology, 15(10):5682-5687.

Van Duin, M., J. de Wit, H. Odijk, A. Westerveld, A. Yasui, M. H. M. Koken, J. H. J. Hoeijmakers, and D. Bootsma (1986). Molecular characterization of the human excision repair gene *ERCC-1*: cDNA cloning and amino acid homology with the yeast DNA repair gene *RAD10*. Cell, 44:913-923.

Van Duin, M., M. H. M. Koken, J. van den Tol, P. ten Dijke, H. Odijk, A. Westerveld, D. Bootsma, and J. H. J. Hoeijmakers (1987). Genomic characterization of the human DNA excision repair gene *ERCC-1*. Nucleic Acids Research, 15(22):9195-9213.

Van Duin, M., J. van den Tol, P. Warmerdam, H. Odijk, D. Meijer, A. Westerveld, D. Bootsma, and J. H. J. Hoeijmakers (1988). Evolution and mutagenesis of the mammalian excision repair gene *ERCC*-1. Nucleic Acids Research, 16(12):5305-5322.

Van Duin, M., J. van den Tol, J. H. J. Hoeijmakers, D. Bootsma, I. P, Rupp, P. Reynolds, L. Prakash, and S. Prakash (1989a). Conserved pattern of antisense overlapping transcription in the homologous human *ERCC1* and yeast *RAD10* DNA repair gene regions. Molecular and Cellular Biology, 9(4):1794-1798.

Van Duin, M., G. Vredeveldt, L. V. Mayne, H. Odijk, W. Vermeulen, B. Klein, G. Weeda, J. H. J. Hoeijmakers, D. Bootsma, and A. Westerveld (1989b). The cloned human DNA excision repair gene *ERCC-1* fails to correct xeroderma pigmentosum complementation groups A through I. Mutation Research, 217:83-92.

Van Vuuren, A. J., E. Appeldoorn, H. Odijk, A. Yasui, N. G. J. Jaspers, D. Bootsma, and J. H. J. Hoeijmakers (1993). Evidence for a repair enzyme complex involving ERCC1 and complementing activities of ERCC4, ERCC11 and xeroderma pigmentosum group F. The EMBO Journal, 12(9):3693-3701.

van Vuuren, A. J., E. Appeldoorn, H. Odijk, S. Humbert, V. Moncollin, A. P. M. Eker, N. G. J. Jaspers, J-M. Egly, J. H. J. Hoeijmakers (1995). Partial characterization of the DNA repair protein complex, containing the ERCC1, ERCC4, ERCC11 and XPF correcting activities. Mutation Research, 337:25-39.

De Vries, A., C. Th. M. van Oostrom, F. M. A. Hofhuis, P. M. Dortant, R. J. W. Berg, F. R. de Gruijl, P. W. Wester, C. F. van Kreijl, P. J. A. Capel, H. van Steeg, and S. J. Verbeek (1995). Increased susceptibility to ultraviolet-B and carcinogens of mice lacking the DNA excision repair gene *XPA*. Nature, 377:169-172.

Vogel, U., M. Dybdahl, G. Frentz, and B. A. Nexo (2000). DNA repair capacity: inconsistency between effect of over-expression of five NER genes and the correlation to mRNA levels in primary lymphocytes. Mutation Research, 461:197-210.

Wang, X., C. A. Peterson, H. Zheng, R. S. Nairn, R. J. Legerski, and L. Li (2001). Involvement of nucleotide excision repair in a recombination-independent and error-prone pathway of DNA interstrand cross-link repair. Molecular and Cellular Biology, 21(3):713-720.

Warren, A. J., M. A. Ihnat, S. E. Ogdon, E. E. Rowell, and J. W. Hamilton (1998). Binding of nuclear proteins associated with mammalian DNA repair to the mitomycin C-DNA interstrand crosslink. Environmental and Molecular Mutagenesis, 31(1):70-81.

Weeda, G., I. Donker, J. de Wit, H. Morreau, R. Janssens, C. J. Vissers, A. Nigg, H. van Steeg, D. Bootsma, and J. H. J. Hoeijmakers (1997). Disruption of mouse ERCC1 results in a novel repair syndrome with growth failure, nuclear abnormalities and senescence. Current Biology, 7:427-439.

Wei, D., D. Fabris, and C. Fenselau (1999). Covalent sequestration of phosphoramide mustard by metallothionein - an *in vitro* study. Drug Metabolism and Disposition, 27(7):786-791.

Whitehead, C. M., R. J. Winkfein, M. J. Fritzler, and J. B. Rattner (1997). ASE-1: a novel protein of the fibrillar centres of the nucleolus and nucleolus organizer region of mitotic chromosomes. Chromosoma, 106:493-502.

Williams, T., and M. Fried (1986). A mouse locus at which transcription from both DNA strands produces mRNAs complementary at their 3' ends. Nature, 322:275-278.

Wilson, M. D., C. C. Ruttan, B. F. Koop, and B. W. Glickman (2001). ERCC1: a comparative genomic perspective. Environmental and Molecular Mutagenesis, 38:209-215.

Wood, R. D. (1999). DNA damage recognition during nucleotide excision repair in mammalian cells. Biochimie, 81:39-44.

Yacoub, A., R. McKinstry, D. Hinman, T. Chung, P. Dent, and M. P. Hagan (2003). Epidermal growth factor and ionizing radiation up-regulate the DNA repair genes *XRCC1* and *ERCC1* in DU145 and LNCaP prostate carcinoma through MAPK signaling. Radiation Research, 159(4):439-452.

Yagi, T., R. D. Wood, and H. Takebe (1997). A low content of ERCC1 and a 120 kDa protein is a frequent feature of group F xeroderma pigmentosum fibroblast cells. Mutagenesis, 12(1):41-44.

Yagi, T., A. Katsuya, A. Koyano, and H. Takebe (1998a). Sensitivity of group F xeroderma pigmentosum cells to UV and mitomycin C relative to levels of XPF and ERCC1 overexpression. Mutagenesis, 13(6):595-599.

Yagi, T., Y. Matsumura, M. Sato, C. Nishigori, T. Mori, A. M. Sijbers, and H. Takebe (1998b). Complete restoration of normal DNA repair characteristics in group F xeroderma pigmentosum cells by over-expression of transfected *XPF* cDNA. Carcinogenesis, 19(1):55-60.

Yang, L-Y., L. Li, H. Jiang, Y. Shen, and W. Plunkett (2000). Expression of *ERCC1* antisense RNA abrogates gemcitabine-mediated cytotoxic synergism with cisplatin in human colon tumor cells defective in mismatch repair but proficient in nucleotide excision repair. Clinical Cancer Research, 6:773-781.

Yu, J. J., C. Mu, K. B. Lee, A. Okamoto, E. L. Reed, F. Bostick-Bruton, K. C. Mitchell, and E. Reed (1997). A nucleotide polymorphism in ERCC1 human ovarian cancer cell lines and tumor tissues. Mutation Research Genomics, 382:13-20.

Yu, J. J., C. Mu, M. Dabholkar, Y. Guo, F. Bostick-Bruton, and E. Reed (1998). Alternative splicing of ERCC1 and cisplatin-DNA adduct repair in human tumor cell lines. International Journal of Molecular Medicine, 1(3):617-620.

Yu, J. J., A. Bichner, Y. K. Ma, F. Bostick-Bruton, and E. Reed (2000a). Absence of evidence for allelic loss or allelic gain for ERCC1 or for XPD in human ovarian cancer cells and tissues. Cancer Letters, 151(2):127-132.

Yu, J. J., K. B. Lee, C. Mu, Q. Li, T. V. Abernathy, F. Bostick-Bruton, and E. Reed (2000b). Comparison of two human ovarian carcinoma cell lines (A2780/CP70 and MCAS) that are equally resistant to platinum, but differ at codon 118 of the ERCC1 gene. International Journal of Oncology, 16(3):555-560.

Zhang, N., X. Zhang, C. Peterson, L. Li, and L. Legerski (2000). Differential processing of UV mimetic and interstrand crosslink damage by XPF cell extracts. Nucleic Acids Research, 28(23):4800-4804.

Zheng, H., X. Wang, A. J. Warren, R. J. Legerski, R. S. Nairn, J. W. Hamilton, and L. Li (2003). Nucleotide excision repair- and polymerase η-mediated error-prone removal of mitomycin C interstrand cross-links. Molecular and cellular biology, 23(2):754-761.

Zhong, X., K. Thornton, and E. Reed (2000). Computer based analyses of the 5'-flanking regions of selected genes involved in the nucleotide excision repair complex. International Journal of Oncology, 17(2):375-380.

CHAPTER 6: APPENDIX A

UV/PM Growth Inhibition Assays and Comparisons to Ercc1 Protein Expression for GM00637A Transfectants

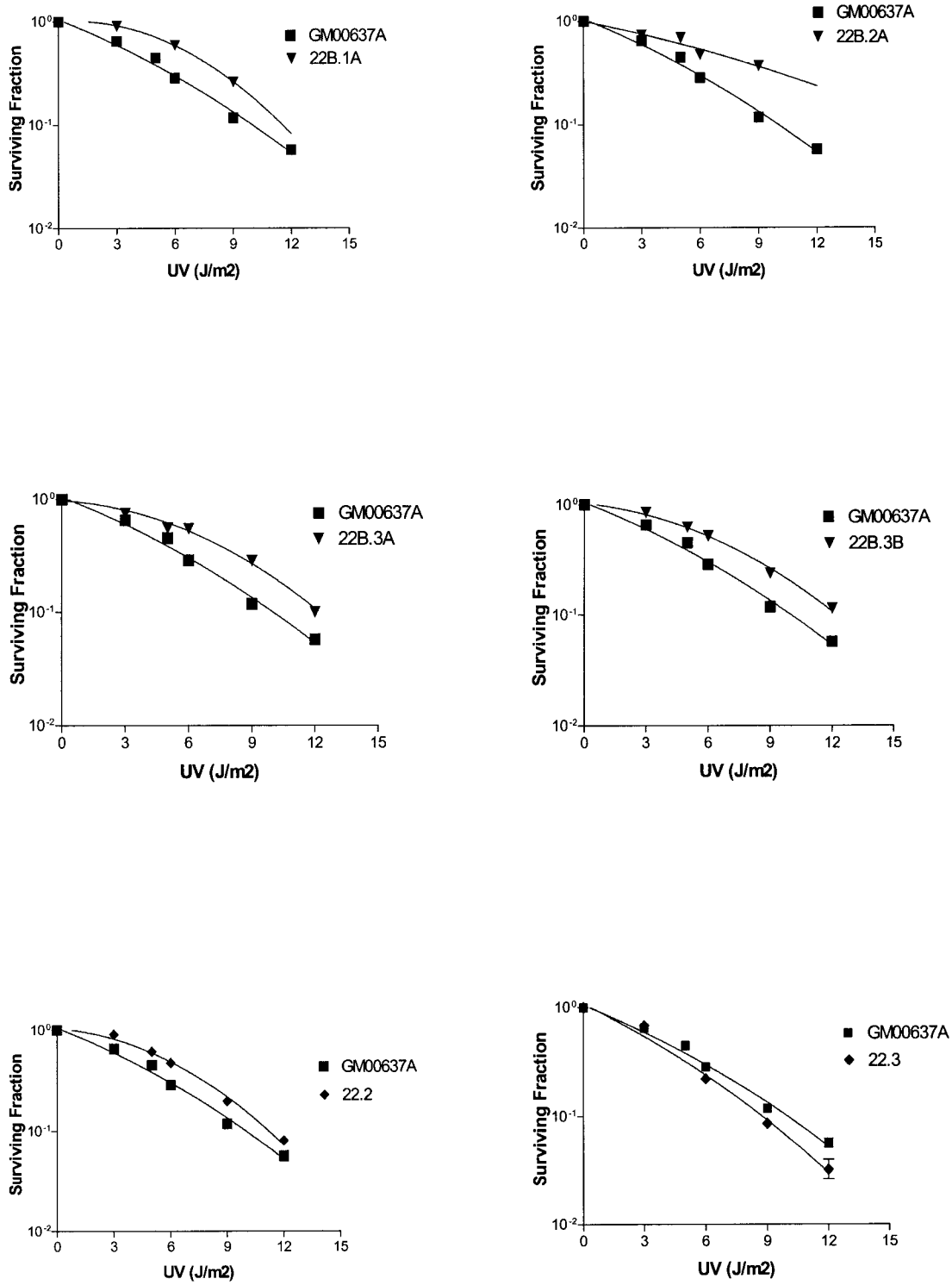

Figure A-1. Sensitivity of GM00637A transfectant cell lines exposed to UV-C as measured using the growth inhibition assay.

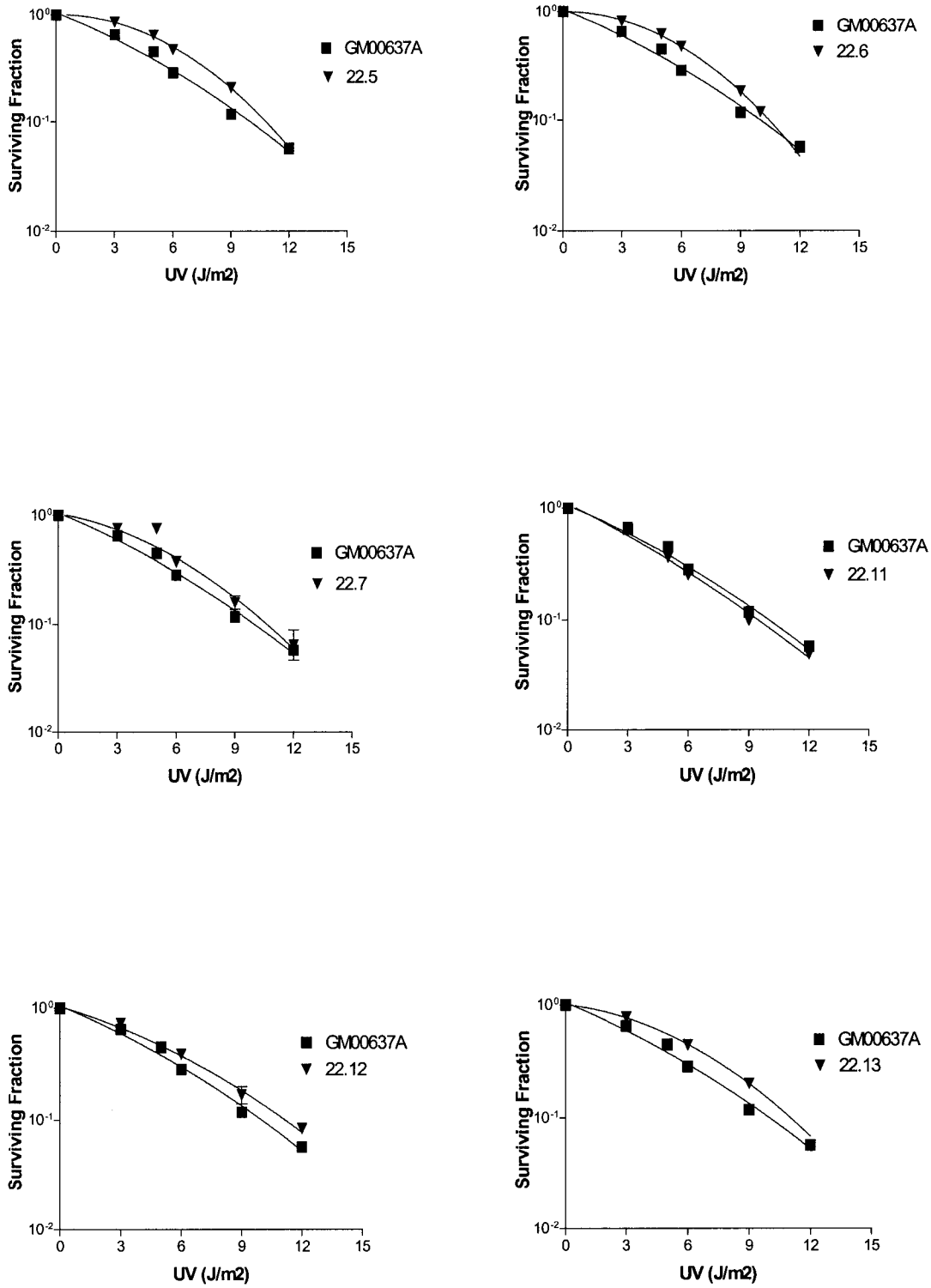

Figure A-2. Sensitivity of GM00637A transfectant cell lines exposed to UV-C as measured using the growth inhibition assay.

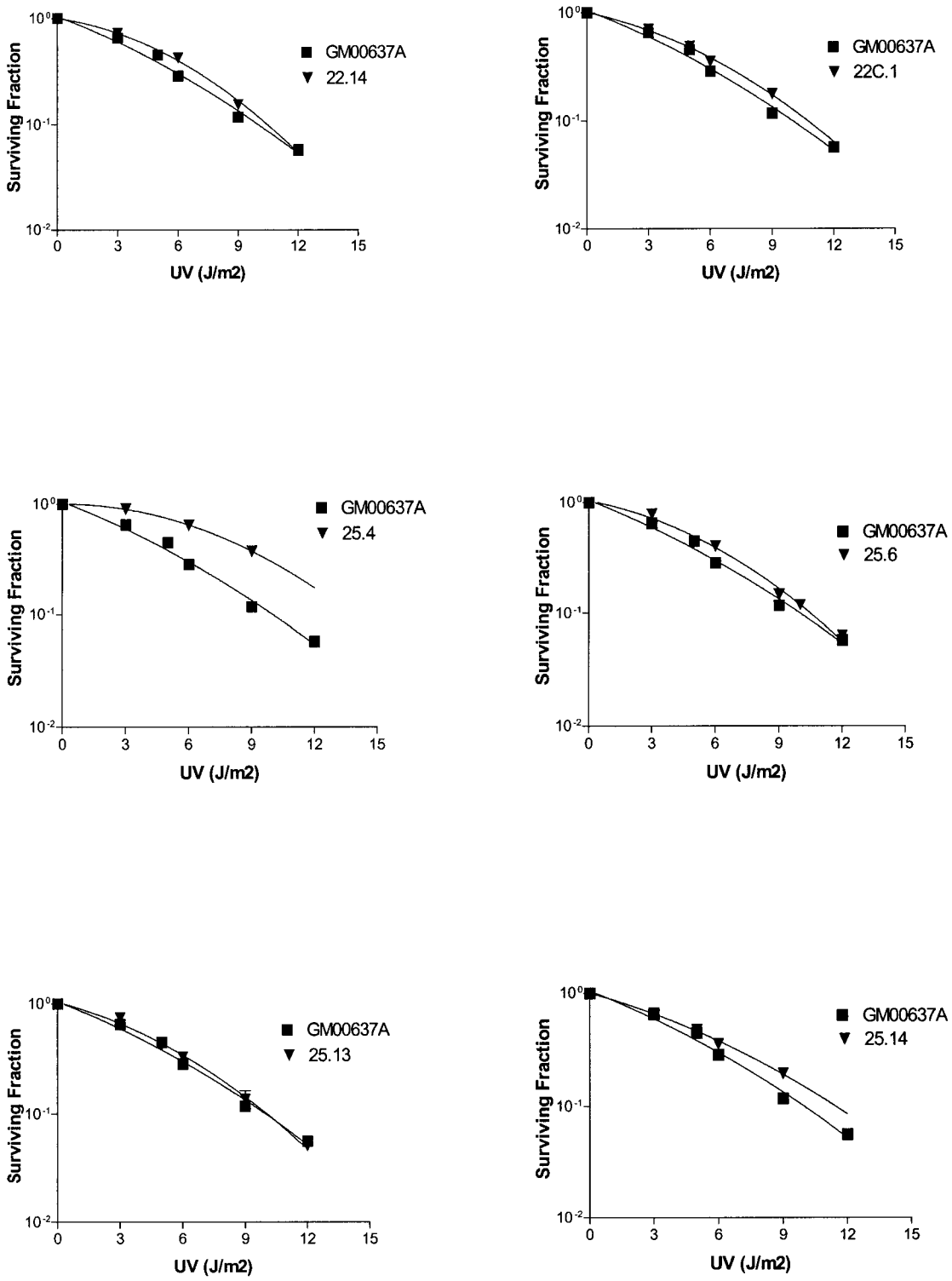

Figure A-3. Sensitivity of GM00637A transfectant cell lines exposed to UV-C as measured using the growth inhibition assay.

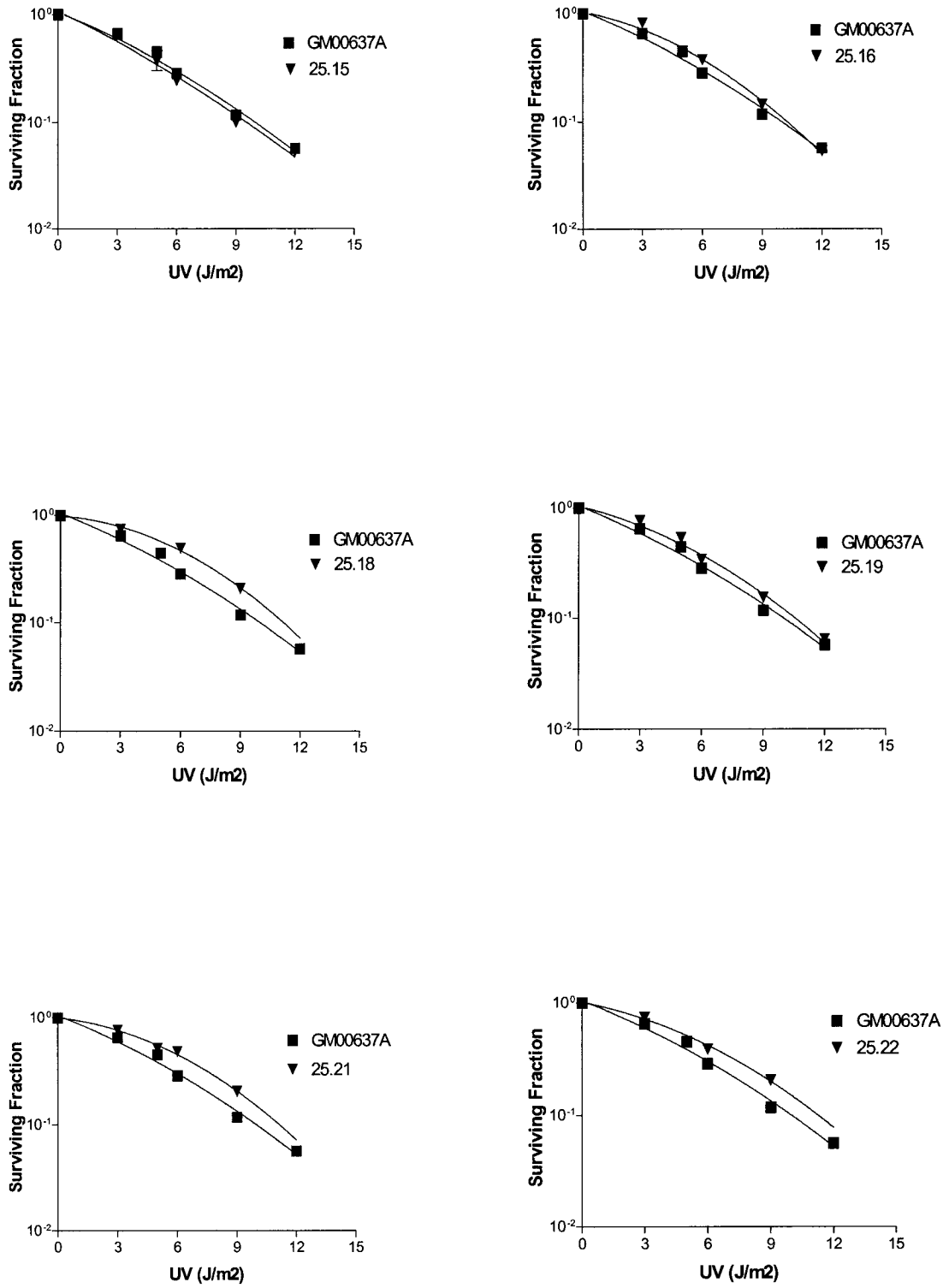

Figure A-4. Sensitivity of GM00637A transfectant cell lines exposed to UV-C as measured using the growth inhibition assay.

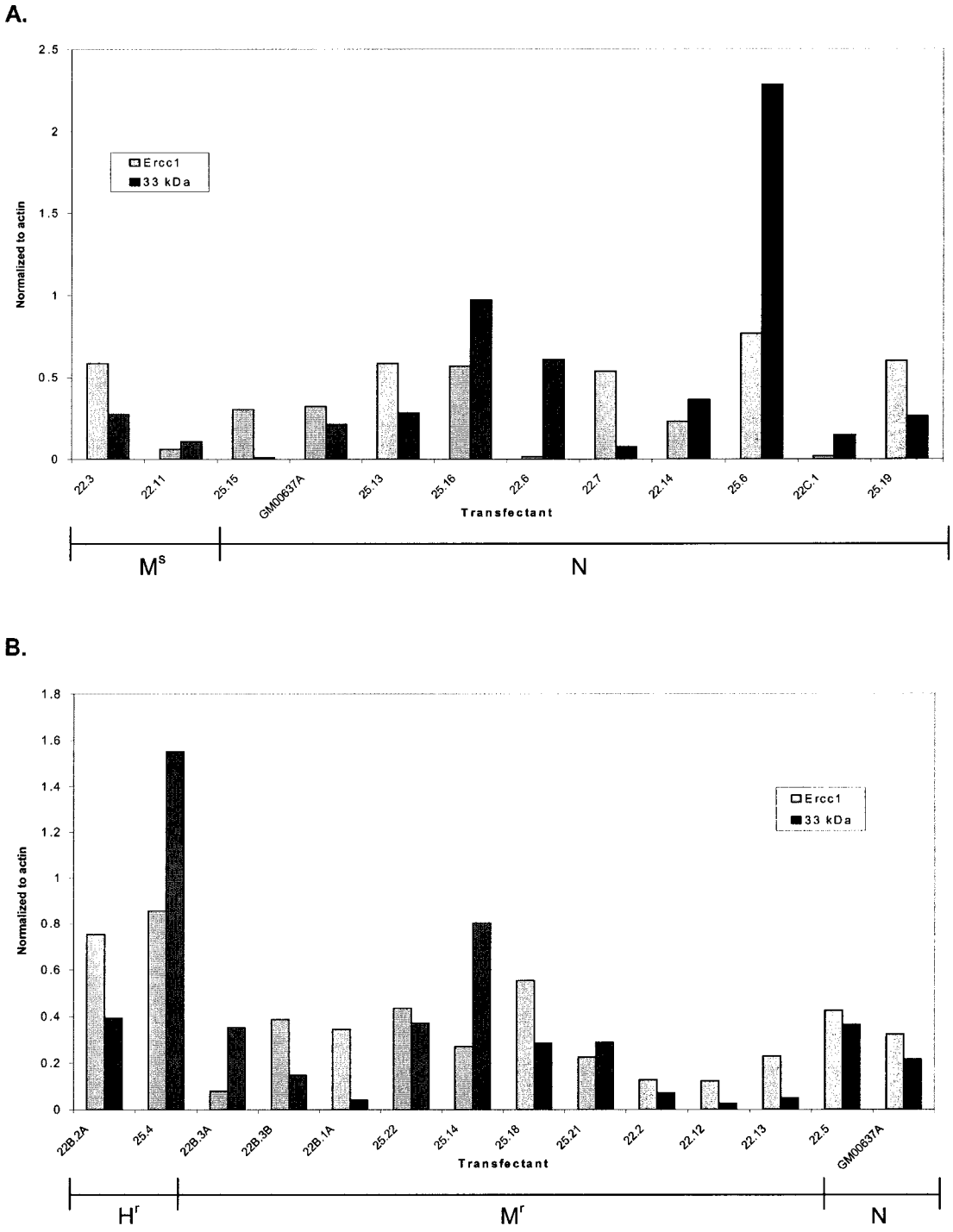

Figure A-5. Ercc1 and 33 kDa protein expression in whole cell extracts of GM00637A transfectant cell lines with respect to their UV-C sensitivity. M^s – moderate sensitivity, N – normal, and H^r – high resistance, M^r – moderate resistance.

A.

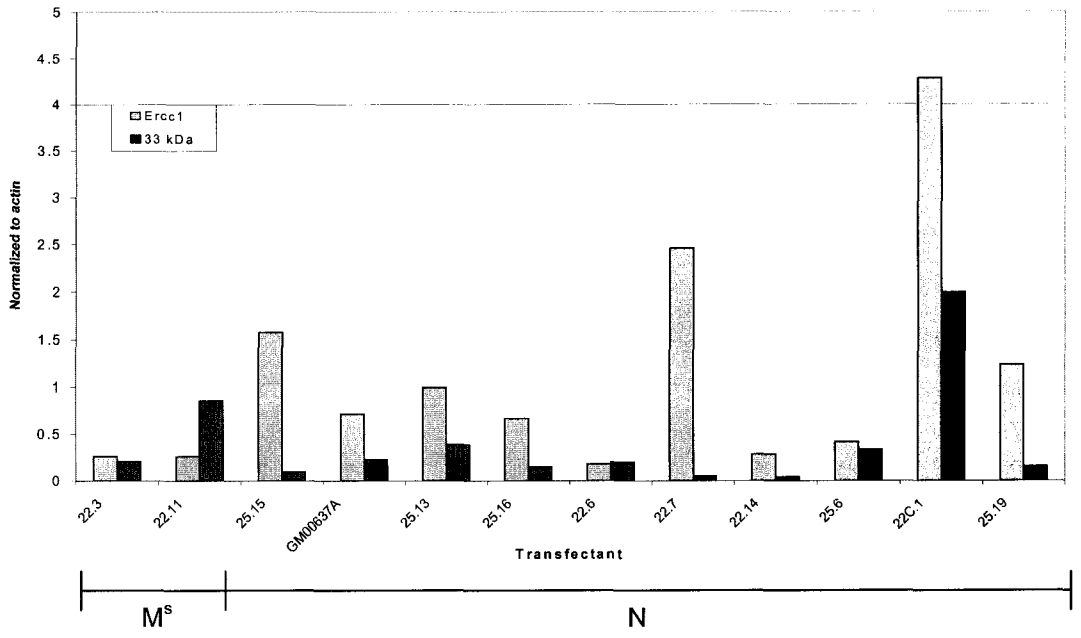

B.

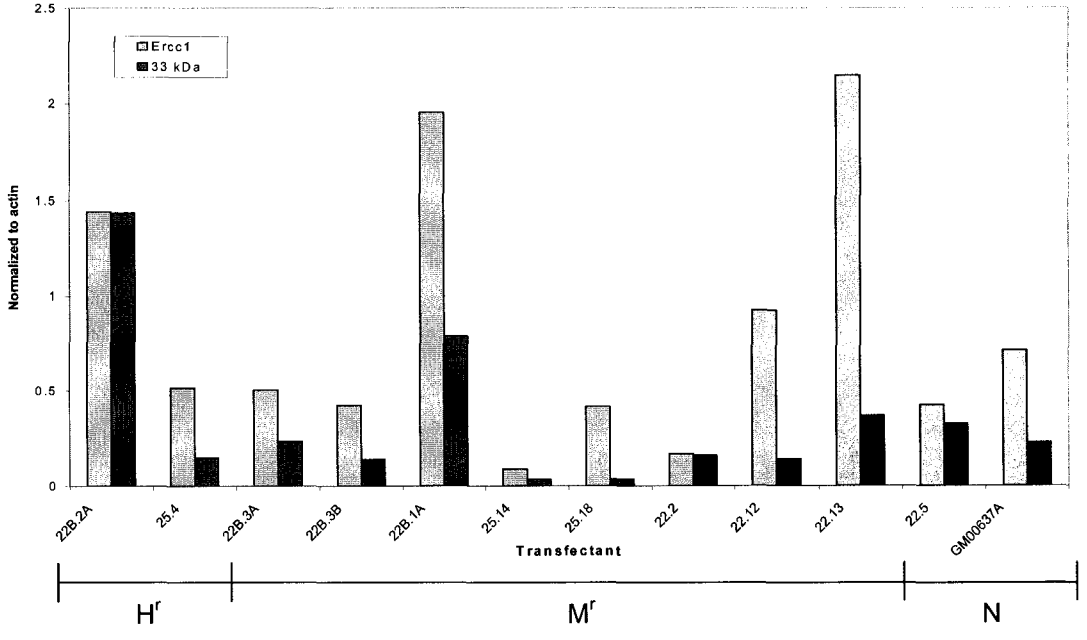

Figure A-6. Ercc1 and 33 kDa protein expression in nuclear extracts of GM00637A transfectant cell lines with respect to their UV-C sensitivity. M^s – moderate sensitivity, N – normal, M^r – moderate resistance, and H^r – high resistance.

A.

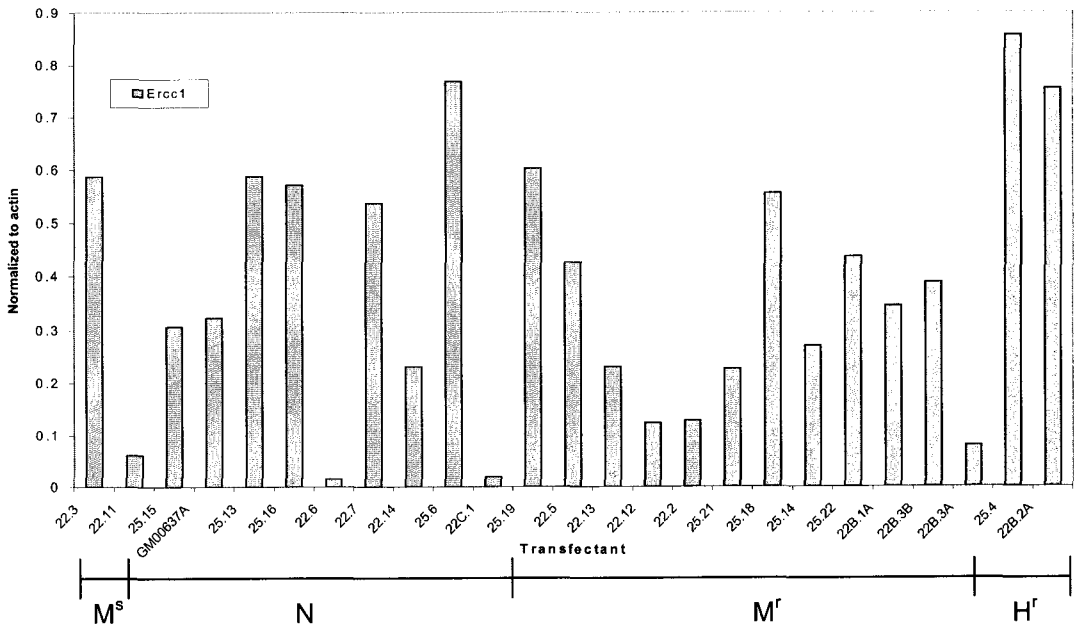

B.

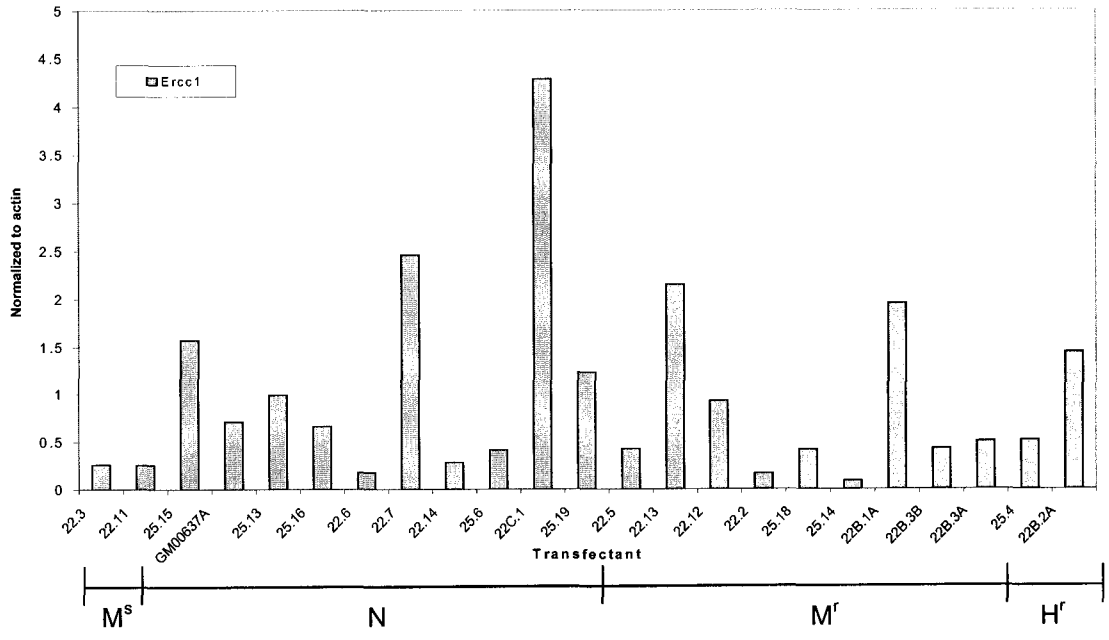

Figure A-7. Ercc1 protein expression in (A) whole cell extracts and (B) nuclear extracts of GM00637A transfectant cell lines with respect to their UV-C sensitivity. M^s – moderate sensitivity, N – normal, M^r – moderate resistance, and H^r – high resistance.

A.

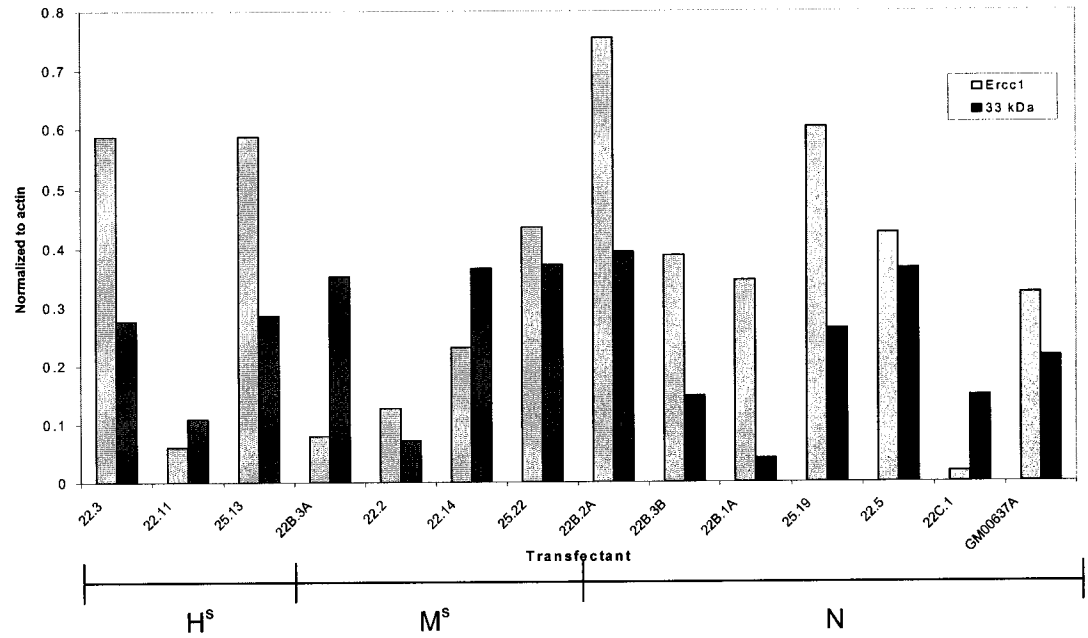

B.

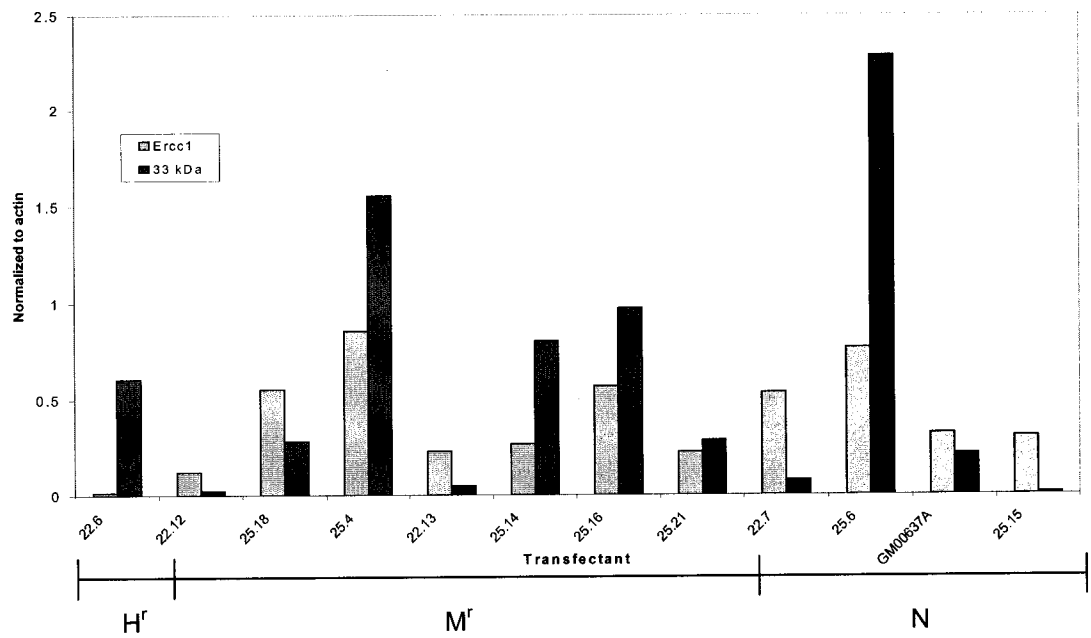

Figure A-8. Ercc1 and 33 kDa protein expression in whole cell extracts of GM00637A transfectant cell lines with respect to their PM sensitivity. H^s – high sensitivity, M^s – moderate sensitivity, N – normal, H^r – high resistance, and M^r – moderate resistance.

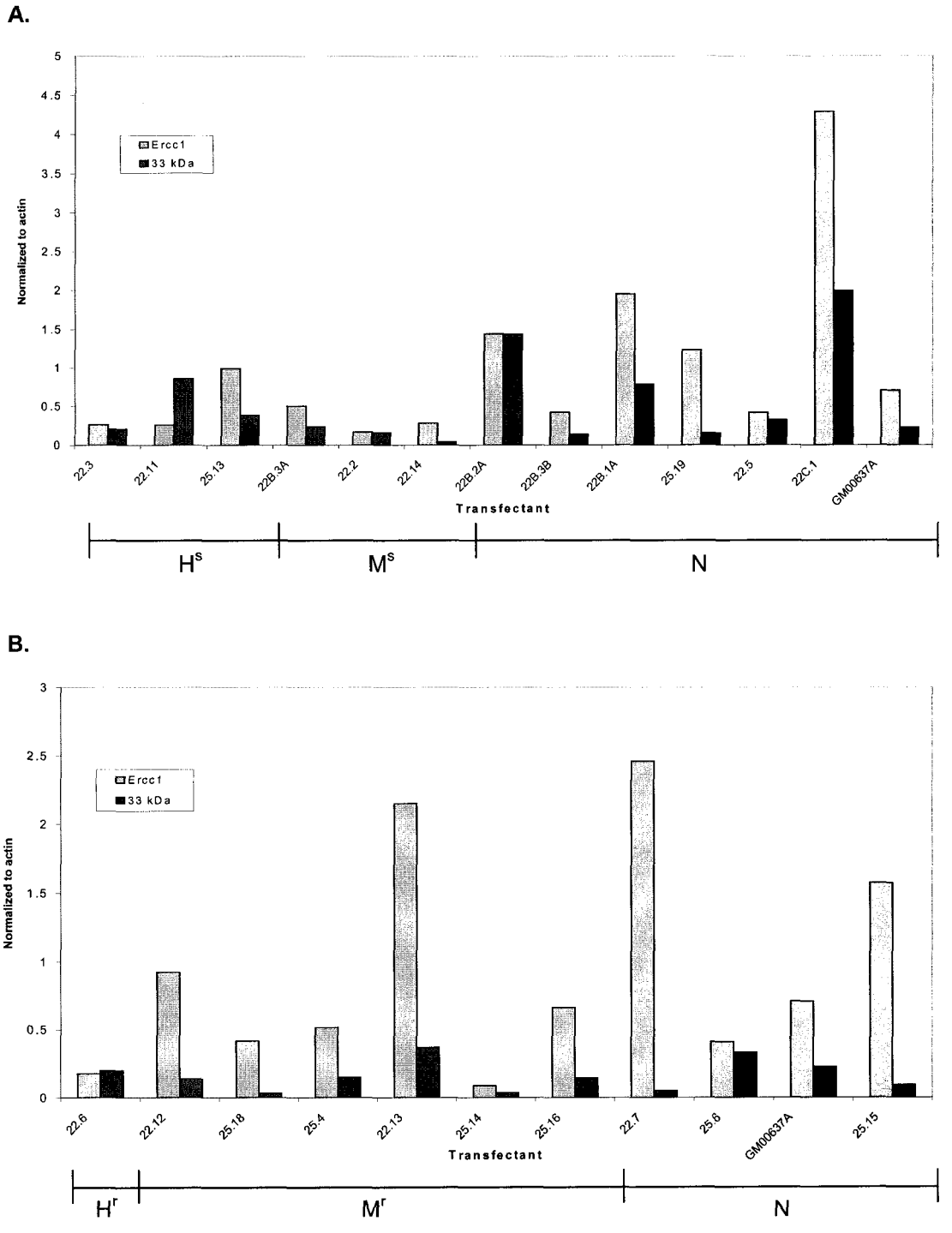

Figure A-9. Ercc1 and 33 kDa protein expression in nuclear extracts of GM00637A transfectant cell lines with respect to their PM sensitivity. H^s – high sensitivity, M^s – moderate sensitivity, N – normal, H^r – high resistance, and M^r – moderate resistance.

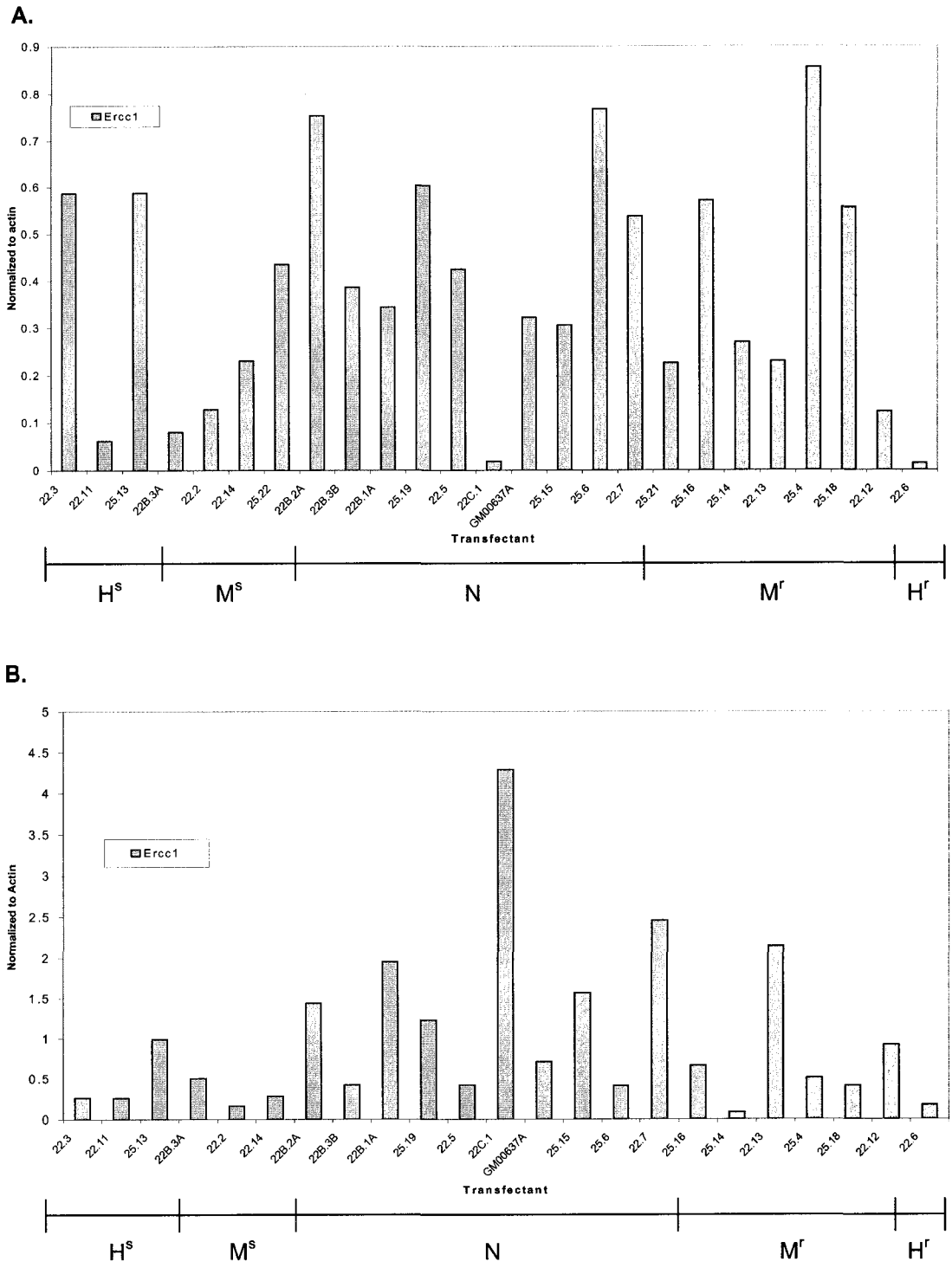

Figure A-10. Ercc1 protein expression in (A) whole cell extracts and (B) nuclear extracts of GM00637A transfectant cell lines with respect to their PM sensitivity. H^s – high sensitivity, M^s – moderate sensitivity, N – normal, M^r – moderate resistance, and H^r – high resistance.